# OPTIMIZATION OF A CITRUS HARVESTING SYSTEM BASED ON MECHANISTIC TREE DAMAGE AND FRUIT DETACHMENT MODELS

By

SUSHEEL KUMAR GUPTA

A THESIS PRESENTED TO THE GRADUATE SCHOOL
OF THE UNIVERSITY OF FLORIDA IN PARTIAL FULFILLMENT
OF THE REQUIREMENTS FOR THE DEGREE OF
MASTER OF SCIENCE

UNIVERSITY OF FLORIDA

2013

To my parents for supporting me in every possible way to achieve my goals and fulfill my dreams

ACKNOWLEDGMENTS

Firstly, I would like to thank my parents for their encouragements, blessings and never ending supports which has helped me achieve one of the most cherished dreams of my life-to study and participate in the cutting edge research in USA. I would like to thank Dr. Nam-Ho Kim for taking me on as a master's student and providing his unstinted guidance, inputs and supervision during the course of my thesis. I am grateful to Dr. Reza Ehsani for giving me chance to work on this challenging, demanding yet exciting research project and supervising and motivating throughout the research. Without their support and guidance, I would have not able to grown and matured as a student and a researcher. I would like to thank Dr. Peter Ifju, and Dr. Arthur Teixeira for their guidance and assistance in the experiments. Very special thanks to Jinsang Chung and Garret Waycaster who helped me in understanding the concepts and principles required for my research. I am grateful for the suggestions and feedbacks from my lab mates in the mdo group especially Shu Sang, Yong Min Chung, Anirban Choudhuri, Diane C. Villanueva, and Taiki Matsumara. I am would also like to thank my labmates from CREC especially, Amanda L. Valentine, Joe Mari Maja, Sherrie Buchanon, Sweeb Roy, Ali Mirzakhani, Jaafar Abdulridha, Luv Khot, and Ying She for guiding me and assisting me in experiments, and data collection.

A special thanks to my friends Mayank Amin, Rajesh Metta, Chirag Mistry, Bhavin Parikh, Bhavesh Patel, Mitesh Patel, Thirumalesh Rao, Akshay Panchal, Varun for their continued support and motivation. Lastly, I would like to thank my brothers: Sudhir and Satish because without their support and encouragement; I would have not been able to achieve my endeavors.

TABLE OF CONTENTS

page

LIST OF TABLES

LIST OF FIGURES

## LIST OF ABBREVIATIONS

| | |
|---|---|
| AL. | Aluminum |
| CAD | Computer aided design |
| CANOPY | Aboveground portion of a plant or crop, formed by plant crowns |
| CCSC | Continuous canopy shake and catch harvester |
| CREC | Citrus research and education center |
| CV | Coefficient of variation |
| DOM | Drawn over mandrel |
| DI | Damage index |
| FEM | Finite element model |
| FDI | Fruit detachment Index |
| Hz | Hertz |
| LIMB | Main branches of a tree |
| LIMB PROTOTYPE | Non-physical or virtual model of a tree limb |
| META-MODEL | Analytical models to predict the function when true function is unknown |
| PA | Polyamide |
| PAN | Polyacrylonitrile |
| PCHIP | Piecewise cubic Hermite interpolating polynomial |
| PF | Pareto front |
| PO | Pareto optimal |
| $PRESS_{RMS}$ | Root mean square of prediction residual sum of squares |
| PRS | Polynomial response surface |
| RBNN | Radial basis neural network |
| RESPONSE SURFACE | metamodel |
| RMS | Root mean square |

| | |
|---|---|
| RSM | Response surface methods |
| SCAFFOLD BRANCHES | Primary limbs radiating form the trunk of a tree |
| TDCS | Tractor-drawn canopy shake harvester |
| TINE | Long tube or rod like structures of canopy shaker which perform the shaking of a tree canopy during harvesting |
| UTM | Universal testing machine |

Abstract of Thesis Presented to the Graduate School
of the University of Florida in Partial Fulfillment of the
Requirements for the Degree of Master of Science

OPTIMIZATION OF A CITRUS HARVESTING SYSTEM BASED ON MECHANISTIC TREE DAMAGE AND FRUIT DETACHMENT MODELS

By

Susheel Kumar Gupta

August 2013

Chair: Nam-Ho Kim
Major: Mechanical Engineering

Mechanization of fruit and nut harvesting is becoming increasingly important because of a significant rise in the cost of manual harvesting. Timely adaptation of technological advancement and innovation is utmost important in the fruit and nut crop industries to ensure their continued profit and global competitiveness. However, the slow pace of research in the design and development of these harvesters is barely able to satisfy the demands of these industries.

The classical method of designing a harvester based on the field experiments is tedious, time consuming and expensive. The goal of this study is to propose a framework for the design and optimization of a harvester using numerical methods: the goal is pursued by optimizing a continuous canopy shaker for citrus crops-specifically orange (*Citrus sinensis*). A progressive design approach is presented consisting of determining the properties of wood, statistical modeling of tree limb prototypes, developing mechanistic models and, integrating numerical simulation with optimization tools. Response Surface Methods (RSM) and Pareto optimal solution search techniques were applied in order to obtain the optimal designs.

Three sets of machine parameters which consist of three different configurations of tines or shaking members and operating parameters of a shaker were proposed to minimize the tree damage and maximize the fruit removal based on the configurations of the tree limbs and distribution of the fruits in a medium size citrus tree. As reference to the current configuration of the tines in a canopy shaker, it was found that by changing the configuration of tines in the middle and the bottom section of a canopy shaker to the tine made of polyamide rods having 50% long glass fiber and hardened steel tube in the ratio of 3:1 by length and vibrating at high frequency of 7-8 Hz and low amplitude of 1.5-2.5 inches has resulted in 25-30% reduction in the damage of limbs which are long, thick and hang down sharply due to the weights of fruits. Changing the top section of a canopy shaker with the tines made of polyamide rods having 60% long glass fiber and vibrating at a frequency of 6.5-7.5 Hz and amplitude of 3-3.5 in. has resulted in a 40-45 % reduction in the damage of limbs which are thick, long, and grow straight up to a height of 100-130 inches before curving down slightly due to the weight of fruits.

# CHAPTER 1
# INTRODUCTION

Mechanical harvesting equipment is becoming increasingly important due to current manual harvesting costs and labor shortages. Continued profit and competitiveness in the global market demands an efficient harvesting system. Many mechanical harvesters for harvesting fruits and nuts have been developed in the past five decades, but only few of them have been successfully adopted and commercialized (Futch and Whitney, 2004). Most current research focuses on increasing the amount of mechanical harvesting either by redesigning existing systems or by developing an entirely new harvesting mechanism. Many commercialized harvesters for fruits and nuts are designed to induce either free vibration or forced vibration to the trunk or tree limbs/canopy (Fridley et al., 1971; Peterson et al., 1972; Markwardt et al., 1964; Halderson, 1966). These vibrations are then transmitted throughout the tree, creating the necessary force to cause the detachment of fruits. The harvesters essentially comprise of two parts: a mechanical system which generates vibratory motions, and a mechanical interface which transmits vibrational energy to the tree crops. Examples of mechanical interface are: a movable tongs which grip the trunk or limbs and force them to vibrate; or a vibrating rod which impacts the tree limbs to cause them to vibrate freely.

## Motivation

Most accomplishments in a design of vibratory harvester have been achieved using heuristic methods (Fridley, 1966). This involves designing the harvesting system using rules of thumb, educated guesses or assumptions validated by extensive field trials. However, field trials are usually very demanding and time-consuming. Moreover, the specific problem areas are very difficult to evaluate by experimental studies because

of high variability and randomness associated with the trees and their interaction with a harvesting machine. However, experience from these field trials had provided a general understanding of the dynamic response of tree crops, but the parameters that can be used to design a shaker has not yet been formulated. The explanation for good results under some conditions and excessive tree damage in other situations has found to be related to the tree structure and their interaction with a machine (Fridley and Adrian, 1966). Extensive field trials are necessary to formulate these interactions in order to find the optimum harvesting parameters but would be prohibitively expensive and time consuming.

An alternative approach for designing an efficient harvesting system is to use numerical methods (Archer, 1965; Hurty and Rubinstein, 1964). Experimentally-verified numerical models allow designer to economically iterate various designs to select the optimum one. Finite elements methods are a widely used numerical technique in structural design. However, the application of these methods in the design of a harvesting system is limited because of the complicated and non-uniform nature of a biological structure such as tree limbs. The randomness in the spatial configuration of the tree limbs and their interaction with a harvesting system makes this physical phenomenon very difficult to simulate using numerical methods. Some assumptions and generalizations should be made to efficiently approximate the physical models and their interactions. These methods can prove to be an economical way to optimize a harvesting system because of their capability to iterate a large number of designs in a significantly less time as compared to the experimental methods.

## Design Problem

Mechanical harvesting of citrus specifically oranges (Citrus senensis) in Florida was started in the late 1990s. Figure 1-1 shows that the harvesting of citrus crop rose gradually thereafter because of implementation of various mechanical means in the harvesting of citrus crops as summarized by Savary (2009). However, with the advent of a canopy shaker (Peterson, 1998), the mechanical harvesting of citrus has reached to its peak in the years spanning from 2005-2009. The continuous canopy shakers are the most recent and widely used type of mechanical harvesting system in Florida for the harvesting of citrus. This system has gained popularity and acceptance over any other harvesting equipment because it does not stop at each tree during harvest and provides a high harvesting yield of approximately 95-96 % (Whitney, 1999).

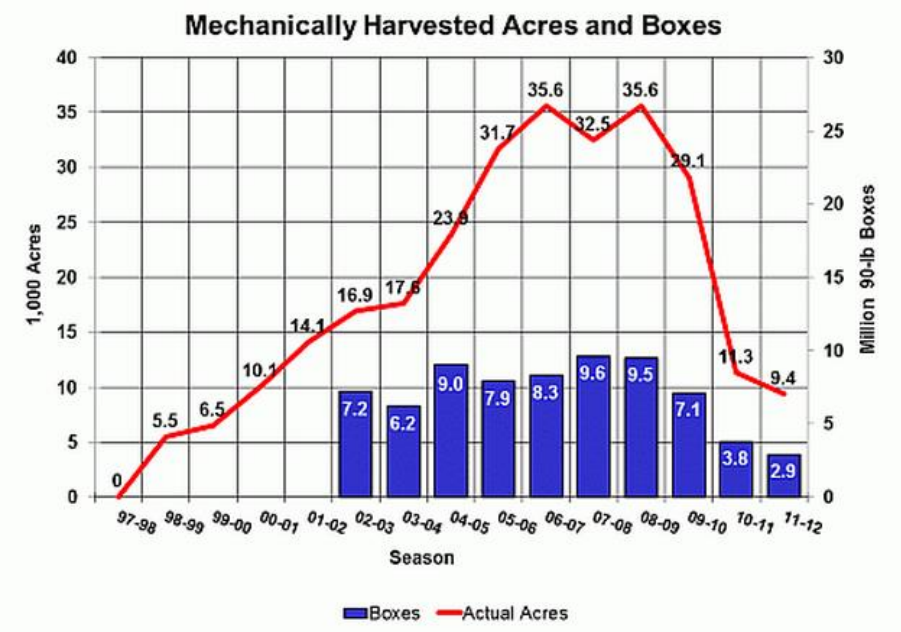


Figure 1-1. Mechanical harvested acreage of Citrus in Florida (Data provided courtesy of Florida Department of Citrus).

However, mechanical harvesting of citrus in Florida has been declining sharply after the seasons of 2008-2009 because of problems associated with extensive use of

canopy shakers. The operation of these machines causes excessive tree damage or injury. The tree damage or injury makes trees vulnerable to disease which girdles and kills not only scaffold branches or a whole tree but sometimes a whole orchard if unnoticed. Therefore, Florida growers are reluctant to use canopy shaker for harvesting of citrus crops as they severely damage the scaffold branches and reported to reduce subsequent years fruit yield (Spann and Danyluk, 2010). In order to increase the mechanical harvesting, the growers concerns should be addressed.

**Design Idea**

The reluctance of the growers to employ these machines for mechanical harvesting can be solved by either modifying the existing machines or developing a new machine with can minimize the tree damage without significantly reducing harvesting efficiency. The idea of adaptive shaking of the tree canopy has been proposed to improve current continuous canopy harvester which can potentially solve the growers' concerns. The adaptive shaking of tree was realized by providing a variable shaking force to the tree limbs depending on the distribution of fruits and limbs (spatial configuration and stiffness) in a tree canopy as shown in Figure 1-2.

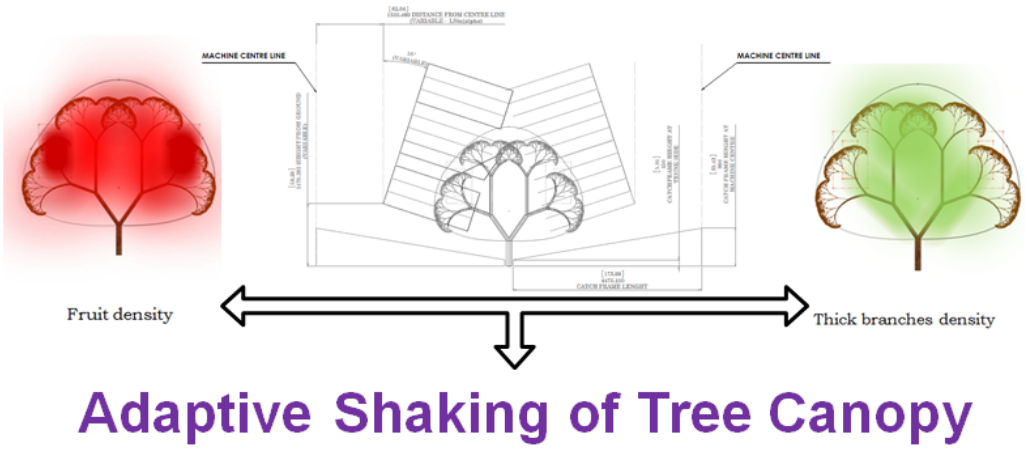


Figure 1-2. Design idea based on the distribution of fruits and thick branches in a tree canopy.

The variable shaking force to different parts of the canopy was provided by setting different configuration of a canopy shaker. The limbs with similar dynamic response owing to their spatial configuration and property distributions were classified in in three zones of a tree canopy as shown in Figure 1-3. Three sets of tine (or shaking member) configurations and combinations of frequency and amplitude of the canopy shaker were proposed based on dynamic response of the three sets of tree limbs.

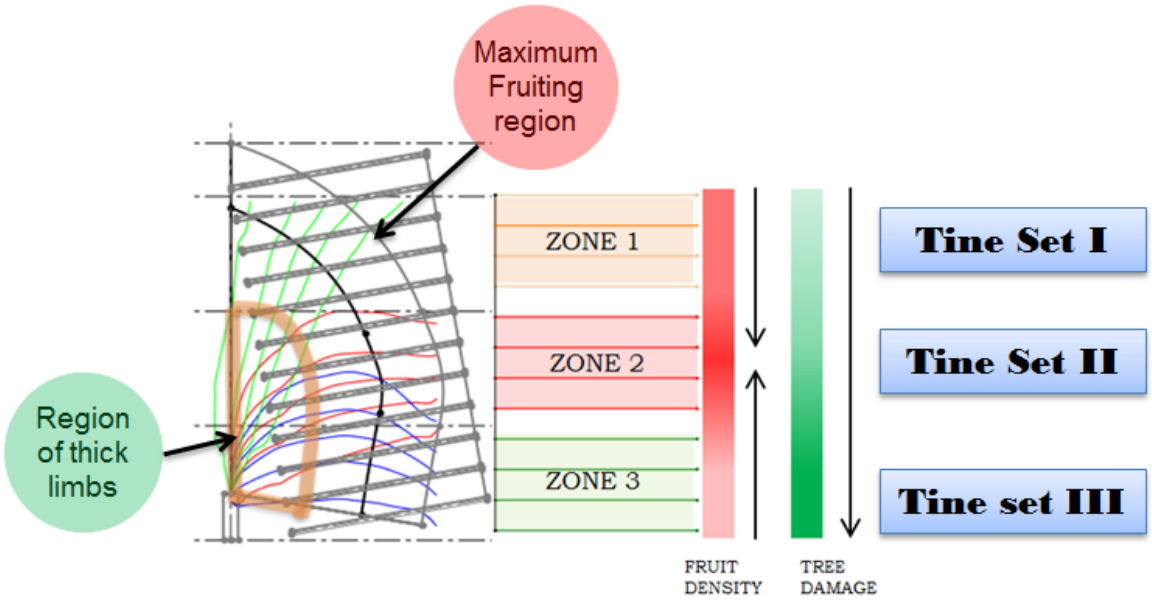


Figure 1-3. Classification of the shaker tines and a citrus tree canopy based on the limbs configurations and the fruits distribution.

**Objective of this Study**

The purpose of this research is to develop a methodology for the optimization of a canopy shaker employing computer aided numerical and optimization techniques. In order to address growers' concerns about tree damage and efficiency of a canopy shaker: this study reports an economical way of defining the machine-tree interactions and modeling the tree limbs based on parameters derived from the statistical prototypes rather than the random individual trees. A progressive design approach is adopted

which involves the determination of the properties of the wood, accumulating and organizing statistical information for modeling tree limbs, performing dynamic analysis, and building mechanistic models for the optimization a canopy shaker. The schematic of the design process employed to predict an optimal set of machine structural and operating parameters is shown in Figure 1-4.

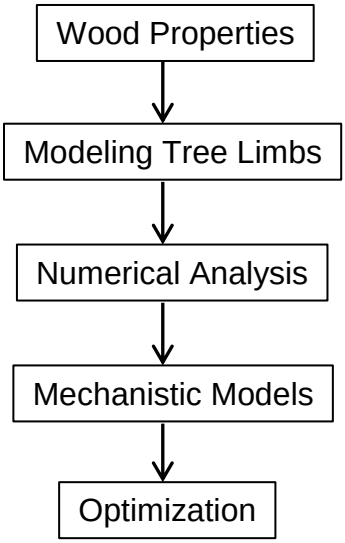


Figure 1-4. Schematic of process involved in the realization of adaptive shaking of tree canopy using numerical simulation.

**Methodology Adopted**

The proposed design idea is implemented using computer aided techniques rather than experimental means as the latter is more expensive and time consuming. Computer simulation provides an efficient tool to determine the response of the whole tree to practically any vibratory force by dividing it into a large number of small element sections, with the mass and stiffness properties of each section known from the measurements (Philips, 1970; Fridley and Yung, 1975; Savary and Ehsani, 2010). However, it is unlike that a harvester designed based on the response of few sets of trees will perform satisfactorily for all other trees. Thus, instead of analyzing a whole

tree, the statistical prototypes of limbs derived from random individual trees were used. This process involves the prediction of the parameters of the primary limbs based on the statistical information accumulated from a large number of trees. The response of the tree limbs with known properties of mass, stiffness and damping is obtained using numerical techniques. The response of limbs is then used to optimize the structural and operating variables of the harvester. This methodology provides an economical way to optimize a canopy shaker for harvesting citrus crops and can be successfully extended to harvest other fruits such as citrus, peaches, apple, almonds, blueberries, raspberries, olives, grapes, and coffee.

## Report Organization

Chapter 2 summaries the previous studies done for the design of mechanical harvesters and various techniques used in this research. Chapter 3 is about determination of physical and mechanical properties of a green citrus wood. Chapter 4 explains the methodology to predict the statistical prototypes of a tree limb to be used in the finite element analysis. Chapter 5 describes the finite element modeling of machine, tree limbs, and their interaction. Chapter 6 identifies and quantifies the objective functions for the optimization of a shaker using mechanistic models. Chapter 7 is about the multi-objective optimization of the canopy shaker. The conclusions of this study are summarized in Chapter 8. Appendix A provides the lab view program to acquire strain gauge and acceleration data. Appendices B and C provide the tables and the figures associated with phase-1 and phase-2 optimization of canopy shaker.

# CHAPTER 2
# HISTORY AND LITERATURE REVIEW

## History

### Mechanical Harvesting

Mechanical harvesting has been successfully adopted for many crops including some fruit and nuts crops. Harvesting method varies with crops. Therefore, a specialized harvesting is needed depending on the type of a crop. Wide varieties of harvesters are available for grain crops, vegetables, forage crops and some fruit and nut crops. For grain crops, harvesting is a process of cutting and threshing the crop to separate the grain from stalk (Kutzbach and Quick, 1999). In case of forage crops, baling for grasses and cutting for forage cereals (Cavalchini, 1999) is required. For vegetables, the harvesting is very complex process and depends on the type of vegetable being harvested. For root crops, harvesting is accomplished by digging as in potatoes or pulling as in the case of leeks (Manfredi and Peters, 1999). For surface crop combing (peas, green beans), stripping (cucumbers), shaking (tomatoes), de-stemming (onions, garlic), threshing (peas from their pods), and cutting (cabbage, cauliflower etc.), operation are employed for harvesting. Mechanical harvesting of fruits is mostly done for process industry. Small fruits and wine grapes are harvested by a combination of contact and non-contact methods. The small fruit's like strawberries, raspberries etc. are harvested using combination of shaking and soft combing. This is achieved by shaking the crops with a finger like structure mounted radially on oscillating drums. Grapes are harvested using straddle type harvester which shake the vines to remove the grape clusters from them. The grape harvester uses horizontal rods to shake the vines with frequencies ranging from 10-20 Hz.

For fruit and nut crops, the most common method of harvesting is to shake the trees which cause oscillatory motion of fruit's. When a fruit vibrates, it experiences traction, twisting, bending, and shear force. These forces results in creating necessary stress at the point of contact, either at the branch-stem junctions or at the stem-calyx which cause the detachment of the fruit. Various fruits such as citrus, prunes, apples, olives, almonds, blueberries, raspberries etc. are currently harvested using the similar methods.

**Mechanical Harvesting of Citrus**

Mechanical harvesting of citrus was started in 1950s in an attempt to reduce the manual labor (Whitney, 1995). Efforts were made to mechanize citrus handling as summarized by Hedden and Churchill (1984). First ever mechanization of citrus handling was achieved by employing two-wheel trailer for handling fruits to both process industry and fresh fruit market. In the late 1950s, loader boom mounted on high lift truck was used for the handling of the processing fruits. In later years, fruit collection system based on vacuum was developed for fruit handling. In such a system, fruits are transferred to the closed cylindrical hopper by the picker, which are dumped directly into a roadside truck by vacuum system. While the handling of citrus was being mechanized, studies were being conducted to improve the efficiency of the machines which picks the fruits from a tree. Jutras and Coppock (1958) conducted time and motion studies on hand harvesting. They investigated different scenarios to design harvesting aids to cut down on non-productive time. Different type of harvesting aids were studied to make manual harvesting efficient by partially mechanizing the process of harvesting (Coppock and Jutras, 1960). Various harvesting aid such as vertical lift worker positioner, multi-boom vertical position, and multi-worker positioner was developed in the course of time.

However, they were not economically very advantageous over conventional methods of picking.

In the 1960s, efforts were made to duplicate manual harvesting by developing harvesting machines. Lenker (1970) developed an auger based harvester. This system used a series of parallel augers having flexible flights to gently twist the fruit from citrus branch and convey it away from the tree to a collector. Later Chen et al (1982) developed a contact harvester which had flexible fingers to harvest the mature fruits selectively. Two other detachment devices have been developed for the removal of individual citrus fruit (Schertz and Brown 1968, Brown et al. 1969). A vacuum twist device was developed which pull the fruits into a large rotating rubber sock like tube and detach the fruits by twisting. The amount of twisting torque applied depends on the friction between the rubber sock and the fruit. To harvest a citrus fruit, a rotating cut-off device which uses pair of concentric cylinders was developed. This machine was composed of outer rotating cylinder with a hood that engaged the stems and draws them against a knife supported on the stationary inner cylinder. Another concept for citrus was the roller head harvester concept. This concept consisted of a series of rubber covered rollers equally spaced in a horizontal bank. All rollers rotate in the same direction and were positioned to comb vertically through the tree canopy. However, due to low harvesting yield, the focus was shifted from contact harvesting to mass harvester like trunk shaker and limb shaker.

Beginning in early 1960s, investigation into development of mass fruit harvester started. Research and development to harvest citrus has resulted into trunk shaker, limb shaker, foliage, and canopy shaker. One of initial inertial shaker to harvest citrus was

designed based on the work of Adrian and Fridley (1965). Some of the early mass harvesters were primarily trunk and limb shakers. Various studies were conducted to investigate the efficiency of these harvesting systems which was found to be significantly low. Various studies were performed analytically and experimentally to improve the performance of these systems. In the 1970s, a vertical foliage shaker was designed which applies force to the canopy of a tree in an attempt to increase the fruit harvesting. Comparative trails performed by Hedden and Coppock (1971) concluded that the foliage shaker had performed better than any other harvester tired in their study. The air shaker designed by Whitney 1968, and Whitney and Patterson, 1972 did not come in contact with fruits, therefore does not cause any fruit bruising. However, these systems were efficient only with abscission chemicals. In late 1990s, a prototype similar to the current canopy shake was designed and developed by Peterson (1998). Harvesting trial using canopy shaker had indicated the fruit removal efficiency ranging for 80-90%.

**Current Harvesting System for Citrus**

The current mechanical harvesting system to harvest citrus fruits in Florida is a continuous canopy shaker which is enhanced version of the design proposed by Peterson (1998). There are two versions of this system: (1) Continuous canopy shake and catch harvester as shown in Figure 2-1 which has a catch frame for collecting harvested fruits; (2) Tractor drawn canopy shaker as shown in Figure 2-2 which is only equipped to harvest the fruits and the harvested fruits are hen picked up from the ground manually or by pick-up machines. The principle mechanism to detach the fruits is same in both the harvesters and is accomplished by impacting the tree limbs periodically by sinusoidally vibrating tines. The tines are 78 inches long and arranged

radially on 12 wheels mounted on a cylindrical frame as shown in Figure 2-3. The sinusoidal motion of tines is provided by slider crank mechanism which is powered by a hydraulic motor.

Figure 2-1. Continuous canopy shake and catch (CCSC) harvester. (Photo courtesy of Ehsani and Sajith.)

Figure 2-2. Tractor-drawn canopy shake (TDCS) harvester. (Source: http://citrusmh.ifas.ufl.edu/images/history/current/025.jpg. Last accessed July, 2013.)

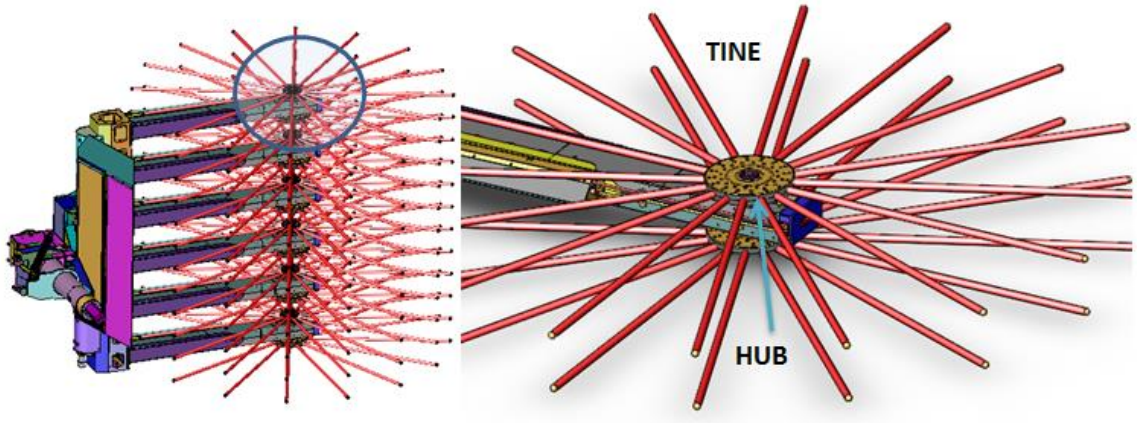


Figure 2-3. CAD model of a canopy shaker showing hub and tines. (Source: Courtesy of Oxbo International Corp.)

## Related Literature

In the past, analytical models have been developed for modeling tree crops and their interactions with various types of harvesting machines such as trunk shakers, limb shakers, canopy or foliage shakers and over-the-row harvesters. The dynamic characteristics of the tree limb and fruit system were predicted using various types of numerical techniques. Yung and Fridley (1975) used finite element methods to model a whole tree, including the fruit-stem system. They have developed three special finite elements to mathematically describe a tree system and have evaluated the natural frequencies, mode shapes, and dynamic internal stress of the complete tree structure for steady-state forced vibration. Rumsey (1967) modeled the fruit-stem system as an elastic beam with a concentrated load at one end and studied the effect of inertial forces due to mass of the fruits on the bending and shear of a limb model as a beam. Pestel and Leckie (1963) studied the vibration response of non-uniform beams using matrix methods. Later, the method of transfer matrices was applied by Rumsey (1967) to solve the forced response of non-uniform beams using finite element methods. Fridley and Lorenzen (1965) simulated the tree shaking by modeling the limb as a four-cell

cantilever beam. They used classical Euler Bernoulli beam theory to formulate partial differential equations. The equations were solved using finite element methods to predict the beam response when vibrated with constant force and varying frequency. Schuler and Bruhn (1973) applied Timoshenko beam theory with structural damping to formulate the differential equations for the dynamic response of the limbs. They concluded that rotary inertia has very little effect on the beam response while the presence of deflection due to shear had a significant effect.

Philips et al (1970) used Euler Bernoulli theory and the Rayleigh-Ritz method to formulate the forced vibration of tree limbs having variable cross-sections. Also, in their study, various methods to model secondary branches were investigated and a computer algorithm was programmed to determine the vibrational characteristic of limbs with secondary branches. Hussain et al. (1975), Ruff et al. (1980), Upadhaya and Cooke (1980), and Upadhyaya et al. (1980b) studied the fruit-stem system using Lagrange's equation. Upadhyaya et al. (1980b) used Galerkin approach to solve the partial differential equations formulated based on the Bernoulli-Euler beam theory. Transient response of the limb under base impact was solved using Newmark's direct integration method. Adrian and Fridley (1965) modeled the tree limbs as a single degree of freedom cantilever beam with viscous damping. Ebner and Billington (1968) investigated the response of an internally damped non-uniform beam under force vibrations. Hoag and Hutchinson (1970) studied the effect of proportional damping (internal damping proportional to stiffness or mass distribution), non-proportional damping (external damping proportional to the leaf distribution), and non-linear external

damping (or viscous damping) which is proportional to the $n^{th}$ power of the velocity of the system on the dynamic response of the tree limbs.

The objective quantification in the damage analysis using mechanistic models is widely employed in the earthquake science. The design based on mechanistic models was first reported by Park and Ang (1985) where they evaluated structural damage in reinforced concrete structures under earthquake ground motions. Veletsos and Newmark (1960) applied these concepts to formulate damage index in terms of ductility ratio defined as the ratio of the maximum deformation to the yield deformation. Lybas and Sozen (1977) has proposed a similar model to estimate the damage potential in structures using the ratio of the pre-yield stiffness to the secant stiffness corresponding to the maximum deformation. Roufaiel and Meyer (1987) defined a damage index based on the flexural flexibility, which is the ratio of the rotation to moment before and after earthquake and the ultimate flexibility. Powell and Allahabadi (1988) presented two concepts for damage assessment: one was based on demand versus capacity, and the other was on the degradation of structural properties. The demand vs. capacity assessment includes strength, displacement, deformation, and energy dissipation whereas a degradation concept uses degradation in stiffness, strength, energy dissipation capacity.

The numerical techniques for the optimization were developed and successfully employed in the structural design (Arora, 1995; Baier, 1977; Leitmann, 1977; Stadler, 1988 and 1992; Koski, 1979 and1980; Carmichael, 1980; Choi and Kim, 2005). The application of numerical techniques for the optimization of a structure has increased and gained popularity with the development of the finite element method (Kristensen and

Madsen, 1976; Pedersen and Laursen, 1983; Santos & Choi, 1989; Bathe, 1996; Kim, 2009). Many engineering problems in the structural design consist of more than one objective, thus require a special techniques. Marler and Arora (2004) described the main characteristics, advantages, and drawbacks of various numerical and random methods used to solve the multi-objective (MO) problems. Messac et al. (2003) provided a review and comparison of several MO algorithm based on numerical optimization. Das and Dennis (1997), Cheng and Li (1999), Das and Dennis (1998), and Messac and Ismail-Yahaya (2003) have respectively developed weighted- sum algorithm, compromise programing, normal boundary intersection method and normalized normal constraint method to find optimum designs in multi-objective optimization.

# CHAPTER 3
# DETERMINATION OF PROPERTIES OF CITRUS WOOD

The material properties of the wood were determined from the fresh samples cut randomly from the primary limbs of Valencia orange trees (Botanical name: *Citrus Sinensis*). The samples were machined to the sizes recommended by ASTM D143-09. The dimensions were measured at the two edges and at the center of specimen using electronic digital calipers of 0.0005 inch resolution. The mean values were used in the calculations of the wood properties. An electronic weighing instrument was employed for accurately weighing the samples. The average values of mechanical and physical properties of citrus wood were used in the numerical model.

## Materials and Methods

### Mechanical Properties

Six samples of wood were cut from the citrus trees growing at the University of Florida- CREC research orchard. The samples were machined to a size of - 1.5 in. x 1 in. x 18 in. A 3-point bending testing of the wood samples were performed using a Universal testing machine (UTM) (Series 313, Tabletop- 11,250 lb., Test Resources Inc, Shakopee, MN, USA). The samples were simply supported between the knife edges of the 3-point bending support as shown in Figure 3-1. The crosshead of the instrument was adjusted to come in proper contact to the top surface at the mid plane of samples. The load was applied continuously throughout the test at a rate of motion of movable crosshead of 0.1 inches per minute. The load cell of the instrument was set to continuously record the reaction force until the specimen fractured or failed to support a load of 50 lbf. The fracture due to static bending failure was identified as the appearance of brash or fiber delamination of the wood specimens. The load-deflection

data was acquired from each specimen using Test Resource R-series software (Test Resources Inc, Shakopee, MN, USA). The wood was assumed to be isotropic and homogenous and the mechanical properties were calculated from the load-deflection curve as discussed below.

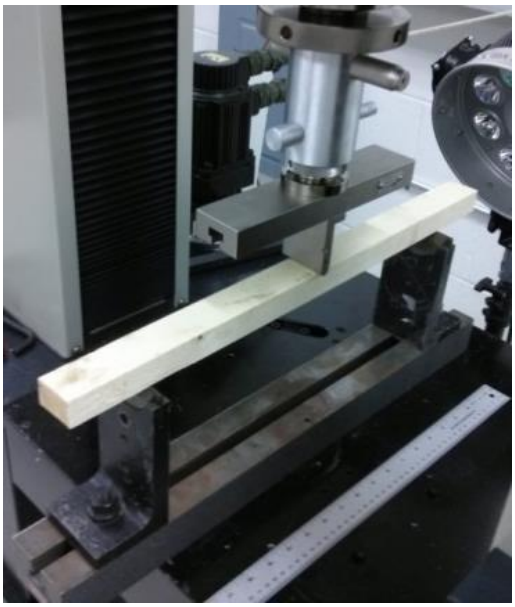

Figure 3-1. A three-point bending test of a citrus wood specimen. (Photo courtesy of S. K. Gupta.)

**Modulus of elasticity**

Elasticity implies that deformation produced by low stress is completely recoverable after the load is removed. The modulus of elasticity (*E*) was calculated from load-deflection $(P-\delta)$ curve of the specimens expressed as:

$$E = \frac{ML^2}{12I\delta} \tag{3-1}$$

where *M* is the bending moment, *I* is the moment of inertia, *L* is the length of the specimen, and $\delta$ is the deflection at the mid span of the specimen. For the 3-point bending test, the bending moment (*M*) is calculated as given in Equation 3-2.

$$M = \frac{PL}{4} \tag{3-2}$$

**Modulus of rupture**

Modulus of rupture (*R*) is equivalent to the fracture stresses and reflects the maximum load bearing capacity of a member in bending. It is an accepted criterion of strength for wood and is computed as:

$$R = \frac{3P_{max}L}{2bh^2} \tag{3-3}$$

where b and h are the width and the height of wood sample respectively.

**Stress at proportional limit**

The stress at the proportional limit ( $\sigma_{PL}$ ) is a stress proportional to the load at which the load-deflection curve is a straight line. The point at which $P - \delta$ curve is no longer linear is called the elastic limit and is expressed as:

$$\sigma_{PL} = \frac{3P_{PL}L}{2bh^2} \tag{3-4}$$

where $P_{PL}$ is the load at the proportionality limit.

**Work to maximum load in bending**

Work to maximum load in bending ($W_{ml}$) is the ability of wood to absorb shock with some permanent deformation. Work to maximum load is a measure of the combined strength and toughness of wood under bending stress. It is calculated as the total area under the load-deflection curve to the maximum bending load per unit volume of specimen as given in Equation 3-5 and is expressed in units of kJ per cubic meter.

$$W_{ml} = \frac{A}{bhL} \tag{3-5}$$

where A is the area under $P - \delta$ curve to maximum load.

## Physical Properties

### Volume and density

Three samples of citrus wood were cut from the bending specimen after the 3 point bending test. The weight of the samples was measured using an electronic weighing machine as shown in Figure 3-2 with an accuracy of 0.2%. The change in the pressure values obtained using an Ultra-Pycnometer 1000 (Quantachrome Corporation, Boynton Beach, FL, USA) as shown in Figure 3-3 were used to calculate the volume of the specimens and subsequently the density of the citrus wood. The instrument was calibrated before the experiments with a sphere of a known volume. The sample was placed in the cell and stream of helium is passed through the cell, sample and an additional chamber named $V_{added}$ of the instrument to purge air from the system. All the valves of the instrument then closed and the system was allowed to reach equilibrium. After reaching equilibrium, the valve allowing helium gas to enter the sample cell was opened. The sample cell was pressurized to a pressure approximately equal to that in the regulator of the UHP helium tank. Then the valve to the $V_{added}$ chamber was opened resulting in the increase of the total volume of system and thus, decrease in pressure since no further gas was admitted to the system and the temperature was maintained constant. Eliminating the 'nRT' – term from the ideal gas equations corresponding to two states results in an equation for which volume displaced by the sample can be calculated:

$$P_A(V_{cell} - V_{sample}) = nRT \quad (3\text{-}6)$$

$$P_B(V_{cell} + V_{added} - V_{sample}) = nRT \quad (3\text{-}7)$$

$V_{sample}$ is obtained by solving Equations 3-6 and 3-7.

$$V_{sample} = \frac{(P_A - P_B)V_{cell} - P_B V_{added}}{P_A - P_B} \tag{3-8}$$

Each sample was tested five times and the average value of density, calculated using Equation 3-9, was used in the numerical model.

$$\rho = \frac{Weight_{sample}}{V_{sample}} = \frac{(P_A - P_B)Weight_{sample}}{(P_A - P_B)V_{cell} - P_B V_{added}} \tag{3-9}$$

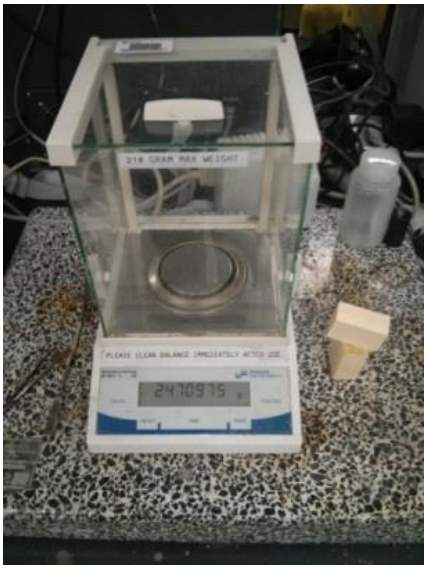

Figure 3-2. High precision electronic weighing scale. (Photo courtesy of S.K. Gupta.)


Figure 3-3. Ultra-Pycnometer to measure the actual volume of the wood samples. (Photo courtesy of S.K. Gupta.)

**Moisture content**

The moisture content of the samples was not required in the formulation of a numerical model but essential in validating the properties of the green citrus wood measured in laboratory experiments. As per Wilson (1932), most of the mechanical properties of wood such as modulus of rupture, the fiber stress at the elastic limit in bending, the flexural modulus, and the fiber stress at 3 % deformation; all vary with moisture content below the fiber saturation point and become invariant to the moisture above this point. Wangrad (1950) defines the 'fiber saturation point' of wood as the point where all the free water in the cell cavity has been removed, but cells are still fully saturated. For most tree species, the fiber saturation point lies between 25-30%. Thus, it is essential that the moisture content of samples used in the bending test should be more than the fiber saturation point in order to accurately simulate the physical phenomena using numerical model.

Nine samples were cut from the bending test specimen as shown in Figure 3-4. The weights of the samples were measured with an electronic weighing machine having an accuracy of ±0.01 grams. The samples were dried to a temperature of 105º C until any significant decrease in the mass was noticed: the mass of wood corresponding to this point is called oven-dry mass of wood. The moisture content of the specimen was determined from the loss in mass, expressed in percent of the oven-dry mass:

$$\text{Mositure content } (\%) = \frac{m_{wet} - m_{dry}}{m_{dry}} * 100 \qquad (3\text{-}10)$$

where $m_{wet}$ and $m_{dry}$ is mass of a green sample and oven dry sample of wood , respectively.

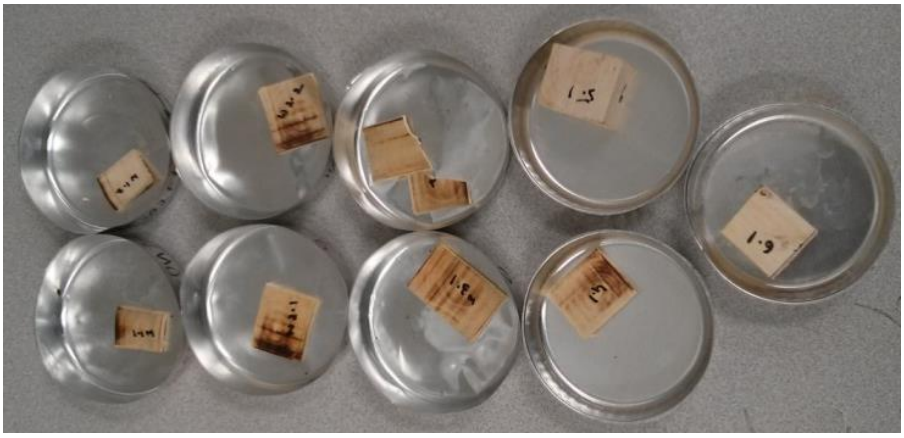

Figure 3-4. The wood samples of the Valencia orange used in the determination of moisture content. (Photo courtesy of S.K. Gupta.)

**Damping coefficient**

The dynamic responses of tree limbs unlike other mechanical structures are greatly affected by the amount and type of damping present in a system (Hoag and Fridley, 1971; Hoag, 1970). The amount of damping determines the amount of vibrational energy dissipated and the amount of energy transferred from the harvesting machine to the fruit bearing branches of a tree. Physically, the damping can be internal, i.e. inherent in the wood and bark, and/ or external due to air resistance. The viscous damping due to air drag on the secondary branches, twigs, leaves and fruits contribute significantly to the damping of the tree crops. The viscous damping is also mathematically convenient to model because it requires the formulation of linear second order differential equation only. Thus, equivalent viscous damping, which models the overall damped behavior of structural system as being viscous, was adopted (-Tompson, 1993). The damping is expressed in terms of damping ratio ($\zeta$) which is a percentage of the fraction of critical damping ($c_0$) as given in Equation 3-11.

$$\zeta = \frac{c}{c_0} \tag{3-11}$$

A system is said be under damped if $\zeta < 1$, critically damped if $\zeta = 1$, and overdamped if $\zeta > 1$. In all the above cases, the response of a system set into motion will eventually decay to zero with time except when ζ= 1. For a single degree of freedom (SDOF) under damped system subjected to an impulse of t=0 exhibits a response x(t) as shown in Figure 3-5 and decays exponentially as given by Equation 3-12.

$$x(t) = x_0 e^{-\varsigma w_n t} \sin w_d t \tag{3-12}$$

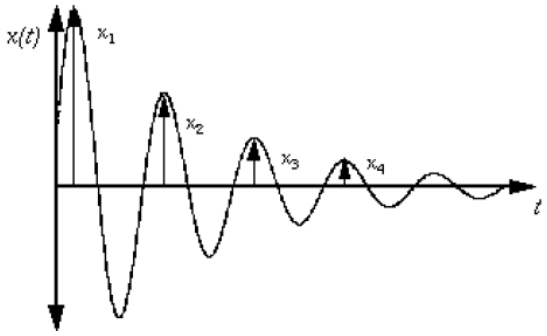


Figure 3-5. Under-damped response of a system having singe-degree of freedom.

The logarithmic decrement method measures the damping of a system as the rate of decay of response for consecutive cycles of the vibration referred as the log decrement (δ):

$$\delta = \frac{1}{n}\left(\frac{X_i}{X_{i+n}}\right) = \frac{2\pi\zeta}{\sqrt{1-\zeta^2}} \tag{3-13}$$

The damping ratio for the system is computed from the log decrement using Equation 3-14.

$$\zeta = \frac{\delta}{\sqrt{4\pi^2 + \delta^2}} \tag{3-14}$$

An experiment was setup in CREC research orchard to measure the damping of the tree limbs of citrus crop. The response of the tree limbs under dynamic testing was measured using an accelerometer (Horvarth & Sitkei, 2005; Chopra, 1995). Two limbs

each from the top, middle and bottom section of the citrus trees were selected and accelerometers (X250-2 Data logger, Gulf Coast Data Concepts LLC, Waveland, MS, USA) were installed on the tree limbs as shown in Figure 3-6. The tip of the limbs were displaced laterally to approximately 30 in. using an in-house mechanism and then released quickly to allow the limbs to vibrate naturally. The responses of the limbs were acquired using a accelerometer data logger and the experiments were repeated thrice for each limb. The damping ratio was estimated using logarithmic decrement method.

Figure 3-6. An accelerometer mounted on a primary limb of a citrus tree. (Photo courtesy of S.K. Gupta.)

## Results and Discussion

### Mechanical Properties

A summary of the mechanical properties calculated from the 3-point bending test as shown in Figure 3-7 is listed in Table 3-1. The mean ($\mu$) and coefficient of variation (*CV*) of mechanical properties were calculated from the load-deflection curves using Equations 3-1 to 3-4. The elastic modulus and modulus of rupture was only used in the formulation of a numerical model. The other two properties provide the knowledge of elastic behavior and shock absorbing capacity of the citrus wood. Figure 3-8 shows the best fit curve and the load deflection curve of 3-point bending test of the citrus wood

samples. The values of the mechanical and physical properties of the citrus wood computed in this research is significant and can also be used in other or future research involving citrus wood.

Figure 3-7. A citrus wood specimen under 3 –point flexural bending. (Photo courtesy of S.K. Gupta.)

Table 3-1. Summary of the mechanical properties of the green citrus wood.

| Mechanical Property | Mean (μ) | Coefficient of variation (CV) |
|---|---|---|
| Flexural modulus (GPa) | 8.5 | 11% |
| Modulus of rupture (MPa) | 67.3 | 4% |
| Stress at proportional limit (MPa) | 45.3 | 13% |
| Work to maximum load in bending ($kJm^{-3}$) | 193.2 | 28% |

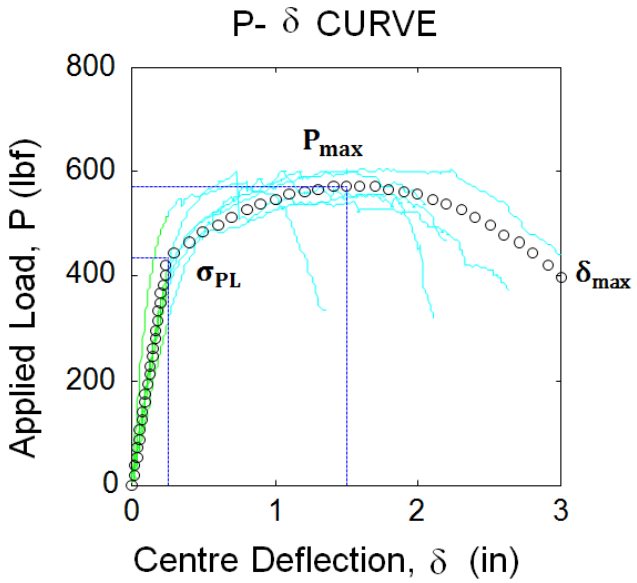


Figure 3-8. The best fit and load-deflection curves of green citrus wood specimens.

**Physical Properties**

A summary of the physical properties measured are reported in Table 3-2. The mean and coefficient of variance are reported for each physical quantity. It was found that the moisture content of the samples of the bending test was more than the fiber saturation point, thus validating the measured mechanical properties of the citrus wood are invariant to moisture content and thus, can be used in numerical formulation. Figure 3-9 shows the under-damped response of a citrus limb when displaced and allowed to vibrate naturally. The average value of damping ratio of citrus limbs was found to be approximately 11. The magnitude of the damping ratio measured by Hoag et al (1970), Hoag et al. (1969), and Horvath and Sitkei (2004) for limbs of other species was found to be close to that of citrus limb. Thus, this suggests that the damping in tree limbs is highly dependent on the air drag on fruits, leaves and twigs (viscous damping) rather than the material property of the wood (structural damping). The friction coefficient between wood and steel was not measured but taken from the research work of McKenzie (1968).

Table 3-2. Summary of the physical properties of the green citrus wood.

| Physical Property | Mean (μ) | Coefficient of variation (CV) |
|---|---|---|
| Density (g/cc) | 1.451 | 2.8% |
| Moisture content (%) | 42.4 | 14.15% |
| Damping ratio (%) | 10.78 | 24.70% |
| Friction | 0.36 | 20.97% |

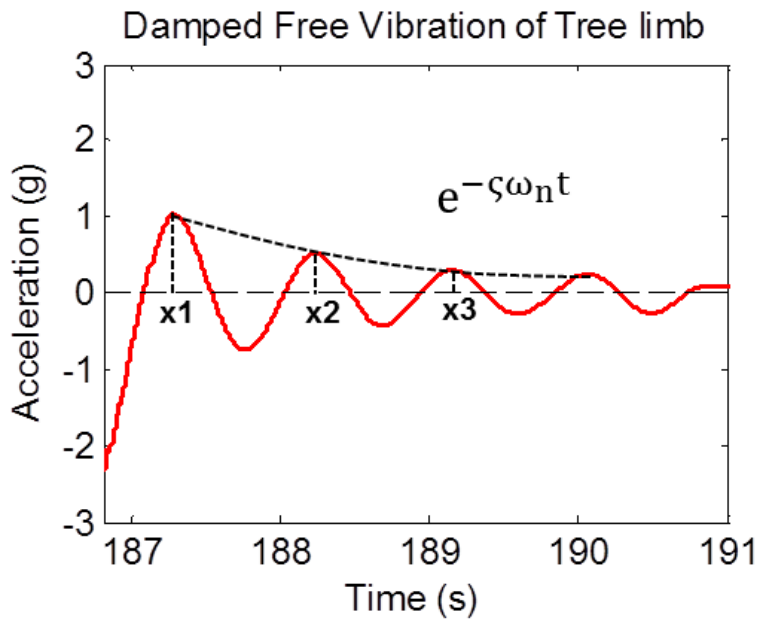

Figure 3-9. Response of a citrus limb measured using an accelerometer.

# CHAPTER 4
# MODELING OF TREE LIMBS

The statistical information based on the data collected from the citrus trees was used to predict the configuration of a citrus limb prototype. A meta-modeling technique (or response surface methodology) was adopted to predict the sectional properties of a tree limb prototype. The tree limbs used to design the limb prototypes were first classified in the multiple sets or zones based on the vibration transmissibility. The vibration transmissibility of a tree limb is defined as the ability of the limb to transmit energy from the input point of excitation to the fruit bearing regions and is a function of mass, stiffness and damping which in turn depends on the configuration of the tree limb (spatial coordinates and location of fruit bearing region) and material properties of wood (O'Brien, 1983). The tree limbs having different vibration transmissibility requires different shaking inputs to effectively detach fruits from them. Therefore, a vibratory harvester equipped to provide multiple values of shaking force effectively minimize the tree damage and maximize the fruit removal. However, only three distinctive sets of machine configuration providing three different shaking forces were proposed to minimize the computational and manufacturing cost. The tree limbs classified in the three zones are analyzed separately to obtain the three set of optimum machine configurations.

## Material and Methods

### Interpolating Technique: Continuous Piecewise Cubic Hermite Interpolation

Piecewise cubic Hermite interpolating polynomial (PCHIP) is an interpolation technique which is based on piecewise polynomials. These are shape preserving piecewise cubic polynomials whose first order derivatives are continuous and are used

to generate smooth curves passing through a series of data points. The polynomial function P(x) on the interval $x_k \le x \le x_{k+1}$, expressed in terms of local variables $s = x - x_k$ and $h = h_k$ is:

$$P(x) = \frac{3hs^2 - 2s^3}{h^3} y_{k+1} + \frac{h^3 - 3hs^2 + 2s^3}{h^3} y_k + \frac{s^2(s-h)}{h^2} d_{k+1} + \frac{s(s-h)^2}{h^2} d_k \quad (4\text{-}1)$$

$$P(x_k) = y_k, P(x_{k+1}) = y_k, \\ P'(x_k) = y_k, P'(x_{k+1}) = y_k, \quad (4\text{-}2)$$

The inbuilt MATLAB function "*pchip*" was used to construct hermit interpolation passing through data points using the polynomial given in Equation 4-1 and satisfying the conditions given by Equation 4-2.

**Surrogate Technique: Polynomial Response Surface (PRS)**

The PRS approximation is a meta-modeling technique which uses polynomial functions to predict the best fit for the data when the true response is unknown (Viana, 2009). The parameters of an approximate polynomial function are obtained by the least squares method. A second degree polynomial model is expressed as given below:

$$y = \beta_0 + \sum_{i=1}^{k} \beta_i x_i + \sum \sum_{i<j}^{k} \beta_{ij} x_i x_j + \sum_{i=1}^{k} \beta_{ij} x_i^2 \quad (4\text{-}3)$$

$$e = y - y \quad (4\text{-}4)$$

where $x = (x_1, x_2, \ldots x_k)$, $\beta$ is a vector of constant coefficients obtained by minimizing the residual error ($e$) between the prediction ($\hat{y}$) and true response ($y$).

**Residual Analysis: Cross-Validation Error**

Cross-validation error is the error at a data point when the surrogate is fitted to a subset of the data points not including that data point (Allen, 1971; Khuri, 1996). A vector of error ($e_p$) is obtained by fitting the surrogate to all the n-1 points and evaluating

the error at that point. This vector of error is called the cross validation error or PRESS vector which stands for “Prediction Residual Sum of Squares”. The measure used to calculate the predictive capability of a response surface is called $PRESS_{RMS}$, which is root mean square of PRESS error and expressed as:

$$e_{pi} = \frac{e_{ri}}{1 - Eii} \tag{4-5}$$

$$E = X(X^T X)^{-1} X^T \tag{4-6}$$

$$PRESS_{RMS} = \sqrt{\frac{1}{n} e_p^T e_p} \tag{4-7}$$

where *Eii* is the diagonal matrix of the idempotent matrix *E* and *X* is vector of data points.

**Experimental Setup: Acquiring Data for the Statistical Model**

Numerical technique to find the dynamics response of a tree limb requires the prediction of the limb configuration. The limb configuration would then be used to model a tree limb as a truncated conical elastic beam. The true response of a limb having infinite degree of freedom is approximated by modeling the limb as a finite set of elements using numerical methods. The information about the distribution of secondary branches and fruits must be included in the numerical model as they considerably modify the response of the tree limbs by changing the overall mass and dissipative properties of the primary limbs. The model and setup presented here are designed in view of its use with FEM; however, it can be extended to any other numerical technique.

A field experiment was set up to find the following information for modeling and analyzing a tree limb using numerical method.

- Spatial co-ordinates of the primary tree limbs
- Sectional property distribution along the length of the tree limbs
- Distribution of secondary branches on the primary tree limbs
- Distribution of the fruits on the primary tree limbs

The tree information were collected from 54 tree limbs of 10 randomly chosen medium sized trees of the Valencia orange variety (*Citrus sinensis*) from the research orchard located at University of Florida- Citrus Research and Education Center from 28 February to 08 Mar 2013. A referenced system based on the Cartesian coordinates with the origin at the trunk base was employed to measure the limb data as shown in Figure 4-1. It was observed that medium size citrus trees generally have 6 to 8 scaffold branches or primary limbs and measuring each and every branching node in detail would be tedious and time-consuming. Therefore, a procedure was laid out which uses the following information to construct the tree limbs models: the length of the limb segments between two branching nodes, the angle from the Z-axis (called vertical angle), and the angle from the Y-Z plane (called the horizontal angle).

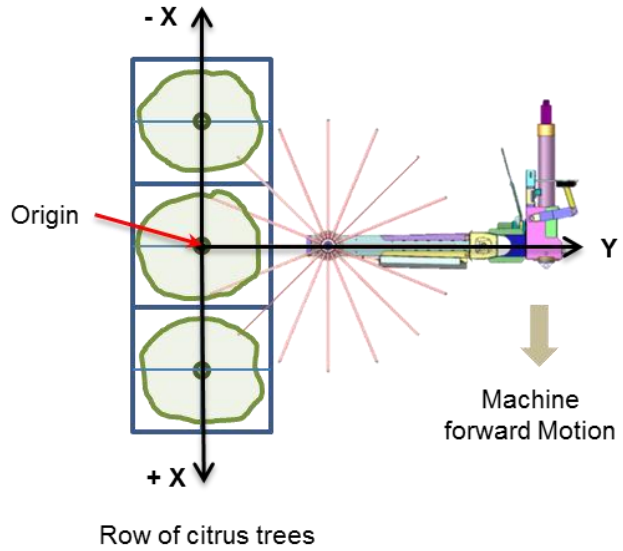


Figure 4-1. Interaction of a canopy harvester with a row of citrus trees.

**Procedure**

The following procedure was adopted during the measurement of the tree limb properties:

- The primary tree limbs were discretized into the nodes (junction where a branch split into two or more branches) which are either the point of origin of secondary branch or other primary limb.
- The length, vertical angle, and horizontal angle of each segment of a primary limb were measured.
- The sectional perimeter of the limb segment was measured near the branching nodes and at the center of the segment.
- The overall length, vertical angle, and horizontal angle of all the secondary branches were measured.
- The sectional perimeter at the origin, center point, and at the tip of the secondary branches was measured.
- The fruits on the secondary branches and on the last segment of the primary limbs were counted.

**Assumptions**

The following assumptions have been made to predict the configuration of the statistical limb prototypes.

- The section of the branch was assumed to be circular.
- A branch originating from a primary limb having base diameter more than 1 in. and less than 2.5 in. was considered as a secondary branch.
- The twigs, stems, and leaves were not considered explicitly in the numerical model but their effect on the response of the limbs was modeled using viscous damping.

The tines of a canopy shaker interact with the tree limbs in the plane Y-Z as shown in Figure 4-2. Therefore, to simplify the limb model and economically optimize the machine parameters using finite element methods, the measured three dimensional data of tree limbs were projected on the Y-Z plane.

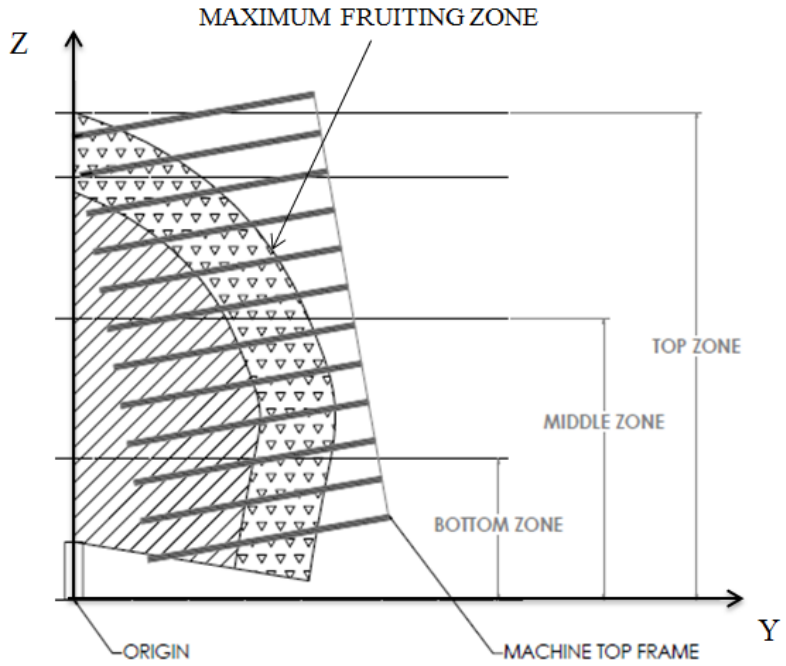

Figure 4-2. Interaction of a canopy shaker with a citrus canopy on YZ plane.

**Classification of Primary Tree Limbs**

The coordinates of the branching nodes of the tree limb were generated from the measured data using a program designed in MATLAB 2011 (Math Works, Natick, MA, USA). The tree limbs were constructed and classified into three distinctive sets based on the spatial configuration of their fruit bearing region (which is generally the last segment of a primary limb having maximum number of the fruits). Mathematically, Equation 4-8 was used in the classification of the limbs in the three zones, referred to as top, middle and bottom zone:

$$\begin{aligned} &\text{TOP ZONE} && = H_{\text{Fruit bearing region}} > 90'' \\ &\text{MIDDLE ZONE} && = 45'' \leq H_{\text{Fruit bearing region}} \leq 90'' \\ &\text{BOTTOM ZONE} && = H_{\text{Fruit bearing region}} \leq 45'' \end{aligned} \tag{4-8}$$

where $H_{Fruit\ bearing\ region}$ is the height of the fruit bearing region of a tree limb measured from the ground level.

**Prediction of Spatial Coordinates of Limb Prototypes**

Since a canopy shaker interacts more or less with the tree limbs in the plane of the tines (Y-Z) as shown in Figure 4-2, it is therefore numerically economical to model a tree limb as a 2-dimensional finite element. Thus, the three dimensional data were projected on the Y-Z plane and projected data were used to construct the individual limbs. However, it is also feasible to model the tree limbs as three dimensional finite element by adding few more parameters but improvement in results will barely able to justify the computational expenses in modeling and analyzing the limbs. The interpolating polynomial, *PCHIP*, was used to create the smooth and continuously differential curve passing through measured data points to model the tree limbs. The interpolated limbs were then used to predict the spatial co-ordinates of the tree limb prototypes or representatives. The following procedure was adopted in the modeling of a limb prototype which is a non-physical model of the tree limb.

- An axis (Y or Z) corresponding to the maximum value of coordinate of any tree limbs in a zone was chosen as the primary axis for that zone and the other axis is referred as the secondary axis.
- Equally spaced points were generated between minimum and maximum value of primary axis-coordinate for each zone. In this research, 30 predefined values of coordinate were chosen along the Y-axis for the top zone and along the Z-axis for the middle and bottom zone.
- The parameters of *PCHIP* interpolating function of a tree limb were determined from the coordinates of the branching nodes of that tree limb.
- The value of secondary axis-coordinate of a limb corresponding to a predefined value of primary axis-coordinate was predicted using the PCHIP parameters calculated for that limb.
- Assuming normal distribution of the secondary axis-coordinates of all limbs in a zone, the $5^{th}$, $25^{th}$, $50^{th}$, $75^{th}$, and $95^{th}$ percentiles values were predicted for that zone.

- The five limb prototypes were constructed for each zone by plotting the values of predefined primary axis coordinate and the secondary axis- coordinate values taken each from the 5$^{th}$, 25$^{th}$, 50$^{th}$, 75$^{th}$, and 95$^{th}$ percentiles of the limb data.

**Sectional Properties of Limb Prototypes**

Perimeter values measured along the tree limbs were used to calculate the diameter of the limbs assuming that the limbs to have a circular cross-section. It was observed that the diameter of a limb at any section decreases as the distance of that section from the limb origin increases. Also, the sectional diameter along the length of a tree limb varies depending on the spatial orientation in a tree structure. Thus, it is concluded that diameter of a limb at any cross-section depends on the actual distance and vertical angle of that cross-section from the limb origin as labeled in Figure 4-3. The actual distance of a branching node and vertical angle of the position vector joining that branching node from the limb origin were measured for all limbs and used to predict the sectional diameter of limbs expressed mathematically as:

$$D = f(L_n, \beta_n) \tag{4-9}$$

where $Ln$ is the actual length of nth branching node from the limb origin and $\beta$ is the vertical angle of the position vector joining the $n^{th}$ node with the limb origin.

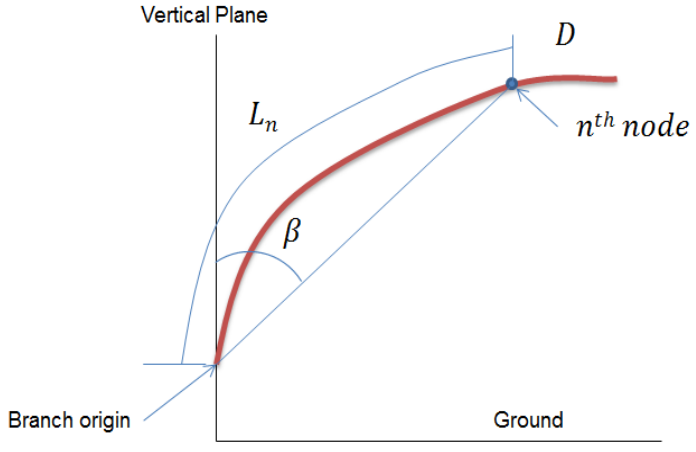


Figure 4-3. Showing a tree limb having diameter at any branching node as a function of the length and the angle of that node from the limb origin.

A meta-model technique (or response surface method) was used to construct regression models to predict the diameter at any section of a tree limb. A polynomial response surface was employed to fit the measured data and predict the diameter of a limb prototype. The surrogate toolbox (Viana, 2010) was used to create a response surfaces with full and stepwise regression. The response surfaces were selected based on the indicator of predictive performance and indicator of quality of fit: cross-validation error ($PRESS_{RMS}$) and adjusted correlation coefficient ($R_a^2$), respectively. The response surface with full regression involves all coefficient terms of polynomial response surface whereas stepwise only involves coefficient terms having $|tstatistics| \geq 1$.

**Distribution of Secondary Branches**

The secondary branches modify the dynamic response by changing the overall mass and dissipative properties of a primary tree limb. The overall length, circumference and coordinates of origin of secondary branch were measured. Based on field observation and data analysis, it was found that around 4-5 secondary branches radiate from the primary limb at the intervals of approximately 20-25 inch. This information was used to add secondary branch effect in the numerical analysis based on some assumptions and idealizations.

**Distribution of Fruits on the Primary Limbs**

Including the effect of fruits is pivotal in determining the dynamics response of a fruit bearing limb under vibratory excitations. The fruits act as an inertia damper and attenuate the dynamic responses of the limbs. The distribution of fruits on a primary limb can be classified in two distinctive groups:

- Fruits attached to the secondary branches of a primary limb
- Fruits attached to the last segment called fruit bearing region of a primary limb

### Fruits on secondary branches

The number of fruits on the secondary branches was counted. The average mass of a citrus fruit-0.186 kg was used to compute the total mass of fruits on the secondary branches of the primary limb.

### Fruits in fruit bearing region

A fruit bearing region of a primary limb is the region near the tip of the limb where the limb branches into large number of small twigs and bears large number of fruits. The information regarding the configuration and the number of fruits in the fruit bearing region is significant as numerical models are evaluated in these regions of the tree limbs to optimize the parameters of a canopy shaker.

## Results and Discussions

The tree limbs were classified into three zones based on their spatial distribution. The models were formulated to predict the spatial configuration and properties of the limb prototypes. The statistical information from the tree limbs data were analyzed and used to predict the distribution of secondary branches and fruits along the primary limbs.

### Primary Tree Limbs Classified in Three Zones

The tree limbs classified in three distinctive sets have similar dynamic responses owing to its property, distribution of secondary branches, and configuration of fruit bearing region. Figure 4-4 shows a three-dimensional representation of the citrus limbs measured to predict the limb prototypes.

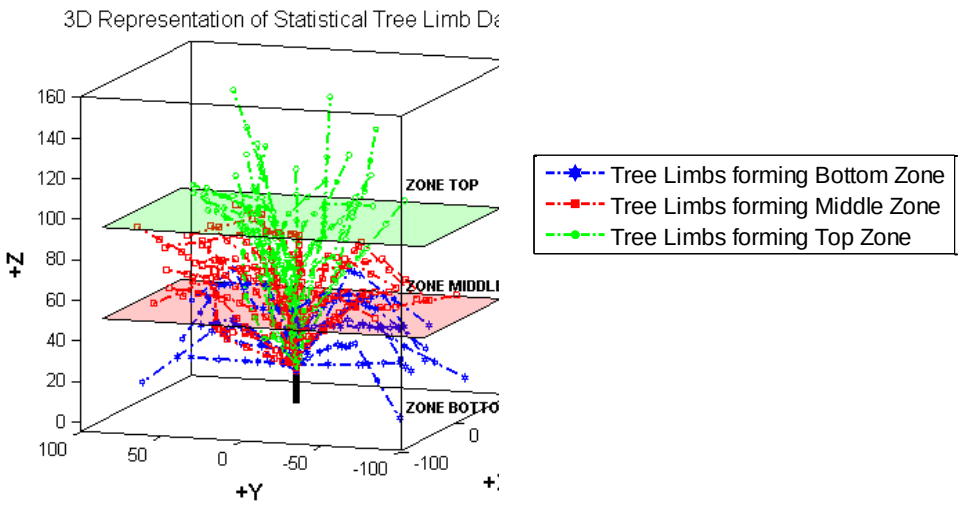


Figure 4-4. Three-dimensional view of the tree limbs of citrus and their classification in three distinctive zones.

**Spatial Coordinates of Limb Prototypes**

Figure 4-5 shows the tree limbs segregated into the three distinctive sets corresponding to the three zones in a citrus tree canopy. Modeling of the tree limbs in the numerical analysis is time consuming and expensive: therefore sets of representative or prototypes of tree limbs were defined for each zone. These representatives of limbs were modeled and analyzed in finite element analysis to optimize a canopy shaker.

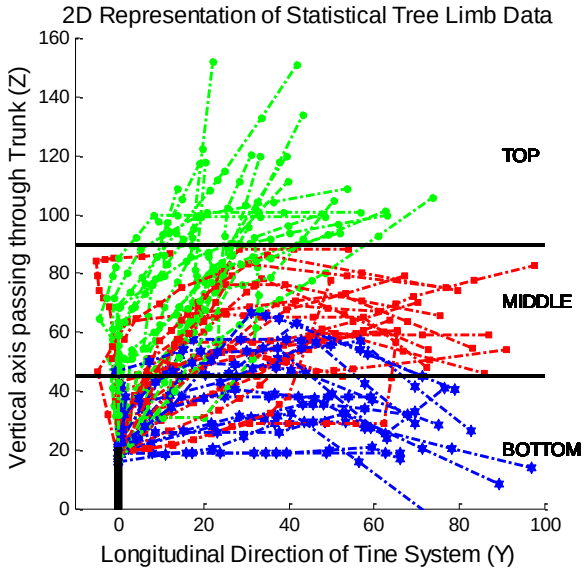


Figure 4-5. Tree limbs classified in three sets and plotted on the plane Y-Z.

Figures 4-6 and 4-7 show the spatial distribution of the limb prototypes capturing the 5$^{th}$, 25$^{th}$, 50$^{th}$, 75$^{th}$, and 95$^{th}$ percentiles of the tree limbs in the top, middle, bottom zone. The dynamic response of five limb prototypes in each zone was used to appropriately balance the cost of optimization and variability in the tree limbs. The dashed lines show *PHCIP* - interpolated limbs passing through measured data points represented by circular markers. It is noticed that the limbs in the top zone radiate at an angle of 0º-20º and grow straight up to a height of 120-130 inches and then curve down slightly because of the weight of the fruits. However, for the middle zone, the limbs are thick, long and hang down gradually after growing approximately 4-5 feet. The limbs in the bottom zone originate and grow near the ground and are comparatively thinner, shorter and hang down steeply at the tip.

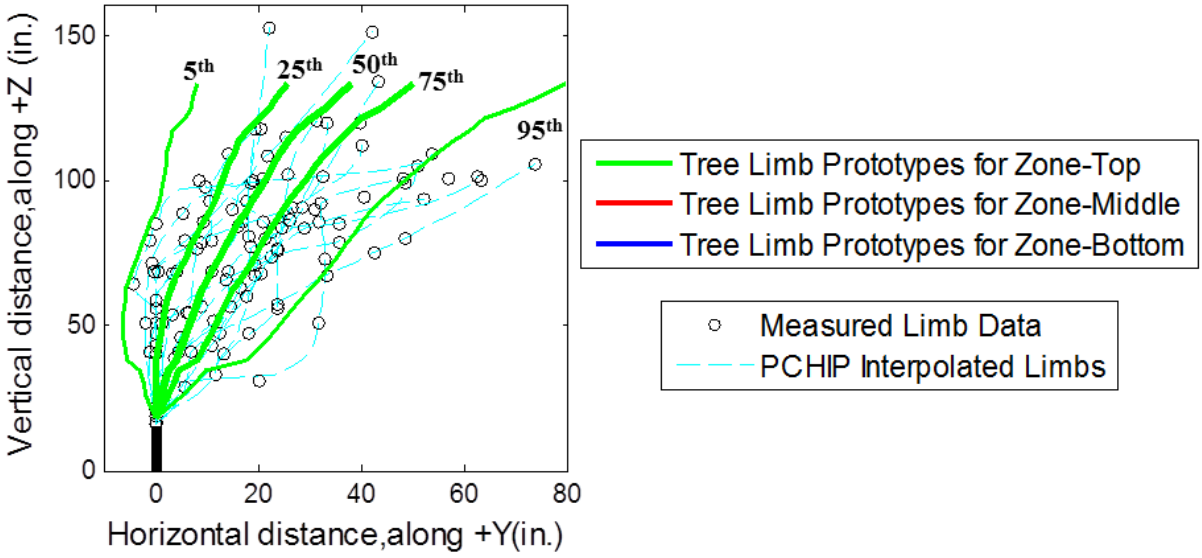


Figure 4-6. Spatial modeling of the limb prototypes for the top zone.

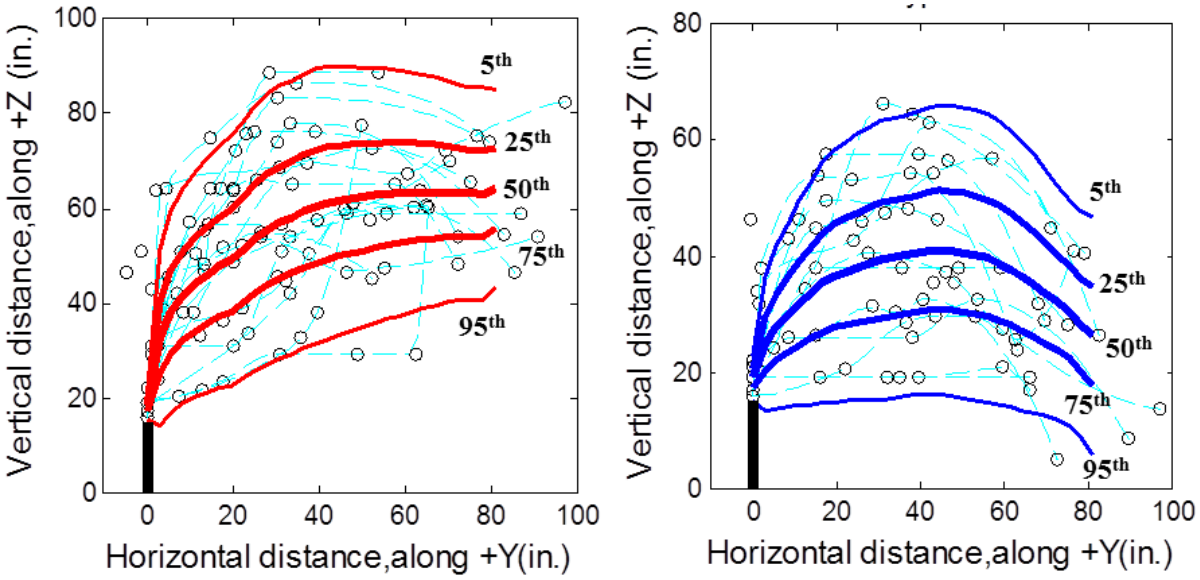


Figure 4-7. Spatial modeling of the limb prototypes for the middle and bottom zone.

Figure 4-8 compares the spatial distribution of the mean and 90% distribution of the tree limbs for the three zones. The tree limbs from number of trees can be statistically interpreted to form a hypothetical tree structure consisting of the tree limb prototypes. The shakers parameters will be optimized based on the interaction of the machine with the limbs of this hypothetical tree rather than any actual tree.

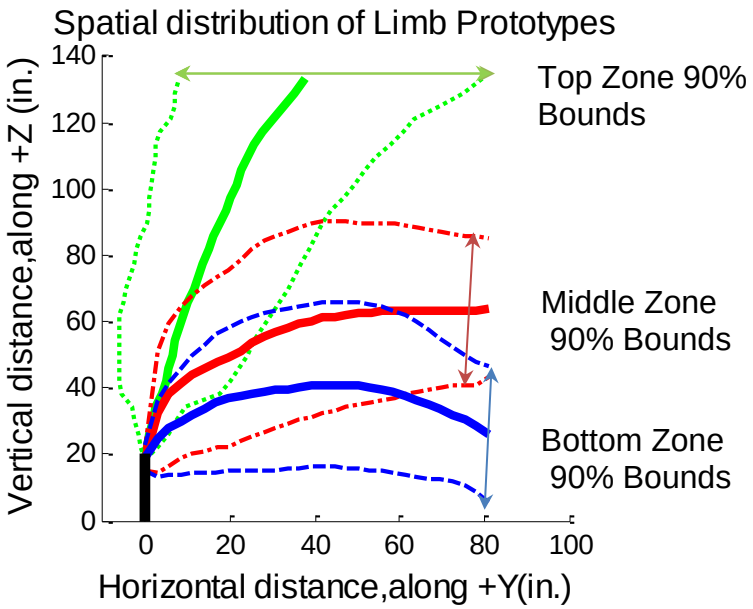


Figure 4-8. Spatial distribution of the limb prototypes of a hypothetical tree.

Figure 4-9 shows the interaction of the shaker and hypothetical tree limbs. Thus, the tines which interact with the top zone of limbs will have a different configuration based on the amount of shaking force required by those limbs to minimum damage and maximum fruit removal as compared to the tines in the middle and bottom zones.

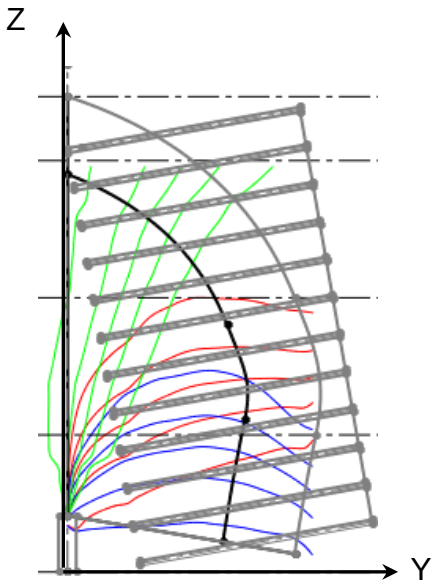


Figure 4-9. Interaction of a canopy shaker with the limb prototypes of a hypothetical tree.

**Error Analysis and PRS model for limbs in the top zone**

Various metal-models were formulated for predicting the sectional diameter of the limbs. Table 4-1 shows the error norms used in determining the best fit meta-model. The third-degree polynomial response surface with stepwise regression was chosen as the best fitting model for the limbs of top zone because it has the lowest value of cross validation error and highest value of adjusted R-square. The parameters of the model are given in Equation 4-10. Figure 4-10 graphically compares the measured diameter for the limbs of top zone shown as marker with a prediction from the meta-model shown as contour plot.

Table 4-1. Meta-models to predict the diameter of limbs of the top zone.

| Error norms | PRS-linear full | PRS-quadratic stepwise | PRS-cubic stepwise | PRS-quartic full |
|---|---|---|---|---|
| % $PRESS_{RMS}$ | 9.4 | 9.1 | 8.8 | 8.9 |
| % Adjusted R-Square | 86.5 | 87.3 | 88.2 | 88.0 |

$$D_{top} = 3.9309 - 0.1044\beta + 0.0026\beta^2 + 0.0011\beta L - 4.8262\times10^{-4}L^2 - 2.844\times10^{-5}\beta^2 L + 2.015\times10^{-6}L^3 \quad (4\text{-}10)$$

where the units of the diameter (D), the length (L) and the angle (β) are in inches and degrees.

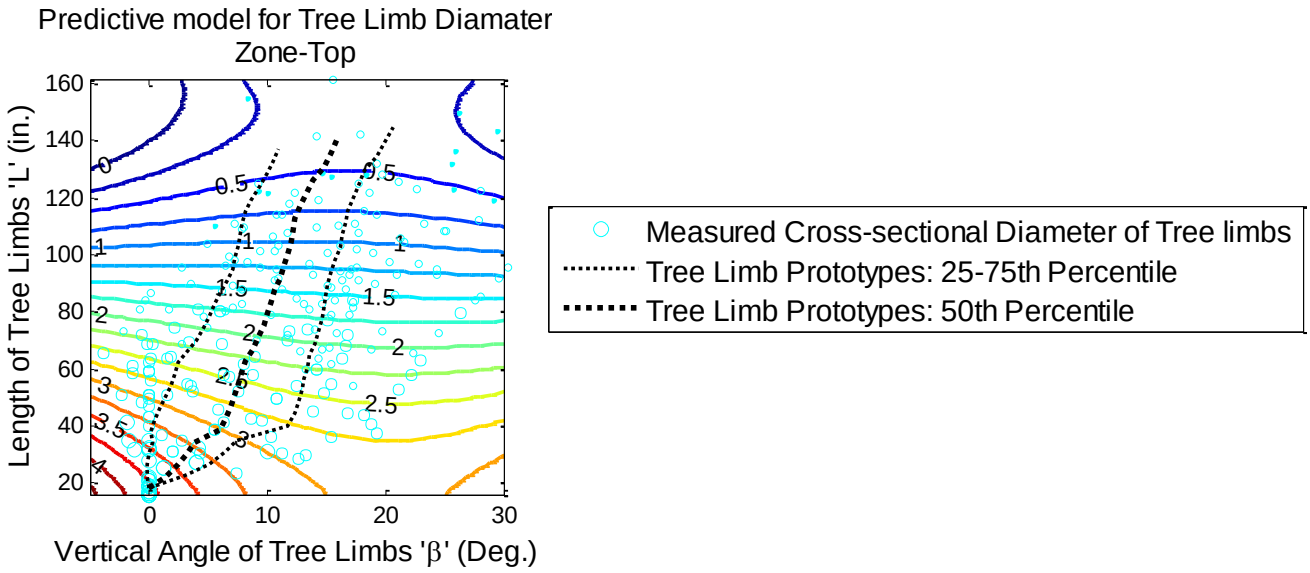


Figure 4-10. Contour plot to predict the sectional diameter of a limb in the top zone.

**Error Analysis and PRS model for limbs in the middle zone**

With the lowest value of $PRESS_{RMS}$ and highest value of adjusted coefficient of determination, the three-degree polynomial with a full regression was used to predict the diameter of the limbs of middle zone. The error norms in the models for predicting the sectional diameter of the limbs of the middle zone are tabulated in Table 4-2. The parameters of this model are given in Equation 4-11.

Table 4-2. Meta-models to predict the diameter of limbs of the middle zone.

| Error norms | PRS-linear | PRS-quadratic | PRS-cubic | PRS-quartic |
|---|---|---|---|---|
| | full | stepwise | full | full |
| % $PRESS_{RMS}$ | 10.6 | 10.0 | 9.9 | 10.0 |
| % Adjusted R-Square | 80.7 | 82.9 | 83.2 | 83 |

$$\begin{aligned} D_{middle} &= 3.7172 - 0.0647\beta - 0.0049L + 7.6411\times10^{-4}\beta^2 \\ &+3.7797\times10^{-4}\beta L - 2.9258\times10^{-4}L^2 + 8.8872\times10^{-6}\beta^3 \\ &-1.9091\times10^{-5}\beta^2 L + 6.1894\times10^{-6}\beta L^2 + 4.1649\times10^{-7}L^3 \end{aligned} \quad (4\text{-}11)$$

**Error Analysis and PRS model for limbs in the bottom Zone**

Similarly, for the limbs of the bottom zone, the three-degree polynomial response surface with a full regression is the best predictive model among all models considered. The error norms are compared in Table 4-3. The parameters of best model are given in Equation 4-12.

Table 4-3. Meta-models to predict the diameter of limbs of the bottom zone.

| Error norms | PRS-Linear | PRS-Quadratic | PRS-Cubic | PRS-Quartic |
|---|---|---|---|---|
| | Full | Stepwise | Full | Full |
| % $PRESS_{RMS}$ | 9.6 | 8.9 | 8.8 | 8.9 |
| % Adjusted R-Square | 81.1 | 84.0 | 84.7 | 84.5 |

$$\begin{aligned} D_{bottom} &= 2.5841 - 0.0645\beta + 0.0357L + 0.0013\beta^2 \\ &-6.8739\times10^{-4}\beta L - 3.9263\times10^{-4}L^2 + 5.2031\times10^{-6}\beta^3 \\ &-2.0646\times10^{-5}\beta^2 L + 1.6265\times10^{-5}\beta L^2 - 1.6425\times10^{-6}L^3 \end{aligned} \quad (4\text{-}12)$$

Figure 4-11 graphically compares the measured data shown as the maker with predicted values from the best fitting model as a contour plot for middle and bottom zones. The spatial distribution of the 25$^{th}$, 50$^{th}$, and 75$^{th}$ limb prototypes are shown in L-β coordinates. The information about the spatial co-ordinates and the sectional

diameters of the limb prototypes obtained from these models was used to model the limbs in finite element analysis.

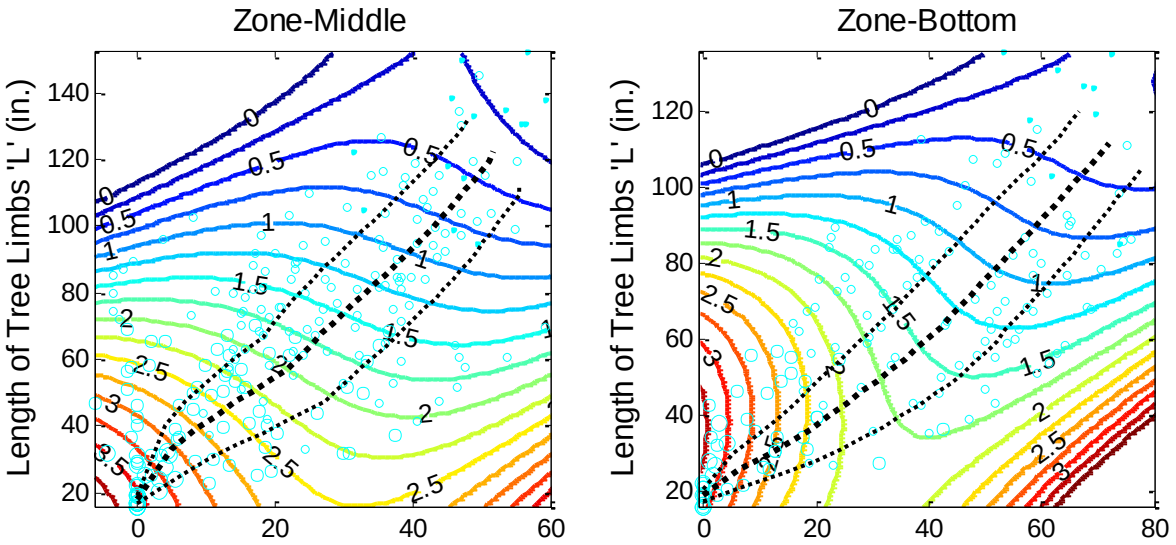


Figure 4-11. Contour plot to predict the sectional diameter of a limb in the middle and bottom zone.

**Distribution of Secondary Branches and Fruits on the Primary Tree Limbs**

Modeling secondary branches and performing dynamic simulation is expensive, thus numerical model was simplified by aggregating mass of the secondary branches and fruits on the primary limbs.

**Distribution of secondary branches**

Figure 4-11 shows the distribution of the mass of secondary branches on the primary limbs of the top, middle, and bottom zones. It is concluded from Figure 4-12 and from the field observations that the secondary branches are thick and long near the limb origin and become thinner near the tip of the limb. It was observed that secondary branching generally starts at a distance of 20-40 in. and ceases at a distance of 100-120 in. from the limb origin for the top and middle zones and 80-100 in. for limbs in the bottom zone. On an average, the limbs of the top and the middle zone radiate five

secondary branches whereas limbs in the bottom zone owing to shorter length bifurcate to only four secondary branches. The average mass of secondary branches was taken over every 20 in. segment of a primary limb and model as a lumped mass on the primary limb in FEM analysis. Table 4-4 provides the information about the average mass of secondary branches in each zone. This indicates that the primary limbs of the top and the middle zone not only have more secondary branching but also weigh 12% and 18 %, respectively, more than the mass of the secondary branches in the bottom zone.

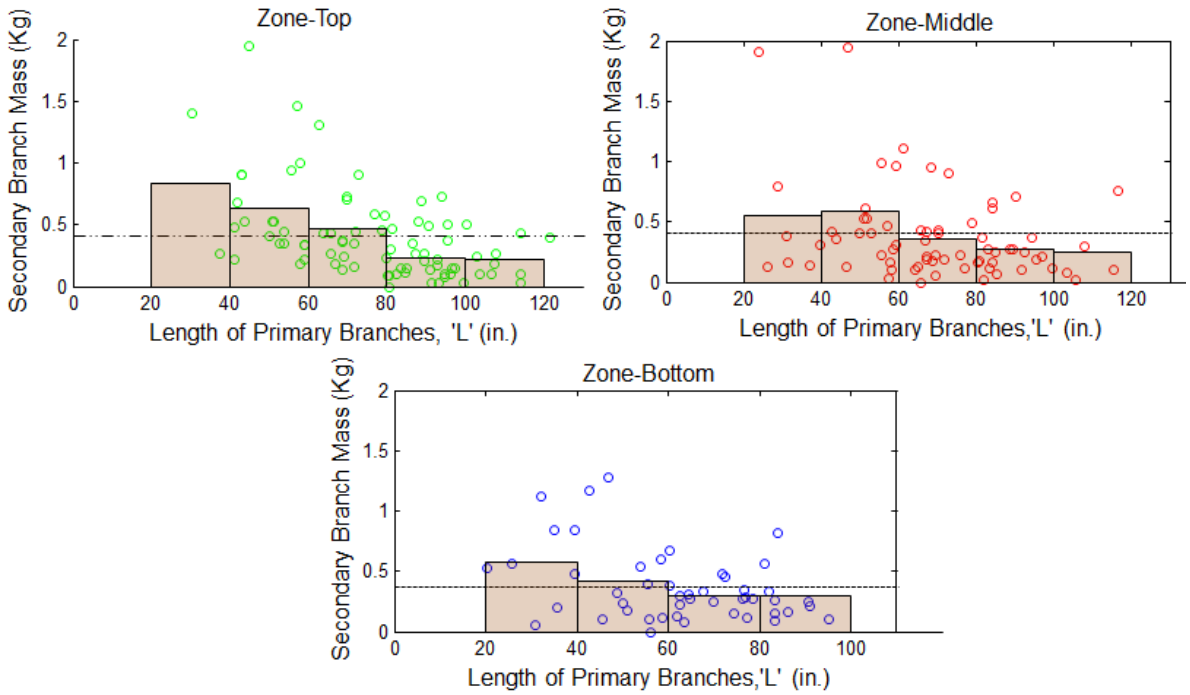


Figure 4-12. Distribution of mass of a secondary branch for all three zones.

Table 4-4. Average mass of the secondary branches in three zones.

| Zone | Mean (kg) |
|---|---|
| Top | 0.4036 |
| Middle | 0.4236 |
| Bottom | 0.3602 |

**Distribution of fruits on primary limbs**

The mass of fruits attached to the secondary branches was modeled by aggregating them at the location of secondary branches on the primary limbs. Figure 4-13 shows the distribution of fruits attached to the secondary branches of the primary limbs for three zones. Table 4-5 provides the average number of fruits attached to the secondary branches. There is no subtle distinction in the distribution of fruits on the secondary branches radiating from the primary limbs for the three zones. However, the average number of fruits attached to the secondary branches in the top and the middle zones are respectively 30% and 21% more than that of bottom zone.

Table 4-5. Average number of fruits on the secondary branches.

| Zone | Mean |
|---|---|
| Top | 12.6 |
| Middle | 11.7 |
| Bottom | 9.7 |

Table 4-6 provides the information to configure the fruit bearing region of a primary limbs for each zone. The information regarding this region is significant because the numerical model would be evaluated at these regions to optimize the shaker. It was noticed that the length of the fruit bearing region is approximately the same for almost all limbs irrespective of zone; however, the distance of fruiting zone from the limb origin is maximum for top and minimum for the bottom zone. The maximum fruiting occurs in the middle zone with an average fruit count of 41% and 13% more than that of top and bottom zone, respectively.

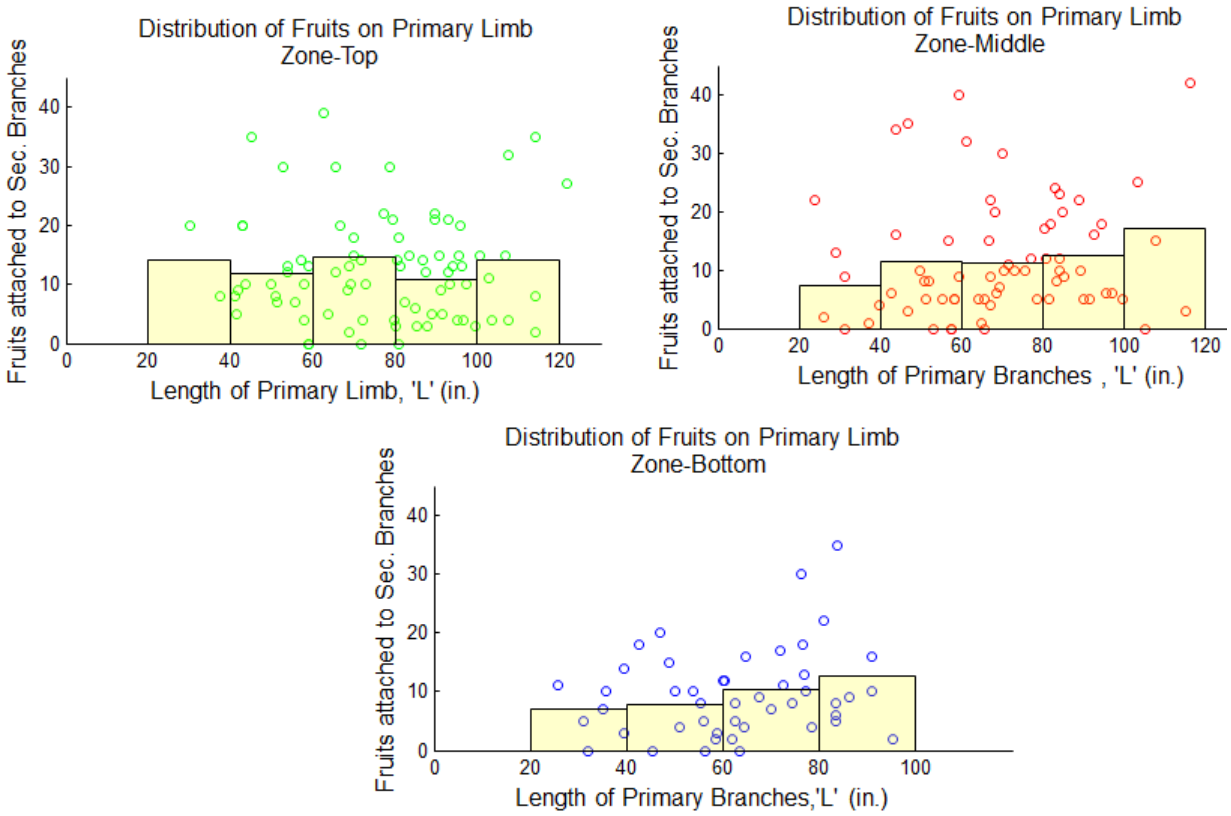


Figure 4-13. Distribution of the fruits attached to the secondary branches.

Table 4-6. Configuration of fruit bearing region of a citrus tree canopy in three zones.

| Zone | Distance from limb origin | Length of fruit bearing region | Fruit counts |
|---|---|---|---|
| Top | 132 | 30.6 | 14.4 |
| Middle | 124 | 32.8 | 20.3 |
| Bottom | 112 | 32.6 | 17.9 |

The information regarding the modeling of limb prototype describes in Chapter 4 is vital in the formulation of numerical model. Various models and idealization formulated here will be used for the optimization of the mechanical harvester in Chapter 7.

# CHAPTER 5
# FORMULATION OF FINITE ELEMENT ANALYSIS

The non-linear dynamic behavior of the tree limbs was analyzed based on the continuum model. The finite element methods were employed to find the response of limbs under the impact load of the tines of a shaker. The responses extracted from numerical analysis of the tree limb prototypes were used in the formulation of mechanistic models for the optimization of a harvester. Figure 6-1 shows the schematic of the process involved in the optimization. The finite element modeling of the interaction between the tree limb and the tine of a shaker will be discussed in Chapter 5.

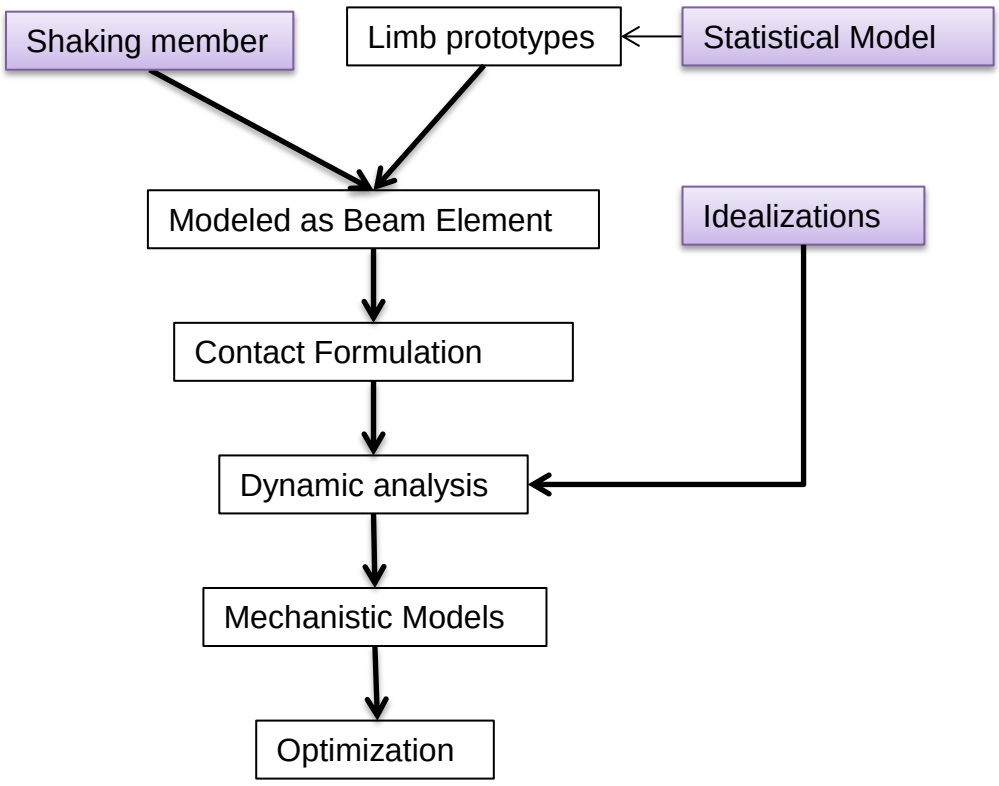


Figure 5-1. Flow chart of process involved in finite element analysis based optimization of canopy shaker.

## Finite Element Model

### Product

The non-linear dynamic response of a tree limb under the excitation force was solved using ABAQUS/Standard. Abaqus input code files were written and integrated with a program in MATLAB to simulate limb prototypes. The Abaqus input code is composed of a set of commands to perform analysis using finite element methods and output analysis results. The software Abaqus was chosen because of the convenience rather than limitation. Other numerical method or analysis software can be used.

### Geometric Modeling

The limb prototypes were modeled as truncated conical three-dimensional cantilever beams. The configurations of the limb prototypes were defined for FE Modeling as discussed in Chapter 4. The limb finite element model was meshed with160 two-node linear beam elements (B31). The sectional properties of the limb finite element models are defined from the meta-models developed in Chapter 4. The tines of a canopy shaker were modeled as three-dimensional beams composed of 100 two-node linear beam elements (B31). The sectional properties of tines were defined as discussed in Chapter 7. Figure 5-2 shows the typical configuration of a limb and a tine in Abaqus.

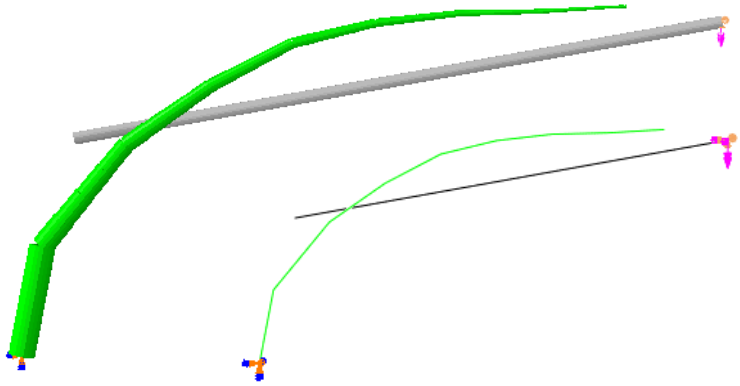

Figure 5-2. Finite element model of a tree limb and a tine modeled as beam element (shown with section and without section).

As discussed in Chapter 4, the secondary branches and fruits were idealized and model as lumped mass on the primary limb to minimize the cost of computation. The mass of secondary branches and fruits were computed and distributed on the limb prototypes as discussed in Chapter 4. Figure 5-3 shows 50th percentile limb prototype of the middle zone lumped with the mass of secondary branches and fruits.

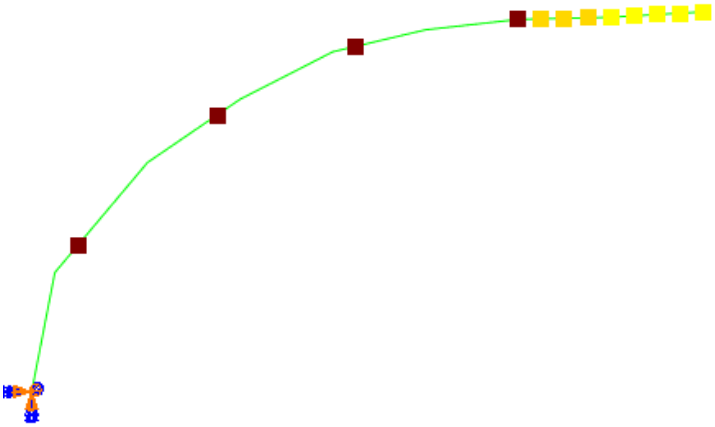

Figure 5-3. Finite element model of a tree limb prototype with secondary branches (brown marker) and fruits (yellow marker) modeled as the lumped mass.

**Material Model**

The isotropic linear elastic material model was considered for both the limb and the tine models. The branch properties were set based on the experiments performed on the green citrus wood as discussed in Chapter 2. The value of Poisson ratio was taken from the studies done by Savary and Ehsani (2010) on citrus wood. The material property of the tine of a shaker was considered as a design variable and will be discussed in Chapter 7.

**Damping Model**

Rayleigh's hypothesis was used to introduce damping in the model. Rayleigh damping is composed of the two parameters as given below:

$$[C] = \alpha[M] + \beta[K] \tag{5-1}$$

where M, K, and C are the mass, stiffness and damping matrices of system, respectively. The parameters $\alpha$ and $\beta$ is mass and stiffness proportional damping of the system, respectively.

**Mass proportional damping (α).** The 'α' factor defines the damping contribution proportional to the mass matrix of an element. The damping forces are caused by the absolute velocities of the nodes of a system. The resulting effect of this damping would be like a model moving through a viscous fluid and motion of any point in the model triggers damping forces.

**Stiffness proportional damping (β).** The β factor defines damping proportional to the elastic material stiffness. A damping stress ($\sigma_d$ ) proportional to the total strain rate is introduced, using the following formula:

$$\sigma_d = \beta D \varepsilon' \tag{5-2}$$

where $\dot{\varepsilon}$ is strain rate and D is initial (Hyperealstic and Hyperfoam Materials) or current elastic stiffness (for all other materials). For linear analysis stiffness proportional damping is exactly the same as defining a damping matrix equal to β times the stiffness matrix.

In this research, mass proportional damping was used to account for the overall damping in the tree limbs. It is appropriate to use this hypothesis because the branch damping ratio is largely correlated to the mass of the main branches, secondary branches and fruits (Moore, 2002). The β coefficient in the damping expression was neglected because the responses of the limbs are predominately in the first mode of vibration (Mayers, 1987). The stiffness-dependent part of damping is effective only for high frequency modes. The parameters of the damping were calculated so that the

mean of the damping ratio measured in the experiments were equal to the damping ratios computed from the test simulations. A value of 87.25 was set for $\alpha$ based on the parametric studies of the 50$^{th}$ percentile limb prototypes of each zone. However, $\beta$ was set to a low value of 0.0001 rather than null value to prevent the numerical noise.

## Contact Formulation

The surface interaction between the limb and the tine which decides the dynamics response of a system when they are in contact was defined using Abaqus tube-to-tube element (ITT3).

### Tube-to-Tube Elements

The tube-to-tube are slide line contact elements used to model the finite-sliding interaction between two tubes or rods like structures which contact each other along their either inner or outer surfaces.

### Master-Slave Assignment

Master surface was defined by the slide line constructed using the nodes of a tine model, whereas the slave surface was defined by the contact elements attached to the nodes of a branch model at the impact region. Figure 5-4 shows FE model of a branch-limb system with the master and slave surfaces. In this setup, the nodes of the branch are constrained not to penetrate the slide line defined on the tine.

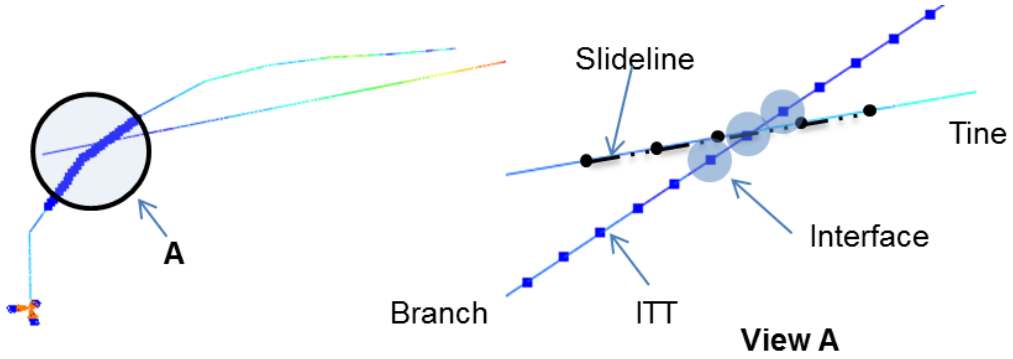


Figure 5-4. Modeling interaction between a tine and a tree limb in Abaqus.

**Contact Property Assignment**

**Pressure-overclosure relationship**

Soft contact was defined which allows small amount of penetration at constraint location. Softened contact was used to resolve the numerical difficulties in applying contact conditions by creating a soft thin layer on one or both surfaces.

The pressure-over closure relationship was prescribed by using a tabular piecewise-linear law. The softened contact was specified in terms of over closure (or clearance) versus contact force as shown in Figure 5-5. The values given in Table 5-1 were chosen based on the observation during the bending test of the citrus wood samples and numerical testing so as to not significantly compromise the accuracy of analysis.

Table 5-1. Pressure-Over closure relationship.

| kPa | Mm |
|---|---|
| 0 | 0E+00 |
| 3.0E-11 | 1E-08 |
| 0.02902 | 1E-02 |
| 0.1275 | 5E-02 |
| 0.22 | 1E-01 |
| 1.5 | 5E-01 |
| 13 | 1E+00 |

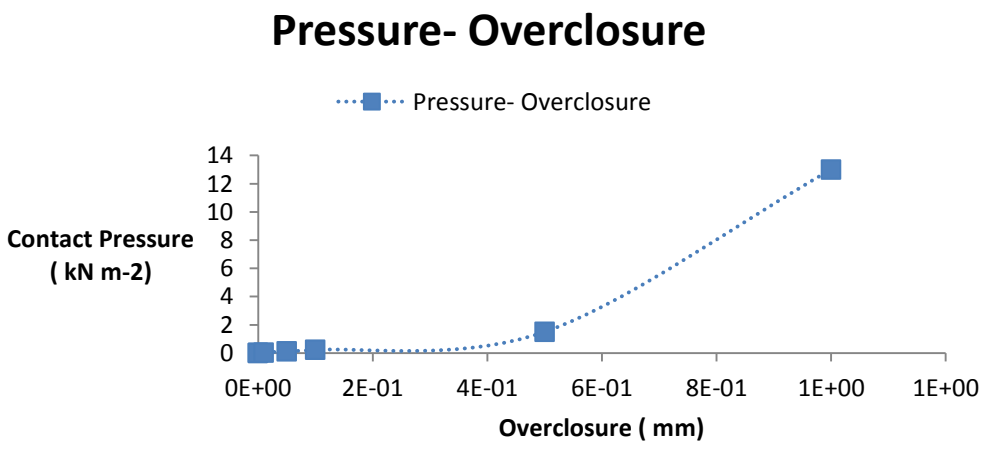


Figure 5-5. Pressure-overclossure relationship used in the contact formulation.

**Friction model**

Classical isotropic coulomb friction model with a coefficient of friction of 0.36 was used to model the frictional behavior of the limb-tine system.

**Contact Constraint Enforcement Method**

Direct methods based on Lagrange multiplier was used to enforce pressure-oveclosure constraint. However, the frictional constraint was enforced using Abaqus penalty method. The choice of method was made to achieve maximum accuracy and minimum convergence time.

**Contact Interface**

The radial clearance between the tine and the limb prototype at point of impact was defined using Equation 5-3

$$radial\,clearance = -(r_{tine} + r_{branch}) \tag{5-3}$$

## Dynamic Analysis

**Analysis Method**

Non-linear dynamic response of a branch was analyzed using an implicit direct integration. The implicit direct integration uses implicit operators to integrate the equations of motion. The integration operator matrix is inverted at each increment to solve the second order non-linear differential equations of dynamic motion. The dynamic motion of a system is expressed as:

$$M\ddot{q} + C\dot{q} + Kq = F(\dot{q}, q, w, t) \tag{5-4}$$

where M, C, K and F is mass matrix, damping matrix, stiffness matrix, and vector of nodal forces of system respectively. $q \in \Re^p$ is a set of generalized coordinates used to represent the configuration of the system.

Hilber-Hughes-Taylor operator is widely used implicit operator defined based on the parameters β and γ and solved using following equations:

$$q_{n+1} = q_n + h\dot{q}_n + \frac{h^2}{2}[(1-2\beta)\ddot{q}_n + 2\beta\ddot{q}_{n+1}] \quad (5\text{-}5)$$

$$\dot{q}_{n+1} = \dot{q}_n + h[(1-\lambda)\ddot{q}_n + \lambda\ddot{q}_{n+1}] \quad (5\text{-}6)$$

where h is an integration step size. The equations 5-5 and 5-6 are used to describe the time $t_{n+1}$ using Equation 5-4. The equation of motion at time $t_{n+1}$ is given as:

$$M\ddot{q}_{n+1} + C\dot{q}_{n+1} + Kq_{n+1} = F_{n+1} \quad (5\text{-}7)$$

Equations 5-5, 5-6, $q_{n+1}$, and $\dot{q}_{n+1}$ are function of the acceleration $\ddot{q}_{n+1}$ which is solved implicitly to find the solution of Equation 5-7.However, to counter the high frequency oscillation and to achieve A-stability, Hilber et al. (1977) induces the numerical damping into the system of equations by defining one more parameter ($\alpha$) defined as:

$$M\ddot{q}_{n+1} + (1+\alpha)C\dot{q}_{n+1} - \alpha C\dot{q}_n + (1+\alpha)Kq_{n+1} - \alpha K\dot{q}_n = F(t_{n+1})$$
$$\textit{where} \quad (5\text{-}8)$$
$$t_{n+1} = t_n + (1+\alpha)h$$

As studied by the Hughes (1987), HHT is stable and achieve second order accuracy when

$$\alpha = \left[\frac{-1}{3}, 0\right]$$

$$\gamma = \frac{1-2\alpha}{2} \qquad \beta = \frac{(1-\alpha)^2}{4} \quad (5\text{-}9)$$

The value of α, β, and γ was taken as -0.05, 0.275625, and 0.55 respectively in dynamic simulation using Abaqus.

**Loading and Boundary Conditions**

The branch was fixed at its base whereas the tine was subjected to sinusoidal vibration defined by frequency (*v*) and amplitude (*a*) as shown in Figure 5-6. The operating parameters such a frequency and amplitude were chosen as the design variables for the optimization of a shaker. The values of these parameters are discussed in Chapter 7. The forward motion of the canopy shaker and rotation of hub were also considered to accurately model the physical phenomena. Based on the information from citrus growers and studies done by Roka et al. (2008), it was found that the canopy shaker travels at the speed of approximately 0.5 miles per hour (or ~ 200 trees per hour) down a row of medium size trees and harvest upto 95% of mature fruits. Field observation and analyzing the video of the canopy shakers, it was found that the tine were allowed to interact with a citrus canopy for approximately one second and during that process, hub rotates at a speed of approximately one cycle per minute. Thus, the tine was subjected to a forward speed of 0.223 m/s and an angular speed of 0.105 rad/sec in the numerical model.

The limb and tine were allowed to interact in numerical model for one second with a maximum step time increments set to 0.0005 second. The results were extracted and used to compute mechanistic index required for the optimization of a shaker.

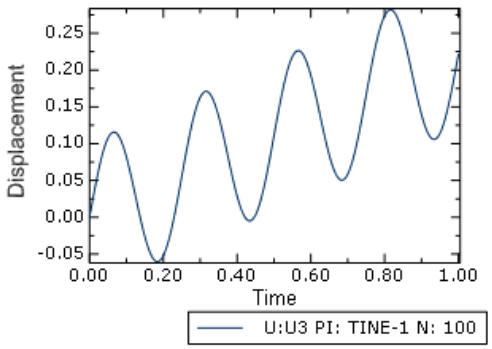


Figure 5-6. Prescribed displacement to the tines of a canopy shaker.

## Finite Element Model Verification and Validation

The tree limb prototypes used to optimize the shaker are non-physical tree limbs which are derived from the statistical data. Therefore, it is impossible to verify the FE model experimentally using limb prototypes because of the uncertainties associated with a structure of biological origin. An alternative must be devised to verify the parameters of finite element model so as to accurately simulate the physical phenomena. Thus, a small scale setup was developed which employed the same vibratory mechanism as used in a canopy shaker to provide the excitation force to the tree limbs. The dynamic response of the tree limbs was measured in terms of longitudinal normal strain and acceleration and compared with the FE simulations.

### Material and Methods

The laboratory test equipment utilizing a slider crank mechanism was built in-house as shown in figure 5-7. An electric motor powers the piston of the test equipment to oscillate the tine up and down with a stroke of 1 in. The supply voltage of the test equipment was adjusted using a voltage regulator to provide four different frequencies: 2.4cps, 3.8cps, 5.1cps, and 6.5 cps. The dynamic response of a branch was measured using strain gauges and accelerometers mounted at the selected test locations on the branch specimen. The configuration of the tine and branch used in the experiments are as follows:

### Tine

Galvanized coated electric metallic tube (EMT), 11/16 in. OD, and wall thickness 0.0625 in., 28 in. length and weighing ~0.7 lbs.

**Branch**

A clear branch specimen was cut from the tree of Valencia variety of orange growing at University of Florida- CREC research orchard. The total mass of the laboratory test specimen was ~ 0.85 lbs. The branch specimen was 70 in. long and has maximum diameter of 21/32 in. which reduced to 17/16 inches at the tip of branch. During the experiment the branch specimen was fixed horizontally with maximum diameter end clamped to solid frame using adjustable clamp as shown in Figure 5-8.

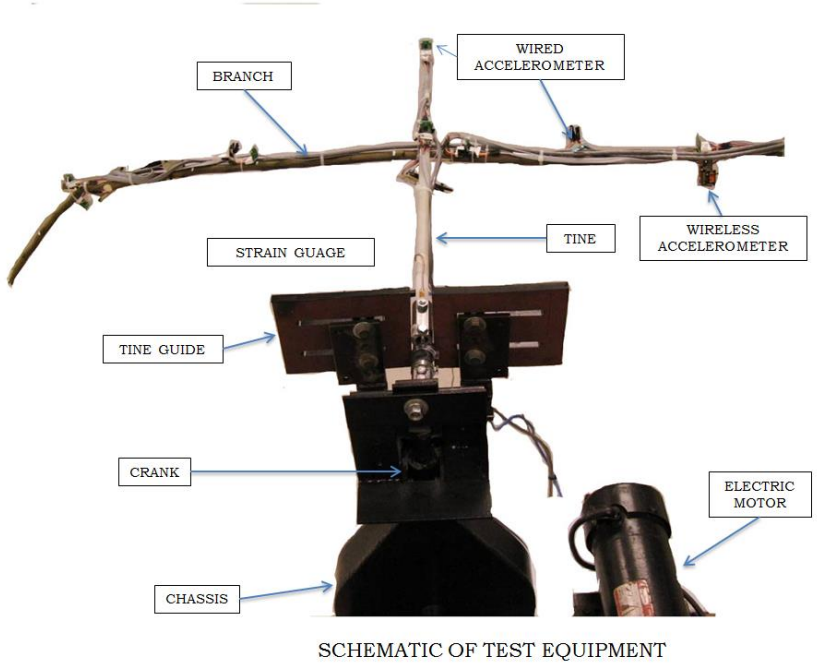


Figure 5-7. Schematic of a laboratory test equipment used to validate the FE model parameters. (Photo courtesy of S. K. Gupta.)

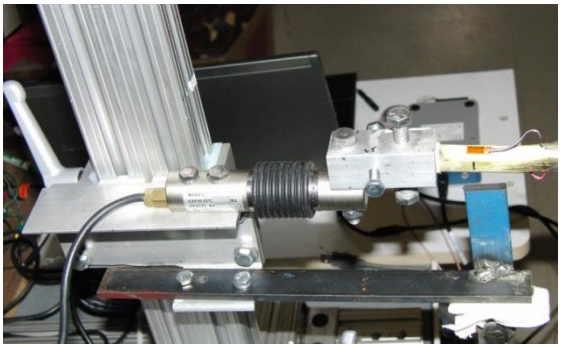

Figure 5-8. Branch specimen fixed to the solid frame with a bracket and a clamp. (Photo courtesy of S. K. Gupta.)

**Acceleration acquisition**

A set of accelerometers (Tri-axis, Model MMA7260Q, Freescale Semiconductor Incorporated, Austin, TX, USA) shown in Figure 5-9 were fixed at test locations of 30 inches and 60 inches from the fixed end of the branch specimen. The data were acquired using compact data acquisition system (Model NI 96211, National Instruments Inc., Texas, and USA). A LabVIEW program was designed as given in Figure A-1 (Appendix-A) to acquire acceleration data from the accelerometers. The sampling frequency for acquiring the acceleration responses of the branch specimen was set to 100 samples per second. The acceleration was computed using formulas as given below:

$$Acceleraton, a = \left( \frac{Sensor\ readingvalue - 0g\,Value}{Senstivity\ of\ the\ accelerometer} \right) \times 9.8\, ms^{-2} \qquad (5\text{-}10)$$

The output voltage range of the accelerometer is 0 - 3.3 V. The 0 g value is reading of accelerometer at zero acceleration. Theoretically, the 0g value is 1.65V; however, this value might have change from sensor to senor, so the accelerometer reading at rest was used as 0 g values. The mean of the first 50 reading of the accelerometer was used as 0g value of that sensor. The sensitivity of 0.2V/g based on 6g setting of the accelerometer was taken for computing acceleration of the branch.

Figure 5-9. MMA7260Q Accelerometer for sensing acceleration. (Source: http://www.robotshop.ca/Images/big/en/sfe-mma7260q-triple-axis-accelerometer.jpg. Last accessed July, 2013)

**Strain acquisition**

Strain gauges (350 Ω, Micro-Measurements, Wendell, NC, USA) as shown in Figure 5-10 were installed near the fixed end of branch specimen to record the strain developed due to dynamic bending of the branch specimen. The strain gauges were installed on both the top and bottom surface of the branch to continuously record tensile and compressive longitudinal strains. The LabVIEW Virtual Instrument (National Instruments Inc., Texas, USA) was designed to communicate between strain gauge and DAQ (Data Acquisition system). The LabVIEW program used to acquire strain data is provided in Figure A-2 and A-3. The data was acquired at the sampling rate of 1000 Hz using quarter bridge strain gage module (Model NI 9236, National Instruments Inc., Texas, USA).

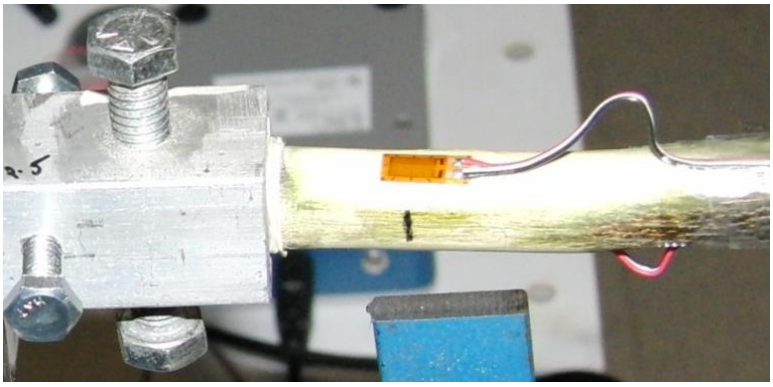

Figure 5-10. A strain gauge installed on the top and bottom surface of the branch specimen. (A photo courtesy of S.K. Gupta)

The branch and tine were installed to form the cross shape assembly as shown in figure 5-7. The tine was allowed to impact the branch at the two sets of locations: 7 inches from tine's free end and 20 inches from branch's fixed end; and 7 inches from tine's free end and 35 inches from the branch's fixed end. The experiments were conducted at both the impact locations with varying vibrating frequencies of 2.4, 3.8, 5.1, and 6.5 cps.

## Simulation

The branch specimen used in the laboratory experiment was modeled with a finite element model. The branch and tine were modeled as an elastic beam element and their mechanical and physical properties were defined in the FE model. The interaction of the branch and the tine was modeled using the tube-to-tube contact element. The FE parameters similar to the parameters described for the FE analysis of tree limb prototypes were set in the simulation of laboratory experiments. The simulation results were computed using Abaqus/Standard and compared with the experimental results.

## Results and Discussion

The values of acceleration and strain used to define objective functions were computed and compared with experiments to validate the FE model. Figure 5-11 shows the comparison of strain computed from the FE model with the experimental results. The regression line for root mean square of longitudinal strains in the branch specimen computed for all loading conditions has a slope of 0.7394, an intercept of 0.0002, and R-square of 93.93 %

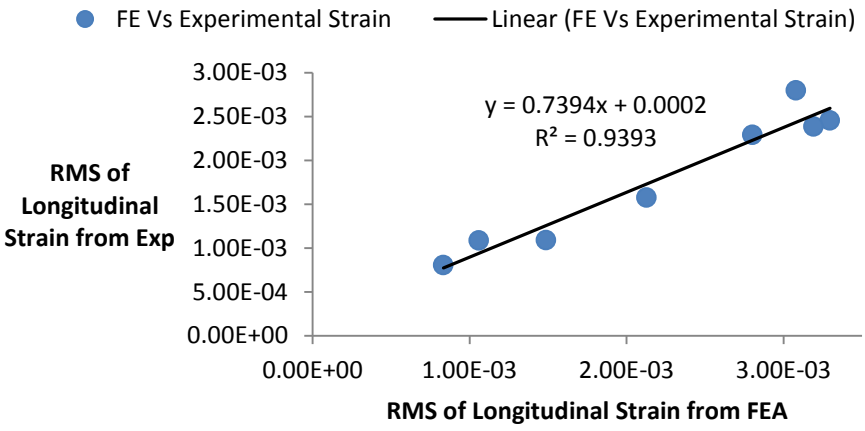


Figure 5-11. Comparison of RMS of maximum strain of branch specimen obtained from FEA and experiments.

The root mean square of acceleration of the branch at test locations was calculated and compared using FE simulations and experiments. The regression line between FE and experiments has a slope of 0.9392, and intercept of 5.19, and R-square of 85.05% as shown in Figure 5-12.

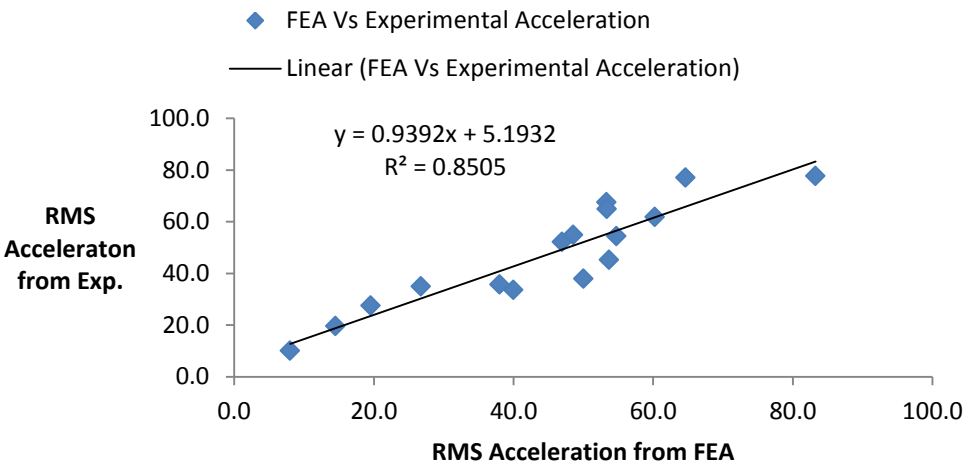


Figure 5-12. Comparison of RMS acceleration of the branch specimen obtained from FEA and experiments.

The longitudinal strain and acceleration computed at the test points for all loading conditions from FE and experiments are highly correlated and respectively have a Pearson coefficient of 0.97 and 0.92. Thus, the proposed FE model is able to predict the mechanical behavior of the branch to acceptable accuracy under the dynamic impact loading conditions and therefore, similar FE parameters were used to analyze the tree limb prototypes for the optimization of a canopy shaker.

# CHAPTER 6
# MECHANISTIC MODELS

The objectives for the optimization of shaker were formulated mathematically in terms of mechanistic index. The mechanistic index is a function of one or more parameters of the objectives, which are structural response quantities that can be computed and correlated with the objectives. The indices are defined based on the demand vs. capacity of a system. The results from the finite element analysis were used in the formulation of the mechanistic models.

## Mechanistic Tree Damage Model

Consistent with the dynamic behavior of the tree limbs due to a vibratory excitation, the dynamic structural damage is estimated using damage index. The damage index is expressed as the ratio of the maximum response of the limbs to the maximum allowable deformation or strength of the tree limbs as described in Equation 6-1. Branches are said to fail when DI ≥ 1, whereas they are elastically deformed for DI < 0.

$$DI = \frac{\delta_m}{\delta_u} \tag{6-1}$$

The response of limbs computed from FEA is used to formulate the damage index. The structural damage response of each limb is expressed in terms of normal stress (S11) obtained by solving partial differential equation of dynamic motion of a system using FEM. The root mean square of normal stress was calculated and used to formulate damage index in order to account for the variations in the stress over a period of cyclic loading. The goal is to minimize the damage of tree limbs or scaffold branches having diameter more than certain critical diameter. For the medium size citrus tree, this value is taken as 2.5 inches because breakage of limbs with more than this diameter

was observed to affect next year fruit yield. Figure 6-1 shows a branch limb with critical region defined by series of dots.

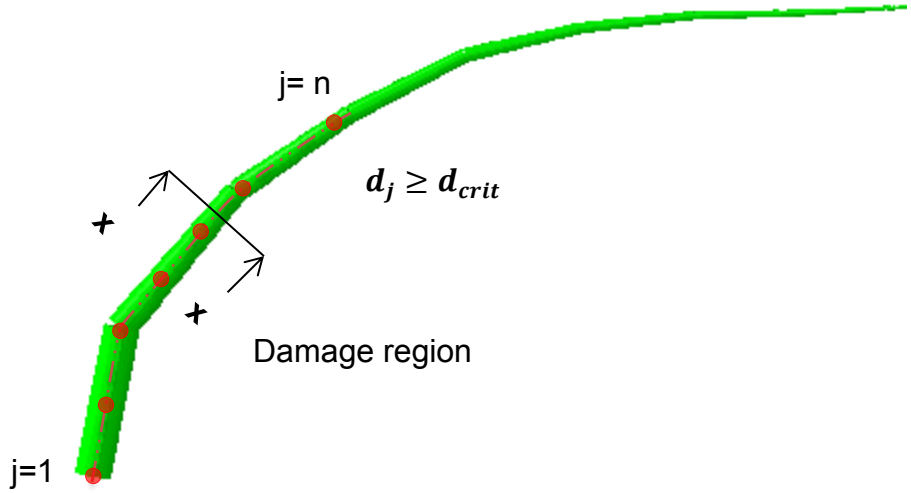


Figure 6-1. A finite element model of a tree limb showing damage region.

The normal stress S11 is evaluated at each section points of the beam element as shown in Figure 6-2. The stress S11 at section points designated as 1, 2, 3, and 4 is given as:

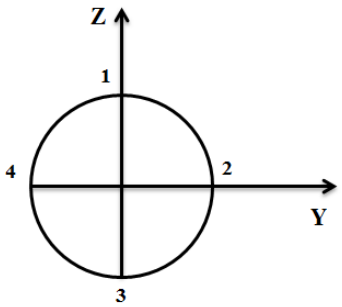


Figure 6-2. Section points of a finite beam element of the tree limb.

$$S11\,(1\,or\,3) = \frac{N_x}{A} \pm \frac{M_y z}{I_{yy}} \qquad \text{Symmetric bending about y axis} \qquad (6\text{-}2)$$

$$S11\,(1\,or\,3) = \frac{N_x}{A} \pm \frac{M_z y}{I_{zz}} \qquad \text{Symmetric bending about z axis} \qquad (6\text{-}3)$$

where My, Mz, Iyy, and Izz are the bending moments and the second area of moment about the Y and Z directions, respectively; y and z are the distance of outer fiber from the neutral axis along the Y and Z direction respectively; and $N_x$ and A is the axial force and the area of cross-section, respectively.

The stress $\sigma$ is a vector of maximum sectional stress (*S11*) computed at all the critical points in the damage region for which $d \geq d_{critical}$ and is given by:

$$\sigma = \max\left(\left\| S11_i \right\|_2\right) \tag{6-4}$$

where i equals to 1, 2, 3, and 4 corresponding to the section points of beam element. The response of the individual limb prototypes $\delta_m$ is computed as the maximum of a section stress $\sigma$ in the damage region of the tree limb prototype and is calculated as:

$$\delta_m = \max\left(\sigma_j\right) \tag{6-5}$$

Damage index of an individual limb prototype is determined by normalizing the maximum response by the capacity of the limb. The capacity is either taken as the strength of wood defined in terms of modulus of rupture ($\delta_U$) or the value of maximum response of limb prototypes when analyze with current machine configuration ($\delta_S$). The current machine configuration uses the 78 inches long, DOM 4130 steel tube hardened to 45 Rc +/- 2 and vibrates at the frequency of 4 Hz with 4 in. amplitude. Minimum of these two capacities was used to formulate the damage index of the limb prototype (D) as given by Equation 6-6.

$$D = \frac{\delta_m}{\min(\delta_S, \delta_U)} \tag{6-6}$$

The damage index *(D)* of all limb prototypes in a tree zone was averaged to provide the damage index of that zone *(DI)* and is expressed as:

$$DI_z = \frac{1}{p}\sum_{k=1}^{p}|D_k| \tag{6-7}$$

where k=1, 2, 3,….p = number of limb prototypes for each zone, and z=1,2,3 corresponds to the top, middle, and bottom zone respectively.

**Mechanistic Fruit Detachment Model**

Fruit detachment model estimates the amount of fruit detached from the limbs when shaken. The mechanism of fruit detachment has been investigated analytically and experimentally by Fridley and Adrian, 1966; Wang and Shellenberger, 1967; Cooke and Rand, 1969; Diener et al., 1969; Liang et al., 1971; Parchomchuk and Cooke, 1972; Miller and Morrow, 1976; Berlage and Willmorth, 1974; Savary and Ehsani, 2010. They found that the amount of fruit removal is highly correlated with acceleration of the fruits. The past studies have suggested that the ratio $\frac{F}{W}$ (the tensile force required to detach the fruit divided by the fruit weight) is a good indicator of fruit detachment by shaking. The typical value of this ratio for fruits like citrus and prunes varies from 1 to 50 depending on the variety and the size of the fruit. Savary (2009) measured the force required to detach Hamlin and Valencia varieties of orange. He concluded that the average static force of 96.1N and shaking force of 17.1N are required to remove these varieties of fruits. Therefore, a system which provides an acceleration of approximately 9g would more likely to detach citrus fruits based on the average weight of 0.186 Kg. However, using this value to define the maximum capacity of fruit detachment model would not be accurate pertaining to high variability in the fruit weight. Thus, maximum capacity is defined in terms of the acceleration obtained by analyzing the limb

prototypes at the current configuration of the canopy harvester, which in the field harvesting provides 96-99% of fruit removal (Roka, 2008).The fruit detachment finite element model computes the fruit detachment index of the limb prototypes as shown in Figure 6-3.

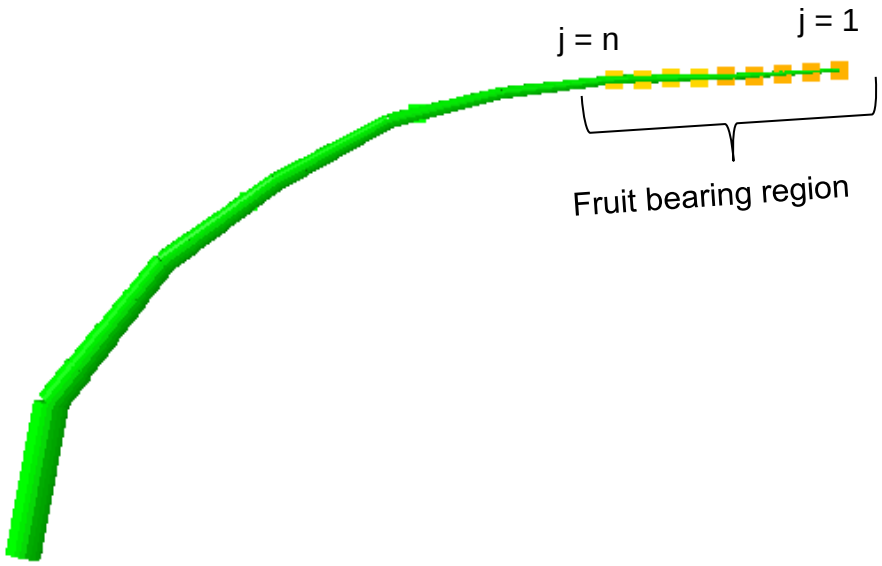


Figure 6-3. A finite element model of a tree limb showing fruit bearing region.

The fruit detachment response ($a^r$) in the fruit bearing region of a limb prototypes was computed as the root mean square of resultant acceleration (a) as given below:

$$a^r = \|a\|_2 \tag{6-8}$$

The resultant acceleration is computed at every node in the fruit bearing region using Equation 6-9.

$$a = \sqrt{a_x + a_y + a_z} \tag{6-9}$$

The fruit detachment response of an individual limb prototype ($a_m$) was calculated as the mean of responses computed at all nodes of the fruit bearing region of the limb prototype and is given as:

$$a_m = \frac{1}{n}\sum_{j=1}^{n} a^r \tag{6-10}$$

The fruit detachment index of a limb prototype ($FD$) was obtained by normalizing the fruit detachment response ($a_m$) by the response obtained using the current machine configuration ($a_S$) and is expressed below:

$$FD = \frac{a_m}{a_S} \tag{6-11}$$

The fruit detachment response of a zone (*FDI*) was obtained by taking the average of responses of all the limb prototypes in that zone and is computed as:

$$FDI_z = \frac{1}{p}\sum_{k=1}^{p} \left| FD_k \right| \tag{6-12}$$

where k = 1,2, … p ( number of limb prototypes) and z= 1,2,3 corresponding to the top, middle, and bottom zone, respectively.

The tree damage index and fruit detachment index were computed from the dynamic analysis of the limb prototypes using Abaqus and MATLAB program to obtain the optimal set of machine parameters.

# CHAPTER 7
# MULTI-OBJECTIVE OPTIMIZATION

An efficient harvester is that which can provide high fruit removal with either no damage or minimal damage to the scaffold branches or primary limbs. Increasing the shaking force to the tree limbs having large number of fruits results in high fruit removal; however, it also cause high amount of tree damage. Therefore, a shaker should be designed to provide the optimum shaking force to the tree limbs based on the distribution of the tree limb and fruits in a citrus tree canopy. This type of design problem generally involves finding the best trade-off between the two conflicting objectives and is hence classified as multi-objective problems. The most widely accepted procedure to solve multi-objective problems is to employ Pareto-optimal solution search technique (Pareto 1906).

Pareto optimal solution guarantees that, if moving from it, no improvement can be achieved on any objective function without worsening others (Deb, 2001). Pareto technique requires significantly high number of functions evaluations to solve multi-objective optimization problems. Thus, a computationally efficient strategy should be developed for the optimization of structures. One of the most effective approaches to minimize the cost of optimization in the recent years is founded on response surface methodology (Myers and Montogomery, 2002). Response surface based optimization methods are based on approximation of a given objective function to be optimized through a set of points belonging to domain of variation of the independent variables the function itself depends on.

The following steps have to be developed in order to implement a multi-objective approach:

- Identification and formulation of different objectives
- Variable definition
- Defining proper design of experiments (DOE)
- Defining numerical model to be evaluated at DOE
- Collection of numerical data to compute objective functions
- Meta-modeling step to analytically develop response surface describing each objective function as a function of design variables.
- Multi-objective optimization formulation to determine optimal Pareto solutions.

## Problem Formulation

The fruit detachment and the tree damage depend on the amount of shaking force applied to the tree limbs by a harvester machine. The shaking force in return, is a function of structural and operating parameters of a harvester. The operating parameters: frequency and amplitude of vibration of a system are only considered in the optimization of a mechanical harvester. In a canopy shaker, the frequency of the vibration can be easily controlled by changing the speed of motor connected to shaft of vibratory mechanism. However, in order to change the amplitude of vibration, the crank design of the slider crank mechanism should be changed. The structural parameter of a harvester is the configuration (geometry and material) of the interface which interacts with tree canopy. For the canopy shaker, the tine acts as an interface and transmits the vibrating motion from machine to tree.

A two piece-design of a tine as shown in figure 12 was proposed to provide the adaptive shaking of a tree canopy considering the following guidelines:

- Easy to adopt and implement in the purchased machines
- Can be tested and verified with the available laboratory equipment
- Overall lost cost of designs

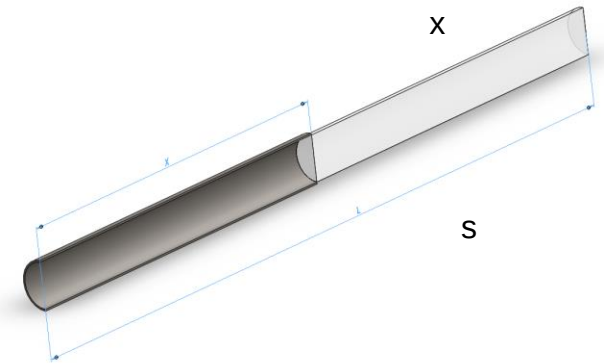


Figure 7-1. Proposed two-piece design of at tine for adaptive shaking of tree canopy

The proposed tine design consists of (1) a current design (steel pipe) forming base and attached to the hub of a canopy shaker; (2) an insert in the form of rod or tube. The configuration of insert was designed to provide variable shaking force to the various parts of a citrus tree canopy. The stiffness (s) of insert which is the property of geometry and the material, and the percentage length of insert (x) were defined as the design variables in the optimization of shaker besides the operating variables: frequency (*v*) and amplitude (*a*). The formulation used in the optimization of a canopy shaker is expressed in Equation 7-1.

$\boldsymbol{find}\ \boldsymbol{s, x, v, a}$ :

$$\underset{s \in \mathbb{R}^n s, x \in \mathbb{R}^n x, v \in \mathbb{R}^n v, a \in \mathbb{R}^n a}{\boldsymbol{Minimize}} \quad \boldsymbol{DI}\ (s, x, v, a)$$

$$\underset{s \in \mathbb{R}^n s, x \in \mathbb{R}^n x, v \in \mathbb{R}^n v, a \in \mathbb{R}^n a}{\boldsymbol{Maximize}} \quad \boldsymbol{FDI}\ (s, x, v, a)$$

Subjected to:

Structural variables:

$$\underline{s} \leq s_i \leq \overline{s}\,, \qquad \forall i = 1, \ldots\ldots n_s$$

$$\underline{x} \leq s_j \leq \overline{x}\,, \qquad \forall j = 1, \ldots\ldots n_x$$

Operating variables:

$$\underline{v} \leq s_k \leq \overline{v}\,, \qquad \forall k = 1, \ldots\ldots n_v$$

$$\underline{a} \leq s_l \leq \overline{a}\,, \qquad \forall l = 1, \ldots\ldots n_a$$

(7-1)

**Design of Experiments (or Design Domain)**

The design of experiments to predict optimum configurations of machine were designed based on past research work and field experiments.

**Design Variables: Stiffness (s)**

The flexural stiffness of an insert is function of the geometry and material of the insert. The different designs of the insert were chosen based on the market availability and conclusion drawn from the various tine configurations experimented by Oxbo® International Corporation (a leading manufacturer of canopy shaker and other farm equipments) and Florida growers. The different variants of polyamide (PA, also called Nylon) having same cross-section denoted as P1-P5 and different cross-section geometries of Aluminum denoted as A6-A9 was chosen as listed in table 7-1. Figure 7-2

shows the variation of stiffness of the various designs of insert considered with respect to stiffness of the current design.

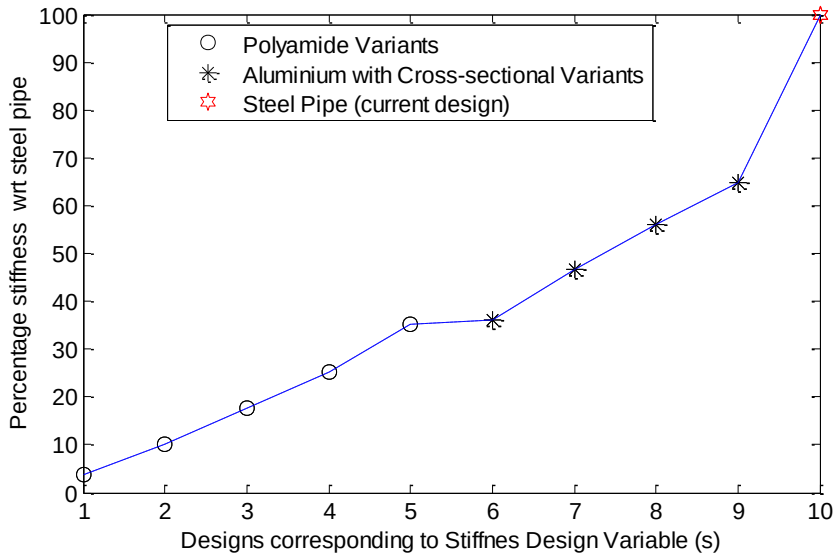


Figure 7-2. Variation of stiffness of multiple designs of insert normalized wrt stiffness of current design of a tine.

Table 7-1. Geometry and material configuration of the designs of the insert.

| Designs | Geometry | Dimension | | Mat. Prop. | Material Type |
|---|---|---|---|---|---|
| | | $r_o$ (mm) | t (mm) | E (GPa) | |
| P1 | Rod | 18.98 | 0 | 3 | PA – Cast, Molding and Extrusion and 15% Glass |
| P2 | | 18.98 | 0 | 8 | PA – 30% Long Glass, 40% Glass and Mineral |
| P3 | | 18.98 | 0 | 14 | PA – 50% Long Glass |
| P4 | | 18.98 | 0 | 20 | PA – 60% Long Glass, 30% PAN Carbon |
| P5 | | 18.98 | 0 | 28 | PA – 50% PAN Carbon |
| A6 | Pipe | 20.64 | 1.5 | 80 | Cast , Wrought Al. Alloy |
| A7 | | 20.64 | 2 | 80 | Cast, Wrought Al. Alloy |
| A8 | | 20.64 | 2.5 | 80 | Cast, Wrought Al. Alloy |
| A9 | | 20.64 | 3 | 80 | Cast, Wrought Al. Alloy |
| Current Design | | 20.64 | 1.65 | 210 | DOM 4130 STEEL |

**Design Variables: Length of Insert (*x*)**

The length of insert is the percentage length of an insert in a proposed two-piece design of the tine. The values of the design variable were chosen as listed in Table 7-2 to balance the computational cost and degree of exploration in the design domain for optimum design. The design value of 0 and 100 corresponds to 0% and 100% of insert respectively. The 0% of insert means that the tine is made of only current design and 100% of insert means tine is made of only new design.

**Design Variables: Shaking Frequency (*v*)**

Shaking frequency corresponds to the number of time shaker tine knocks the tree limbs per second.

**Design Variables: Shaking Amplitude (*a*)**

Shaking amplitude is a maximum displacement of a shaker and determines the amount of flexural deformation imparted to the tree limbs.

Past experiments on many fruit and nut crops have indicated that high frequencies of 20-40 Hz and short strokes of 20-25 mm is effective for the trees having relatively rigid structure. However, for willowy trees which have long and slender branches that curve down sharply due to the weight of fruits, the long stroke (100-125mm) and low frequencies (1.5-6 Hz) are effective for the fruit removal. Based on the experiments conducted on citrus using various harvesters, the good results was achieved using a stroke of 100-125 mm at a frequency of 1.6-5.9 Hz (O'Brien and Fridley, 1983). The conclusions from the past studies were used to sample the frequency and amplitude of a canopy shaker. The values of the design variables are listed in Table 7-2.

Table 7-2. Design of experiments for numerical analysis and optimization.

| Design Variables | Lower bound | Upper bound | Design Values |
|---|---|---|---|
| Length of Insert in % (x) | 0 | 100 | 0:5:100 |
| Shaking Frequency (v) | 2 | 8 | 2:1:8 |
| Shaking Amplitude (a) | 1 | 6 | 1:1:6 |

## Estimation of Cost of Analysis for Optimization

The total optimization time consist of the finite element (FE) analysis calculation time multiplied by the number of optimization iterations. The dynamic FE analysis of a tree limb using single design of a tine takes about 5 min. therefore, the total time required for the optimization of single zone would be the total time required for whole FE simulations of design domain multiplied by number of limb prototypes as shown in Equation 7-2.

$$t = No.\ of\ limb\ proptotypes\ \boldsymbol{X}\ Design\ Domain\ \boldsymbol{X}\ Cost\ of\ an\ analysis$$

$$\mathbf{5} \qquad \boldsymbol{X}\ (9 * 21 * 7 * 6)\ \boldsymbol{X}\ 5\ min.$$

$$\boldsymbol{t = \ 137.8\ days} \tag{7-2}$$

The total computation time of about 138 days for one zone hardly justified the practical value derived from such a long and tedious analysis. Besides high computational effort required by dynamic simulations, the multidimensional optimization requires special techniques for finding the optimum design such as gradient based optimization techniques, and genetic or evolutionary algorithms. These techniques further require special programs as well additional computational resources. Thus, a strategy was hereby put forward which aimed to minimize the computation time and to employ a classical graphical optimization technique instead of special optimization algorithm. The strategy consists of solving the optimization problem in two phases: first

phase of optimization involves only structural variables (*s, x*); and in the second phase optimization, the best designs of phase-1 were used to further improve the objectives defined in terms of machine operating variables (*v, a*). The proposed strategy has an additional advantage of being able to provide designs based on change in structure of the machine and change in the machine operating parameters. Structural parameters of the machine are easier to test and implement as it only involves the procurement of new designs whereas machine operating parameters involve changes to be made in the machine vibratory mechanism. Thus, operating designs are costlier and difficult to implement in the exciting machine but may result in significant improvement in the objective functions.

**Shaker Optimization: Phase – 1**

The phase one of optimization involves the optimization of a shaker based on only structural variables: the stiffness and the percentage length of an insert. The operating variables were fixed to the current machine setting with a frequency and amplitude of 4 Hz and 4 in., respectively. The design of a shaker for the phase-1 of optimization is formulated in Equation 7-3.

$\boldsymbol{find}\ \boldsymbol{s, x}$:

$$\underset{s \in \mathbb{R}^n s, x \in \mathbb{R}^n x}{\boldsymbol{Minimize}} \quad \boldsymbol{DI}\ (s, x, v^0, a^0)$$

$$\underset{s \in \mathbb{R}^n s, x \in \mathbb{R}^n x}{\boldsymbol{Maximize}} \quad \boldsymbol{FDI}\ (s, x, v^0, a^0)$$

$$where\ v^0, a^0 = current\ machine\ operating\ parameter\ (4\ Hz, 4\ in.)$$

Subjected to:

$$\underline{s} \leq s_i \leq \overline{s}\,, \qquad \forall i = 1, \ldots\ldots n_s$$

$$\underline{x} \leq s_j \leq \overline{x}\,, \qquad \forall j = 1, \ldots\ldots n_x \tag{7-3}$$

**Materials and Methods**

The following procedure was adopted to find the optimum tine configuration for each zone.

- The response of the limb prototypes was computed using finite element analysis.
- The fruit detachment index and damage index were calculated for each zone as described in Chapter 6.
- The Pareto-frontiers were constructed for each zone to choose optimum design based on the trade-off between DI and FDI. The Pareto-frontier was constructed based on dominance principle where a set of non-dominated design points are chosen such that no objective functions can be improved further without impairing the other objective. The MATLAB function by Freitas (2012) was used to create Pareto fronts.
- To minimize the computation cost the bi-objective formulation was converted into a mono-objective formulation by converting the fruit detachment formulation into a constraint as given by Equation 7-4. The best Pareto-optimal design was selected to obtain at least of 15 % reduction in the tree damage.

  $Minimum\ (DI - 0.85)$

- $FDI - FDI_{allowable} \geq 0$ (7-4)

The value of $FDI_{allowable}$ was chosen based on the fruit distribution in a citrus tree. The fruit harvesting efficiency can be increased by providing large shaking force to the parts of canopy that have comparatively high fruiting. Theoretically, it can be achieved by setting high value of $FDI_{allowable}$ to those parts of tree canopy. Whitney and Wheaton (1984) have studied the fruit distribution pattern of the citrus trees and they have concluded that most of the fruiting occurs in the middle and outer part of the canopy. To

corroborate their finding for a case of medium sized citrus tree, an experiment was set up and fruit distribution was analyzed for 361 trees. Figure 7-3 shows the distribution of fruits in the three zones of a tree. It is found that the average fruit density in the middle section of a tree canopy is two times as in the top and bottom sections. Thus, overall harvesting efficiency can be improved by setting the comparatively high value of $FDI_{allowable}$ for the middle zone as compared to the bottom and top zones. The values of $FDI_{allowable}$ selected for the phase 1 of optimization for each zone of tree canopy are listed in Table 7-3.

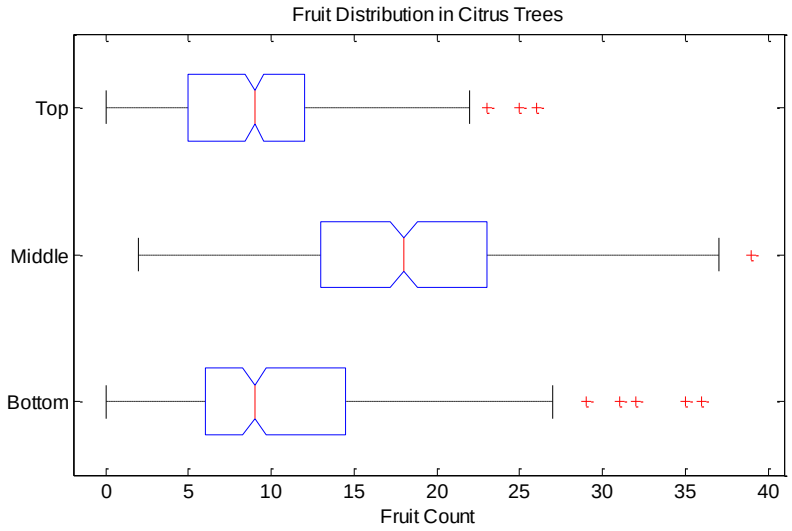


Figure 7-3. Distribution of citrus fruits in the three zones of a citrus tree canopy.

Table 7-3. Allowable Fruit Detachment Index.

| | |
|---|---|
| Top Zone | 0.8 |
| Middle Zone | 0.9 |
| Bottom Zone | 0.8 |

**Results and Discussion**

Optimization results based on structural variables of the harvesting equipment for each zone are presented below. The different optimal design configurations of the tine were proposed. The design of a tine is selected among the proposed designs of the tine

based on the degree of machine improvement desired and amount of expenditure, one is willing to invest.

**Middle zone**

Figure 7-4 shows the Pareto-front between objective functions, damage index (DI) and fruit detachment index (FDI), of the middle zone. The contour plots for the FDI and DI for the middle zone of the limbs are shown in Figure 7-5.

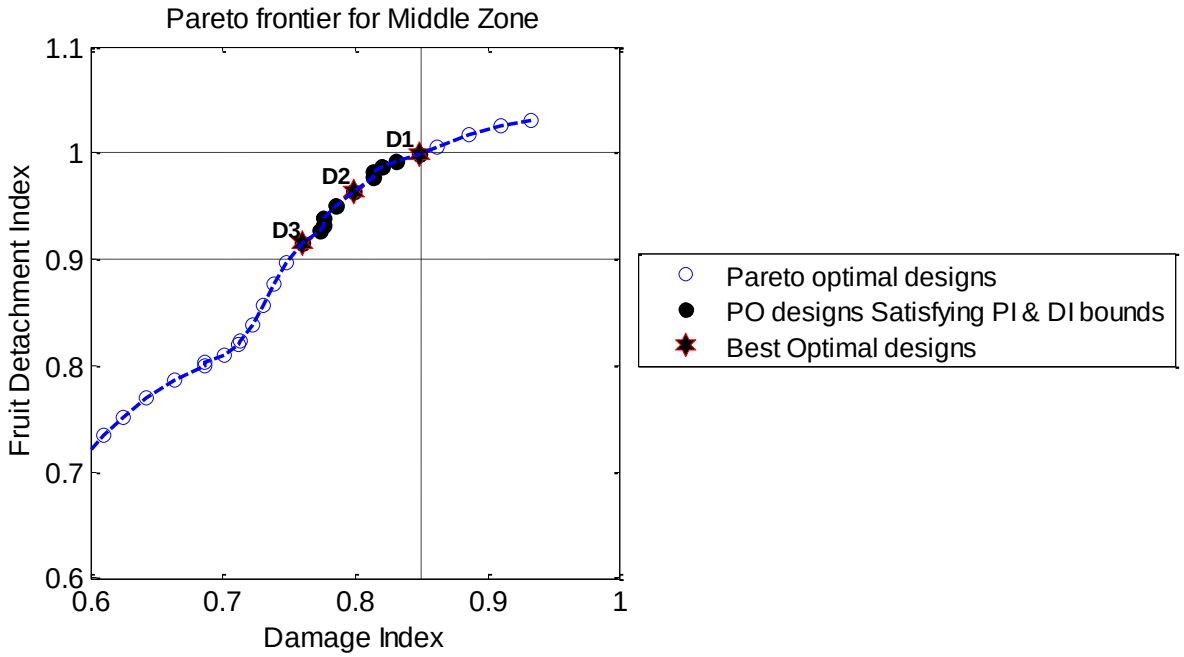


Figure 7-4. Pareto frontier to predict the optimum tine configuration of the middle section of a canopy shaker.

Table 7-4. Optimum configuration of tine for middle section of the canopy shaker.

| ZONE | Best design | | Design Configuration | Reduction in Damage (%) | Fruit Detachment (%) |
|---|---|---|---|---|---|
| MIDDLE | D1 | Design P5 | 70% 28 GPa PA | 15.2 | 100 |
| | D2 | Design P4 | 70% 20 GPa PA | 20.1 | 96.4 |
| | D3 | Design P3 | 65% 14 GPa PA | 24 | 91.5 |

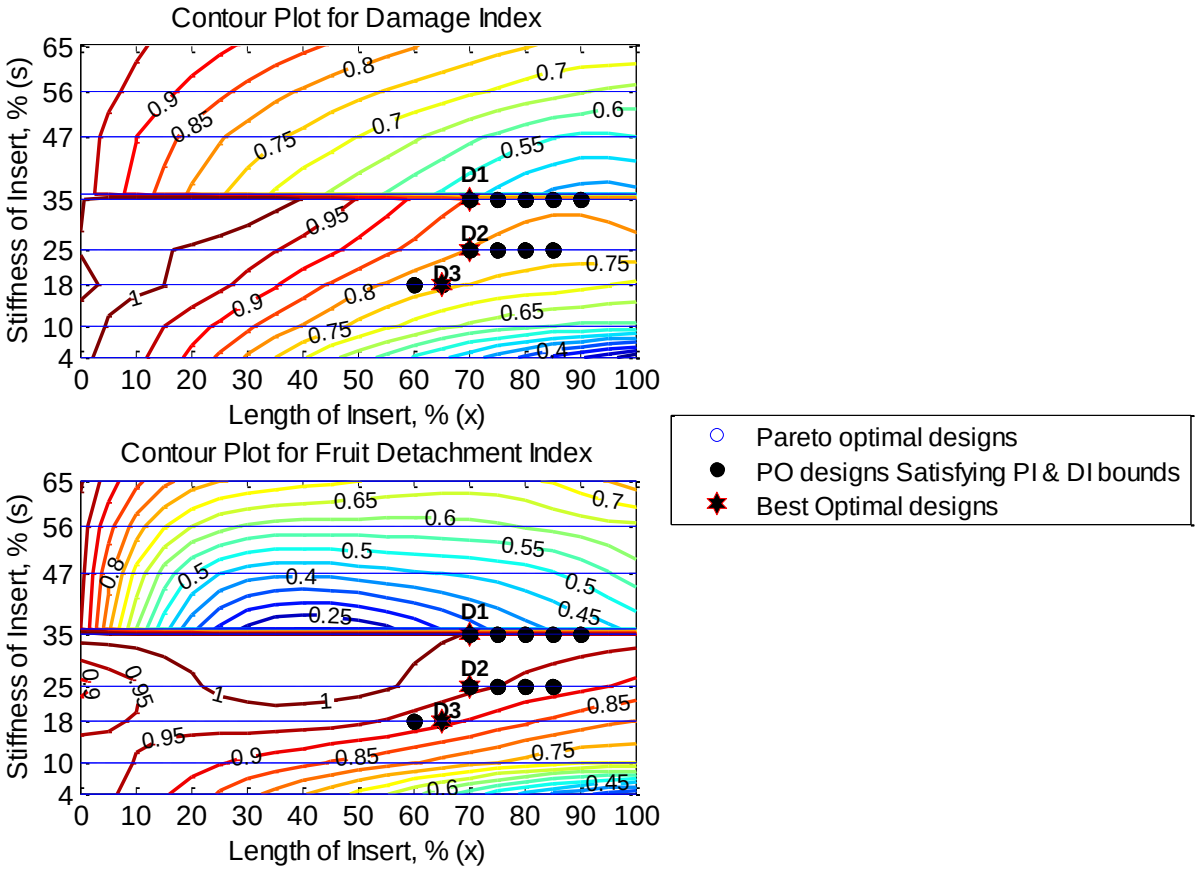


Figure 7-5. Phase-1 optimization: Contour plots for the Damage Index and Fruit detachment Index to predict optimum tine configuration for the middle section of a canopy shaker.

The upper bound on DI and the lower bound on FDI were set to select only those designs which result in at least of 15 % reduction of tree damage and minimum of 90% fruit detachment. Three optimum designs of tine have configurations D1, D2 and D3 shown as six-pointed star in Figure 7-4 and listed in table 7-4 were proposed. The tine configuration of 70% 28 GPa polyamide means that the tine composed of 70% of new design of insert and 30 % of current design by length. As in table 7-4, the tine design D1 results in 15.2 % reduction of tree damage and fruit removal of approximately 100 %. Physically, it means that employing the new design will result in approximately 15% reduction in maximum stress in the critical region of limbs and an average acceleration

of about 100% of the average acceleration in the fruiting zone of the tree limbs in the middle zone of the tree canopy when computed using current design of the tines. In the field experiments, the current tine configuration of a canopy shaker results in the fruit harvesting efficiency of 95-96 % (Roka, 2008). A significant amount of reduction in tree damage can be accomplished by employing the designs D2 and D3; however, this will also result in the considerable reduction in the fruit detachment.

**Top and bottom zone**

Figure 7-6 shows the Pareto frontier constructed for the limbs of the top and bottom zone of a citrus tree canopy. The contour plots for the FDI and DI are provided in the appendix B (Figure B-1). The designs of the top and bottom zone were selected to achieve high reduction in tree damage (more than 20%) as compared to that of the middle zone. Two optimum designs of tine D1 and D2 and three designs of the tines D1, D2, and D3 as listed in table 5 were selected for the limbs of top and bottom zone, respectively to minimize the tree damage and maximize the fruit removal. It should be noted that the design D1 of top zone results in the fruit detachment of 102 % which simply means that the average acceleration in the fruiting bearing region of the limbs of the top zone is 2% more than that could be obtained by the current design of the tines. Physically, more than 100% of fruit detachment index means that there is higher probability of achieving fruit harvesting efficiency of 100% during real time harvesting.

It is noticed that the substantial reduction in tree damage (~30-35) can also be achieved using tine design D2 in the top zone and design D3 in the bottom zone. However, employing the tine design D2 of the top zone and D3 of the bottom zone would result in 15-20% reduction in the fruit removal. This reduction in the fruit removal

can be compromised because of significantly less number of fruits in the top and bottom zone as compared to middle zone.

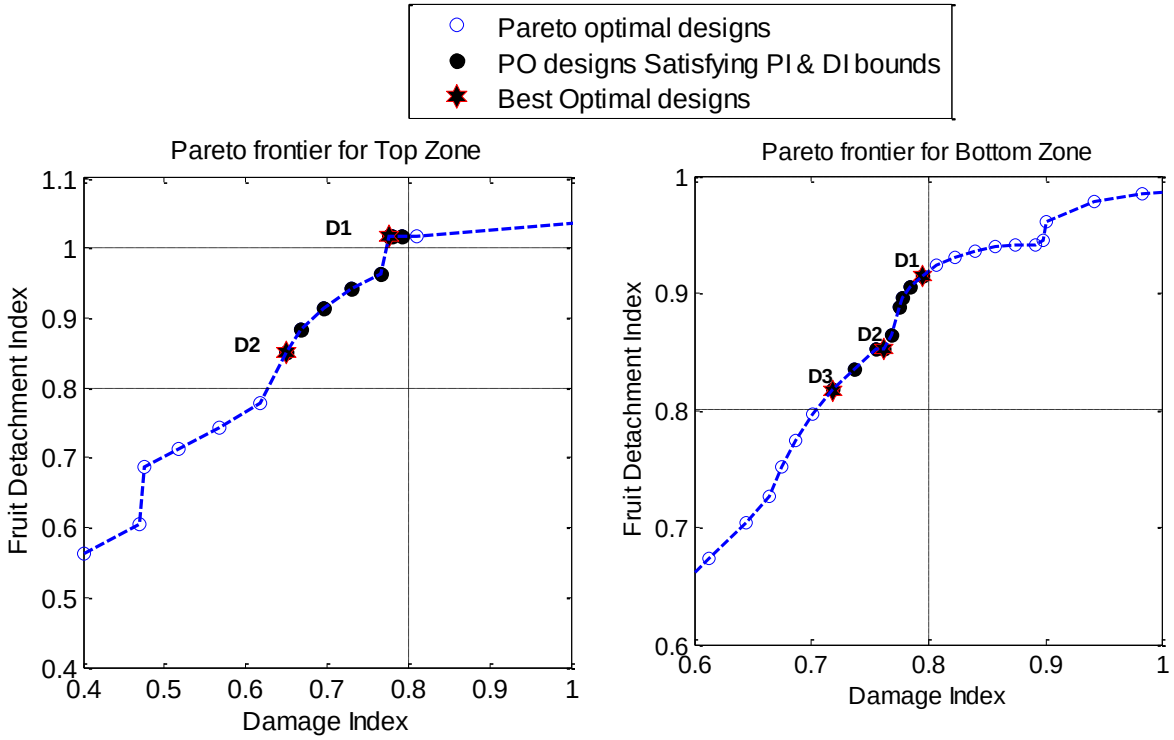


Figure 7-6. Pareto frontier for the top zone (left) and the bottom zone (right) to predict optimum tine configuration for the top and bottom section of a canopy shaker.

Table 7-5. Optimum configuration of tine for top and bottom section of the canopy shaker.

| ZONE | Best design | | Tine Configuration | Reduction in Damage (%) | Fruit Detachment (%) |
|---|---|---|---|---|---|
| TOP | D1 | Design P5 | 100% 28 GPa PA | 22.5 | 102 |
| | D2 | Design P4 | 100% 20 GPa PA | 35 | 85 |
| BOTTOM | D1 | Design P5 | 80% 28 GPa PA | 20.6 | 91.5 |
| | D2 | Design P4 | 80% 20 GPa PA | 23.8 | 85.2 |
| | D3 | Design P3 | 70% 14 GPa PA | 28.2 | 81.7 |

Considering all the proposed designs of all three sections for a canopy shaker, the choice of employing any design is made based on trade-off between the total cost of design and the degree of improvement required in the machine. Figure 7-7 compares

the cost of various polyamide invariants used in the optimization with their respective flexural strength. The flexural strength is the measure of capacity of a structure to bear flexural deformation; and choosing a tine design with high value of flexural strength is desirable. The information regarding the cost and the tensile strength of various variants of polyamide were obtained from the web resources and information available in CES Education Package (version: 2005). The information is listed from the data published in 2005; therefore, absolute value may have changed now but the relative cost would be approximately same. More market exploration would be helpful in making comprehensive decision regarding the choice of design for the three sections of a citrus canopy.

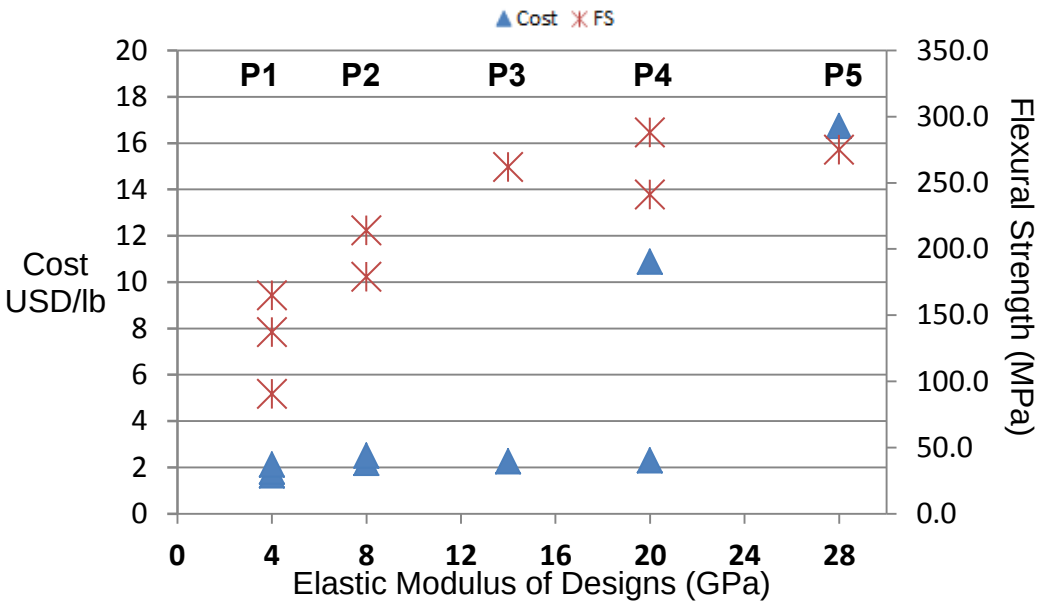


Figure 7-7. Comparison of a cost and tensile strength of the polyamide variants.

It is noticed that both the cost and the tensile strength of polyamide variants increases from the design P1 to P5. However, design P3 and P4 are about 8 times cheaper than design P5 and have only marginal difference in the tensile strength. The decision to choose a tine configuration for each section of a canopy shaker depends on

the amount of financial resources one is willing to put in and degree of improvement one desired to get in the canopy shaker.

**Shaker Optimization: Phase - 2**

In this phase, the canopy shaker is further improved by providing the optimum combination of operating parameters: frequency and amplitude. The best designs from the phase-1 were used in the optimization to find the optimum operating parameters. The problem formulation of the phase-2 of the shaker optimization is expressed in Equation 7-5.

$$\boldsymbol{find} \quad v, a$$

$$\underset{v \in \mathbb{R}^n v,\, a \in \mathbb{R}^n a}{\boldsymbol{Minimize}} \qquad \boldsymbol{DI}\,(s^1, x^1, v, a)$$

$$\underset{v \in \mathbb{R}^n v,\, a \in \mathbb{R}^n a}{\boldsymbol{Maximize}} \qquad \boldsymbol{FDI}\,(s^1, x^1, v, a)$$

Subjected to:

$$\underline{v} \leq s_k \leq \overline{v}\,, \qquad \forall k = 1, \ldots\ldots n_v$$

$$\underline{a} \leq s_l \leq \overline{a}\,, \qquad \forall l = 1, \ldots\ldots n_a$$

$$s^1, x^1 = Best\ optimal\ designs\ from\ phase - 1$$

(7-5)

**Materials and Methods**

The following procedure was adopted to find the optimum operating parameters of the machine for the best designs of the phase-1.

- The FDI and DI were computed for each combination of frequency-amplitude in the design of experiments.
- Performing dynamic analysis is generally computationally expensive, thus meta-modeling technique was implemented to minimize the cost of optimization.

- Radial Basis Neural Network (RBNN) (Park and Sandberg, 1991) was used to construct the analytical response surface of fruit detachment index and damage index as a function of the design variables: shaking frequency and amplitude. The Matlab program for surrogates designed by Viana (2010) was used to construct RBNN response surface. The parameters of *RBNN* were chosen based on the minimum $PRESS_{RMS}$.
- The Pareto-frontiers for the optimum tine designs of each zone were constructed from the FDI and DI response surfaces.
- The best operating combination of frequency and amplitude was determined using Equation 7-6.
- $$\begin{aligned} &Minimum\ \ DI \\ &FDI - FDI_{allowable} \geq 0 \end{aligned} \tag{7-6}$$

**Results and Discussion**

The optimum operating parameters of a canopy shaker for each zone of tree canopy are presented below. The response surfaces were constructed based on results of numerical simulations evaluated for few combinations of frequency and amplitude. These response surfaces were then used to predict objective functions for any combination of operating variables (frequency and amplitude) in the design domain. The Pareto- frontiers were constructed to predict the best combination of operating variables for all designs of tines proposed in phase-1.

**Middle zone**

The parameters of the response surfaces were set to maximize the predictive performances of the response surface obtained by minimizing the $PRESS_{RMS}$. The value of error norms of RBNN response surface for both the objective functions are listed in Table C-1 (appendix C). The response surface of the objective functions for the tine design D1 for the middle zone of a canopy shaker is shown in Figure C-1. Figures C-3, C-4, and C-5 show Pareto frontier for the tine design D1, D2 and D3 computed in

phase-1 of the shaker optimization. The optimum operating parameters for each design of the tine for the middle section of a canopy shaker are listed in Table C-2 and summarized in Table 7-6.

Table 7-6. Optimum operating parameters for the middle section of a canopy shaker.

| Designs | Frequency (cps) | Amplitude (inches) | Reduction in Damage (%) | Fruit Detachment (%) |
|---|---|---|---|---|
| D1 and D3 | 7.8 | 1.5-2 | 20-30 | 90-100 |
| D2 | 3.6 | 4.6 | 20 | 102 |
| | 6.4 | 2 | 26 | 91 |

It is found out that the tine design D1 and D3 if operated at high frequency (~7.8 Hz) and low amplitude of vibration (1.5-2) can result in 20-30% reduction in tree damage and a fruit removal of 90-100 %. For design D2; however, two different optimum combination of frequency was found. The tree shaking with a high frequency of around 6.5 Hz and low amplitude of 2 in. has resulted in 26 % reduction in the tree damage with approximately 91 % of the fruit removal; however, decreasing the shaking frequency to about 3.6 Hz and increasing amplitude to about 4.6 in. has resulted in more than 100 % fruit removal with 20% reduction in tree damage.

**Top zone**

The value of error norms of the response surfaces used in predicting the objective functions for the designs of the top zone are listed Table C-3. Figure C-6 shows the response surface constructed for the tine design D1 of the top zone as a function of operating variables (*v, a*). The optimum operating parameter for both the designs of the top section of a canopy shaker are listed in Table C-3 and summarized in

Table 7-7. Figures C-7 and C-8 show Pareto frontier and contour plots for the optimum tine designs D1 and D2 of phase-1, respectively.

Table 7-7. Optimum operating parameters for the top section of a canopy shaker.

| Designs | Frequency (Hz) | Amplitude (inch) | Reduction in Damage (%) | Fruit Detachment (%) |
|---|---|---|---|---|
| D1 and D2 | 6.5-7.5 | 3 - 3.5 | 40 - 55 | > 100 |

It is can be concluded that for both the optimal designs, high frequency in the range of 6.5-7.5 and mid-range value of amplitude of 3-3.5 inches of vibration has result in the 40-55% reduction in the tree damage. The designs of tine (*D1 and D2*) at these combinations of frequency and amplitude have resulted in more than 100% of fruit detachment index.

**Bottom zone**

The value of error norms of the response surfaces constructed to predict the objective functions of designs of the tine of bottom zone are listed in the Table C-5. Figure C-9 shows the response surface constructed for the tine design D1 of the bottom zone. The optimum operating parameters and improvement in the objective functions for the designs of the tines proposed for the bottom section of a canopy shaker is given in Table C-6 and summarizes in Table 7-8. Figures C-10, C-11, and C-12 show Pareto frontier constructed for the tine designs D1, D2, and D3 computed in phase-1.

Table 7-8. Optimum operating parameters for the middle section of a canopy shaker.

| Designs | Frequency (Hz) | Amplitude (inch) | Reduction in Damage (%) | Fruit Detachment (%) |
|---|---|---|---|---|
| D1, D3 and D3 | 3 - 3.5 | 5.5 - 6 | 35 - 40 | ~ 80 |
| D2 and D3 | 7.5 | 2.5 | 20 - 25 | ~ 100 |

Two sets of optimum combinations of frequency were observed for tine corresponding to design D2 and D3. The tines configurations (D2 *and D3*) when operated at the mid-range frequency of 3-3.5 Hz and high amplitude of 5.5-6 in. has resulted in 35-40% reduction in tree damage and 80% of fruit detachment in the bottom section of tree canopy. However, around 100% of fruit detachment was computed at the high frequency of 7.5 Hz and low amplitude of vibration (~2.5 in.) with a 20-25% reduction in damage. The design D1 of the tine has only one optimum combination of frequency and amplitude (3-3.5 Hz, and 5.5-6 in.) and results in approximately 35% reduction in the tree damage with a fruit removal of only 80% when operated at this combination.

# CHAPTER 8
# CONCLUSION

In this study, the application of finite element analysis and computer aided optimization techniques for the design of a harvester was presented. The main goal of this study was to provide an overview of analytical possibilities available to improve the performance of a vibratory harvester: this goal was pursued by employing numerical methods and optimization techniques in the design of a canopy shaker. A progressive design approach consisting of determining the properties of the wood, modeling statistical prototypes of tree limbs, developing mechanistic models and, integrating numerical simulation with optimization tools was presented. Statistical modeling, objective quantification using mechanistic modeling, response surface methodology, and Pareto optimal solution search techniques were applied in order to obtain optimum machine parameters. The proposed design methodology consists of solving the optimization problem in two phases in order to reduce computational effort. Although the proposed framework has been developed in regards to the optimization of the citrus canopy shaker, it can be easily and effectively applied to the design and optimization of other fruit crop harvesters.

## Summary of Conclusions

The design idea of providing adaptive shaking of a tree based on the distribution of fruits and spatial configuration of the tree limbs was realized in this study. The adaptive shaking of the tree was accomplished by designing three set of tines vibrating at different combinations of frequency and amplitude corresponding to three sets of tree limbs in a tree canopy. The optimal design of the machine was proposed employing

numerical method instead of extensive experiments to reduce the high cost associated with setting up field trials.

Laboratory experiments were set up to find the properties of the green citrus wood to be used in the numerical analysis. The elastic modulus (8.5 GPa), the modulus of rupture (67.3 MPa), specific gravity (1.4508 g/cc) and damping ratio (10.78%) were calculated. The limbs to be modeled in the numerical analysis were defined based on the statistical distribution of the tree limbs rather than random individual trees. The spatial configuration of the limbs were predicted and modeled in the finite element analysis as a three-dimensional beam element. The sectional properties of the tree limbs were predicted using response surface methodology. The effect of secondary branches and fruits on the dynamic response of the primary limbs was considered by modeling them as a lumped mass on the limbs. The distribution of secondary branches and fruits were obtained by analyzing the measured data from the field experimentation. The fruit bearing region, where the objective function was evaluated, was configured based on statistical data of the tree limbs.

The finite element model was developed and the parameters were derived from the experimental results and research literature. The FEA model was verified by setting up small scale laboratory experimentation. Pearson correlation coefficient between the simulations and experiments of 0.97 and 0.92 were observed for the physical quantities: strain and acceleration, respectively. The research objectives (tree damage and fruit removal) for the optimization of shaker harvester were identified and quantified in terms of stress and acceleration of the tree limbs using mechanistic models. The computational cost involved in numerical simulations and optimization was minimized

using response surface methodology and two-phase optimization. Pareto fronts for phase-1 optimization were constructed based on structural variables: stiffness and percentage length of the insert; and Pareto fronts of the phase-2 optimization were designed based on machine operating variables: shaking frequency and shaking amplitude.

Tines made of low stiffness material (polyamides) and high stiffness material (steel) in the approximate ratio of 3:1 by length work best for limbs which are long, thick and hang down due to the weights fruits, typically seen in the middle and bottom sections of a citrus tree canopy. Considering least expensive of the proposed designs, the tine made of 70% of polyamide (PA) rods having 50% long glass fiber (Elastic modulus, E=14 GPa) and 30% of steel tube (DOM 4130) by length when installed in the middle section of canopy harvester, has shown approximately 24 % reduction in tree damage and about 92 % of fruit detachment as compared to current tine configuration. However, using the same configuration of a tine in the bottom section of the canopy shaker, around 28% reduction in tree damage and approximately 82% fruit removal was computed. Around 100% of fruit removal can be achieved in the middle section of canopy using a tine made of polyamide rods having 50% PAN carbon fiber (E=28GPa) but they are expensive and result in comparatively less reduction in the tree damage.

The tree limbs which are thick, long and grow straight up to a height of 100-130 in. and then slightly curve down due to the weight of the fruits; approximately 35% reduction in the tree damage and about 85% fruit detachment can be obtained by installing tines of polyamide with 60% long glass fiber or 30% PAN Carbon (E=20GPa) in the top section of a canopy shaker.

The phase-2 of optimization proposed different combinations of frequency and amplitude corresponding to each zone of a citrus tree canopy to further minimize the tree damage and maximize the fruit removal. From the manufacturing point of view, these combinations of frequency and amplitude are obtained by employing three different vibratory mechanisms in a harvesting system; however, the cost of installing these modifications could be high but can be considered owing to the improvement achieved in the machines. Considering the least expensive of the tine configurations: the tines made of rod of PA having 50% long glass fiber and tube of steel (DOM 4130) in the ratio of 3:1 when vibrates at a high frequency of 7-8 Hz and low amplitude of 1.5-2.5 inches has resulted in 20-30% of reduction in tree damage and 90-100% of fruit removal of the limbs for the middle zone and 20-25% reduction in the tree damage and ~100% fruit removal for the limbs of bottom zone. However, the tines made of rods of only polyamides having 60% long glass fiber or polyamides having 30% PAN carbon fiber and vibrating at a frequency of 6.5-7.5 Hz and amplitude of 3-3.5 inches has resulted in the 40-55% reduction in tree damage and approximately 100% fruit removal for the limbs of the top section of a citrus tree canopy.

Thus, the proposed study offers design alternatives based on adaptive shaking of a tree canopy to improve the current continuous canopy shaker for the citrus crop. We expect this methodology will open up a novel way to optimize the other vibratory shakers based on modeling and analyzing the tree limb prototypes using numerical methods.

## Recommendation for Future Work

In future work, the proposed designs will be evaluated by field trials to determine their efficacy. After evaluation, judgment will be made to determine which optimum

machine configurations should be chosen for the commercial harvesting of citrus. The possibility of redesigning a harvester may be explored further based on the experimental results and the proposed theoretical models. The presented theoretical model, verified in the controlled environment of laboratory experiments, may be refined further depending on its correlation with the field trials. The following recommendations are listed to further improve a canopy shaker, and validate and refine the proposed analytical models to optimize other vibratory harvesters.

- A small scale fruit removal system which works on the principles similar to that of a continuous citrus canopy harvester should be built to validate the simulations.
- The field experiments should be setup to evaluate the proposed design modifications.
- The proposed analytical models can be refined further based on experimental results.
- The techniques of experimental based design optimization (EDO) may be used to further improve the performance of a harvester.
- Effect of vertical shaking of a tree canopy can also be explored using numerical simulation.

# APPENDIX A
# LABVIEW PROGRAM

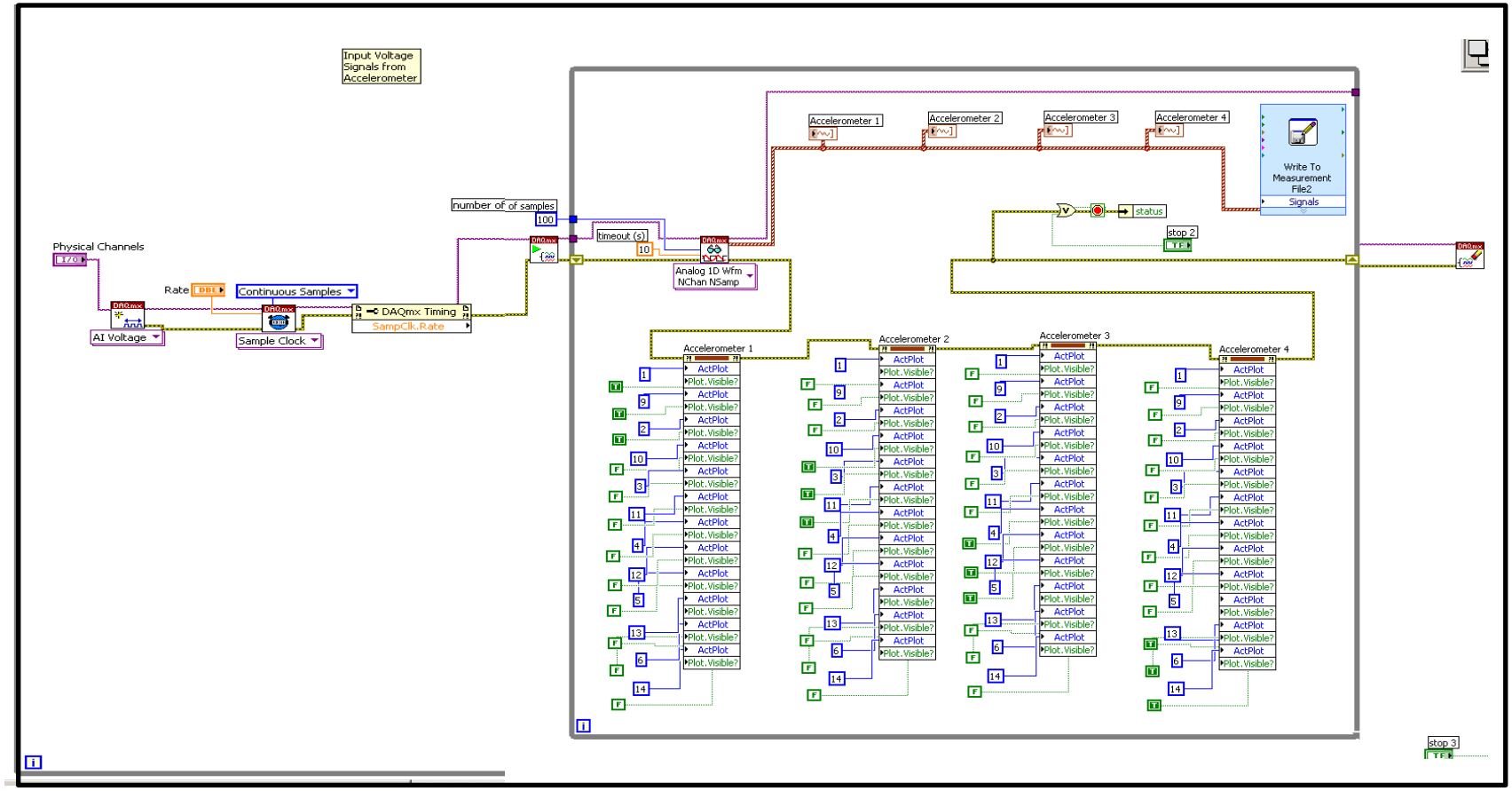


Figure A-1. LabVIEW instrument program to acquire data from an accelerometer.

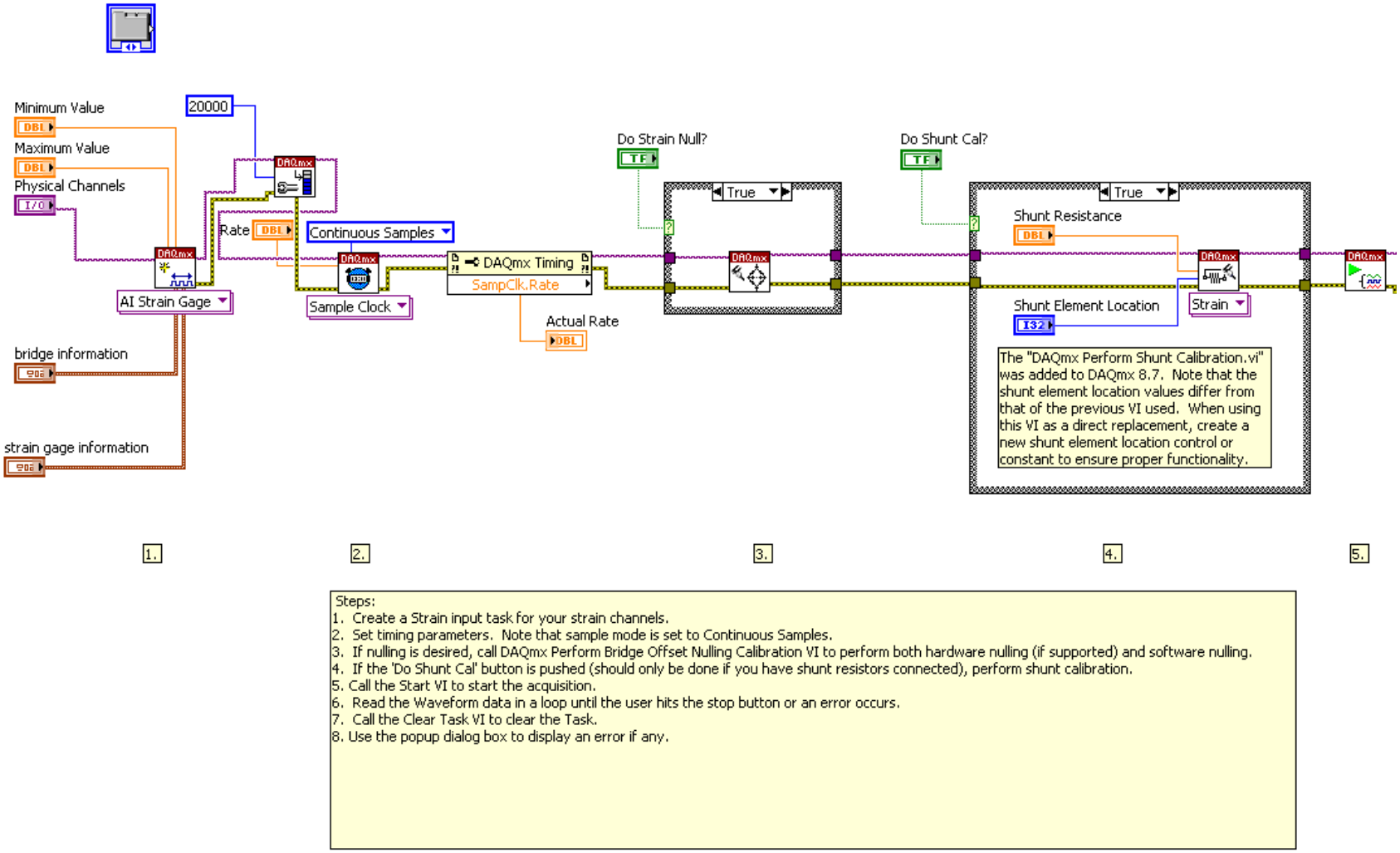


Figure A-2. LabVIEW instrument program to acquire strain data from a strain gauge-left half portion.

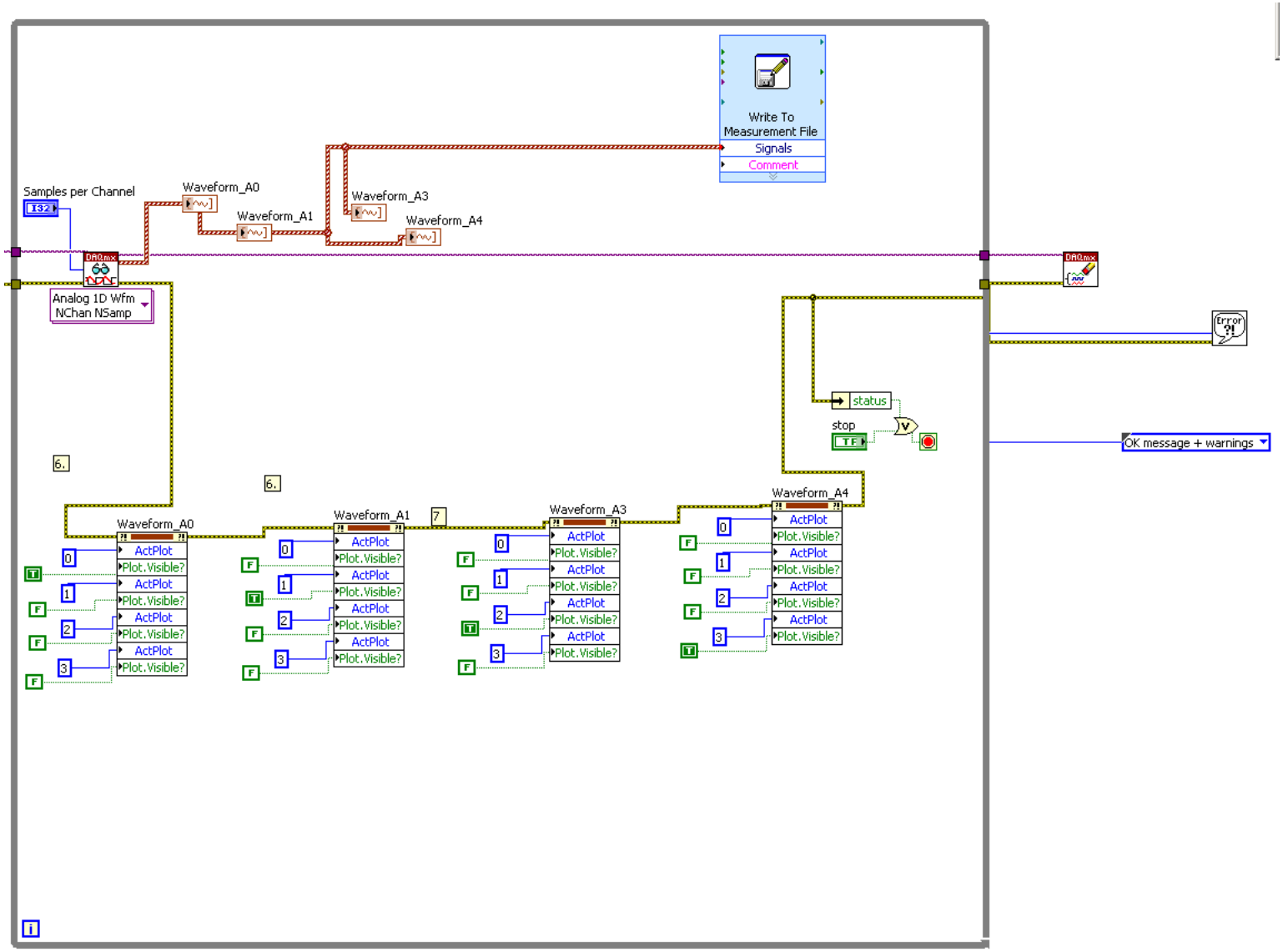


Figure A-3. LabVIEW instrument program to acquire strain data from strain gauge-right half portion.

APPENDIX B
PHASE-1 OPTIMIZATION

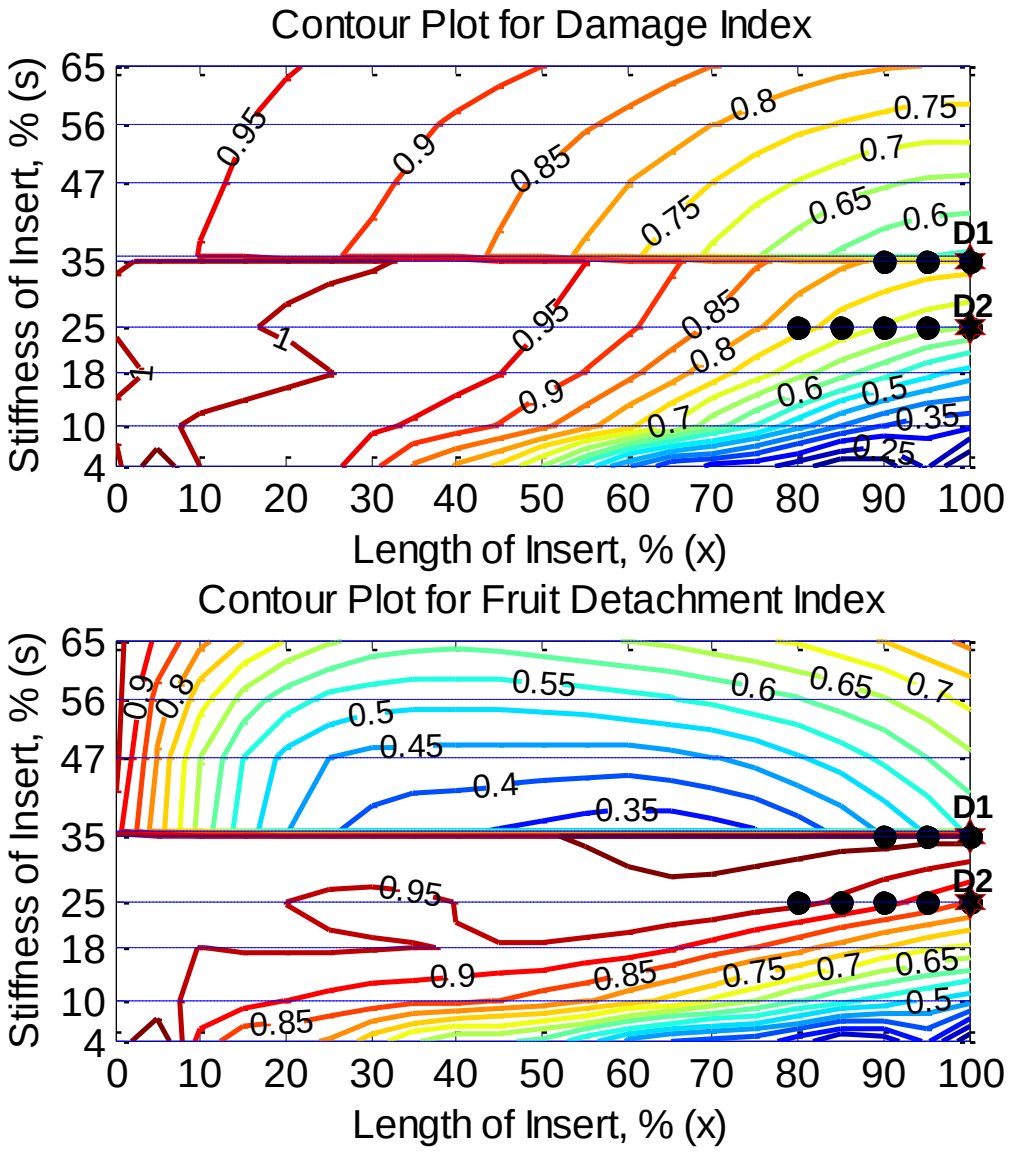


Figure B-1. Phase-1 optimization: Contour plots for the Damage Index and Fruit detachment Index for the top zone tine design.

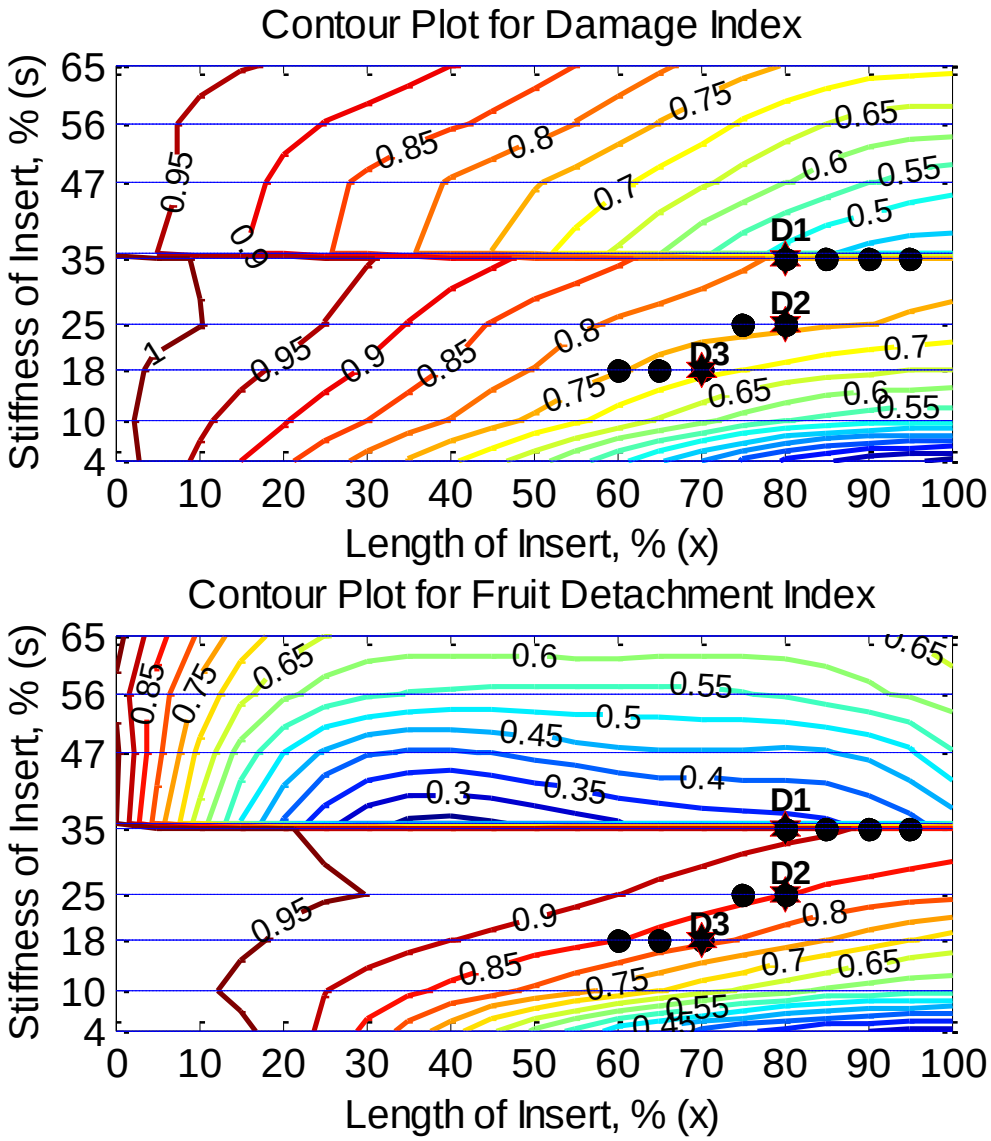


Figure B-2. Phase-1 optimization: Contour plots for the Damage Index and Fruit detachment Index for bottom zone tine design.

APPENDIX C
PHASE-2 OPTIMIZATION

Table C-1. Error norms of RBNN meta models used to predict objective functions for the middle zone tine designs

| MODEL | | Fruit Removal Index | | Damage Index | |
|---|---|---|---|---|---|
| Error Norms | | $PRESS_{RMS}$ | RMS | $PRESS_{RMS}$ | RMS |
| D1 | Design P5 | 0.0483 | 0.0423 | 0.0874 | 0.0429 |
| D2 | Design P4 | 0.107 | 0.0519 | 0.0748 | 0.0521 |
| D3 | Design P3 | 0.0641 | 0.0575 | 0.0784 | 0.055 |

Table C-2. Optimum operating parameters of the tines in the middle section of canopy shaker

| ZONE | Phase-1 Best Designs | Best Operating Range | Frequency | Amplitude | Reduction in Damage (%) | Fruit Removal *(%) |
|---|---|---|---|---|---|---|
| MIDDLE | D1 | OP1 | 7.8 | 1.6 | 19.4 | 99.3 |
| | | OP2 | 7.2 | 1.6 | 27 | 89.3 |
| | D2 | OP1 | 3.6 | 4.6 | 20.1 | 102.4 |
| | | OP2 | 6.4 | 2 | 26.5 | 90.6 |
| | D3 | OP1 | 7.6 | 2 | 21.5 | 103.4 |
| | | OP2 | 7.6 | 1.8 | 32.1 | 89.9 |

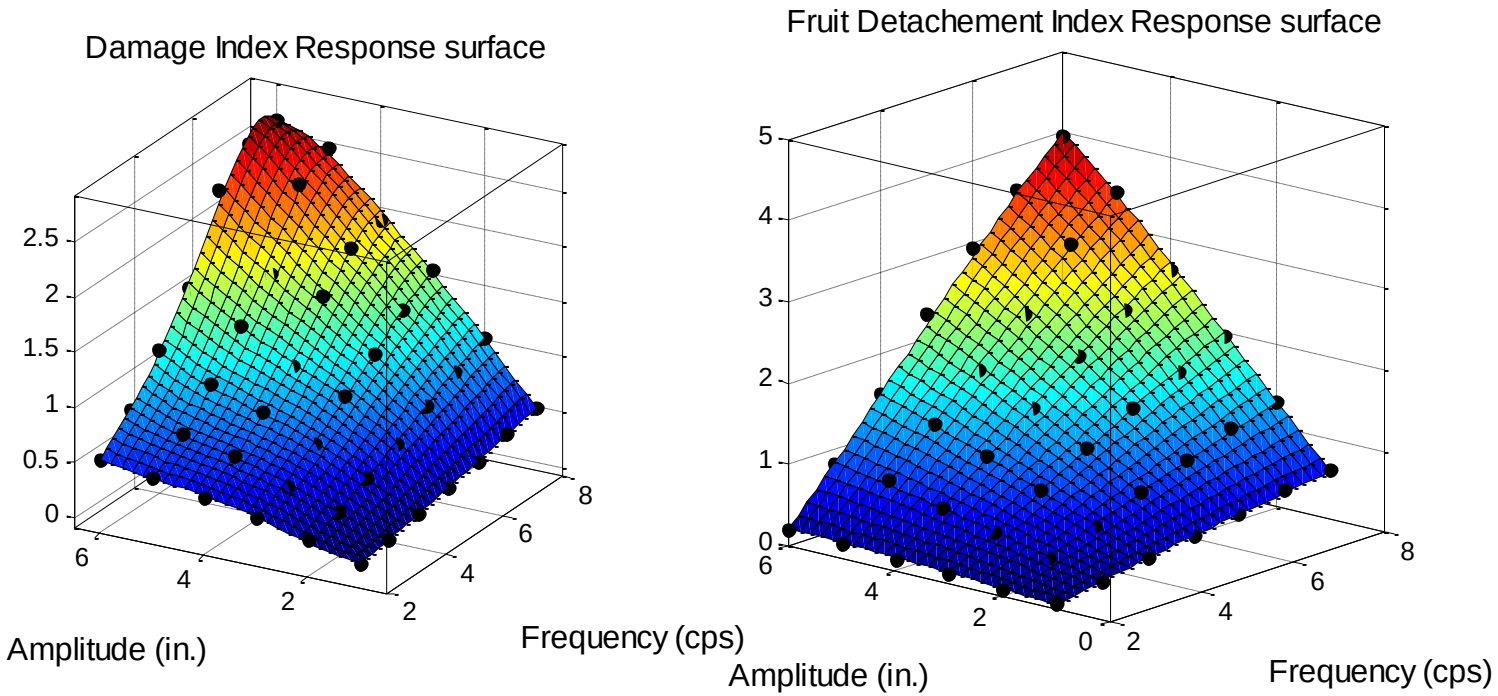


Figure C-1. Response surfaces used to predict the damage index and fruit detachment index of best tine design D1 of middle zone.

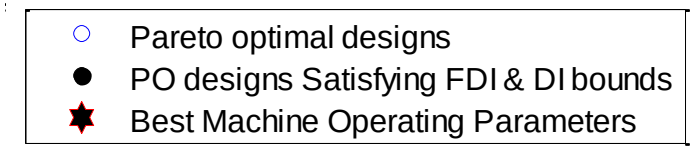


Figure C-2. Legend information used in the Pareto fronts and contour plots.

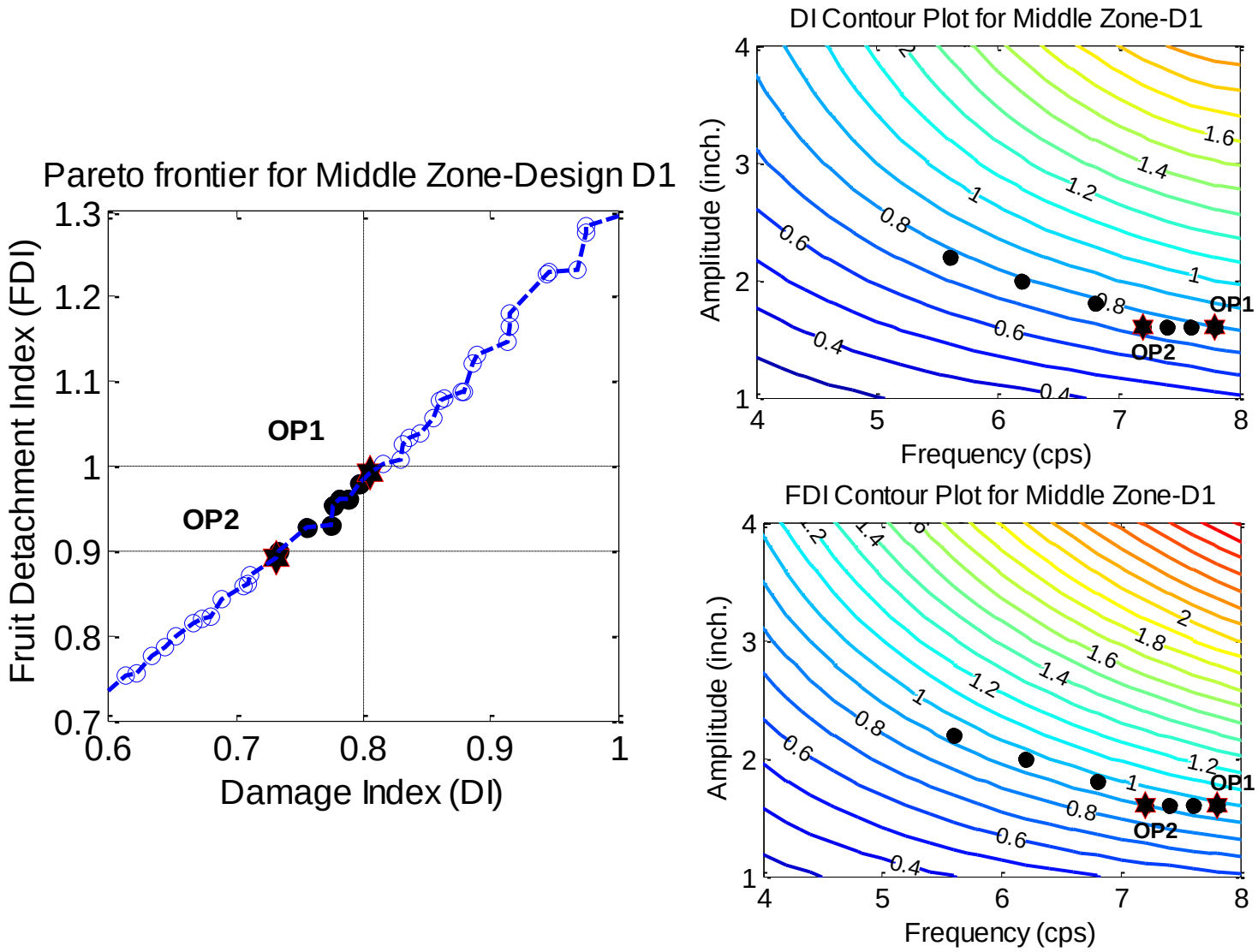


Figure C-3. Pareto front and contour plots of the tine design D1 of middle zone.

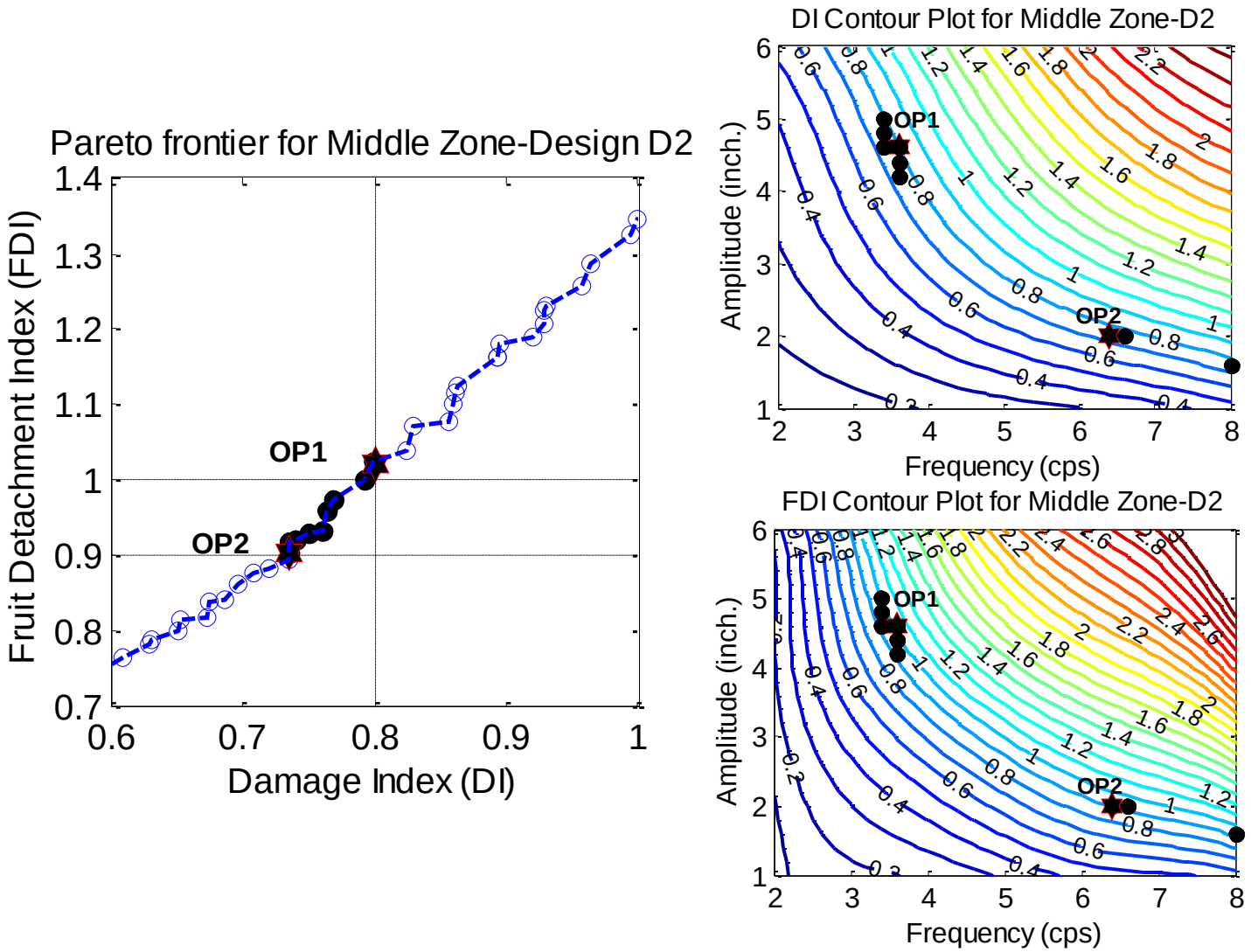


Figure C-4. Pareto front and contour plots of tine design D2 of middle zone.

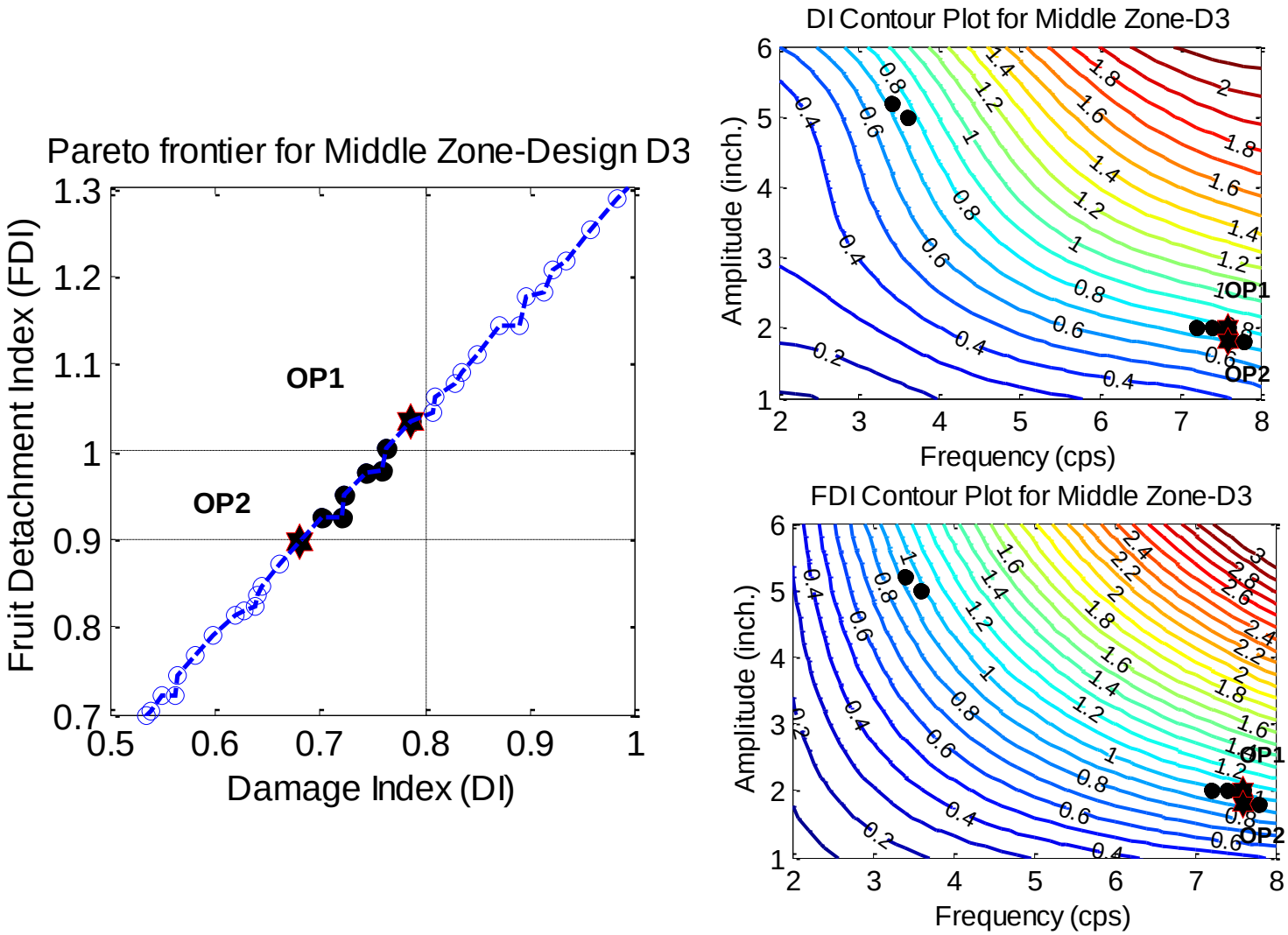


Figure C-5. Pareto front and contour plots of the tine design D3 of the middle zone.

Table C-3. Error norms of RBNN meta models used to predict objective functions for the top zone tine designs.

| MODEL | | Fruit Removal Index | | Damage Index | |
|---|---|---|---|---|---|
| Error Norms | | $PRESS_{RMS}$ | RMS | $PRESS_{RMS}$ | RMS |
| D1 | Design P5 | 0.037 | 0.022 | 0.29 | 0.17 |
| D2 | Design P4 | 0.022 | 0.01 | 0.021 | 0.14 |

Table C-4. Optimum operating parameters of the tines in the top section of canopy shaker.

| ZONE | Phase-1 Best Designs | Best Operating Range | Frequency (Hz) | Amplitude (inch) | Reduction in Damage (%) | Fruit Removal *(%) |
|---|---|---|---|---|---|---|
| TOP | D1 | OP1 | 6.6 | 3 | 40 | 131.1 |
| | | OP2 | 6.8 | 3.6 | 50.6 | 102.3 |
| | D2 | OP1 | 7.25 | 3.75 | 40.1 | 142.8 |
| | | OP2 | 7.5 | 5.5 | 55 | 100.7 |

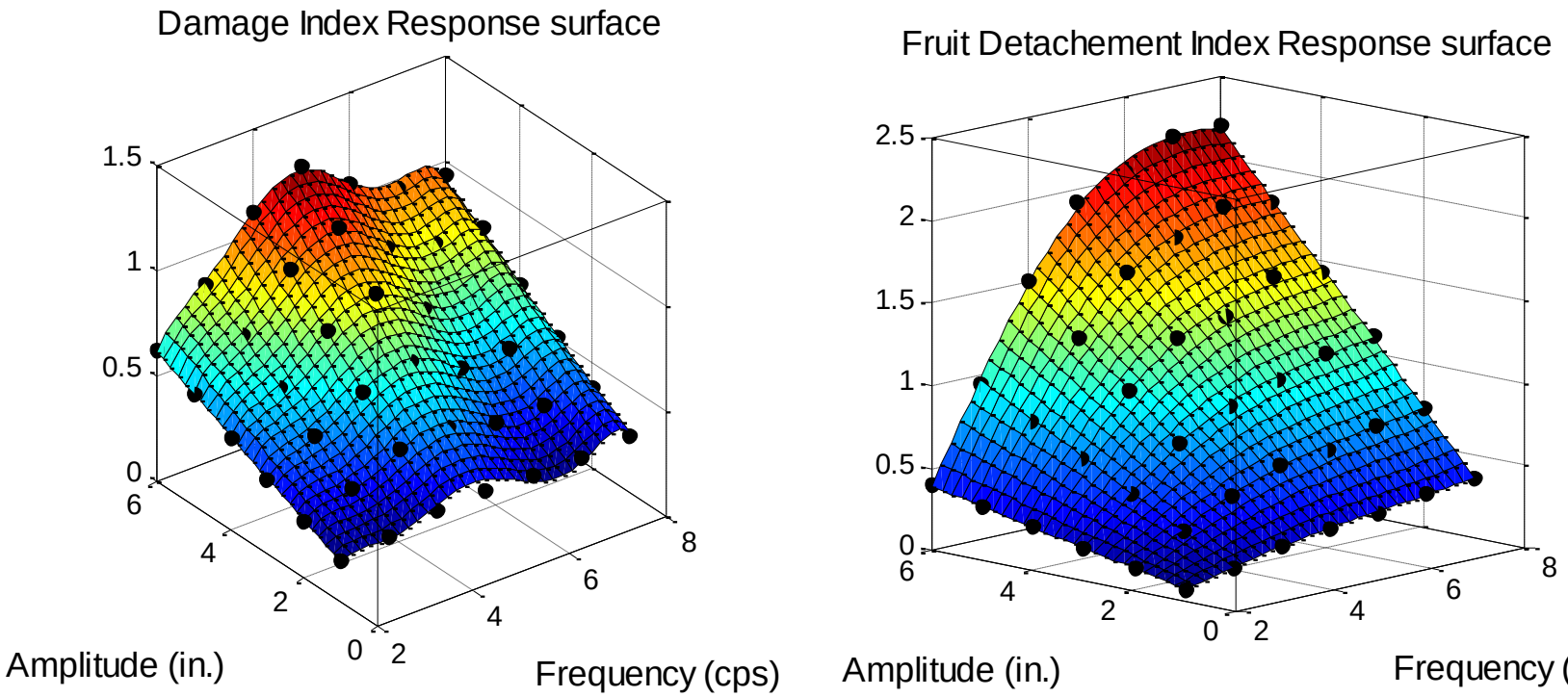


Figure C-6. Response surfaces used to predict the damage index and fruit detachment index of best tine design D1 of top section of a canopy shaker.

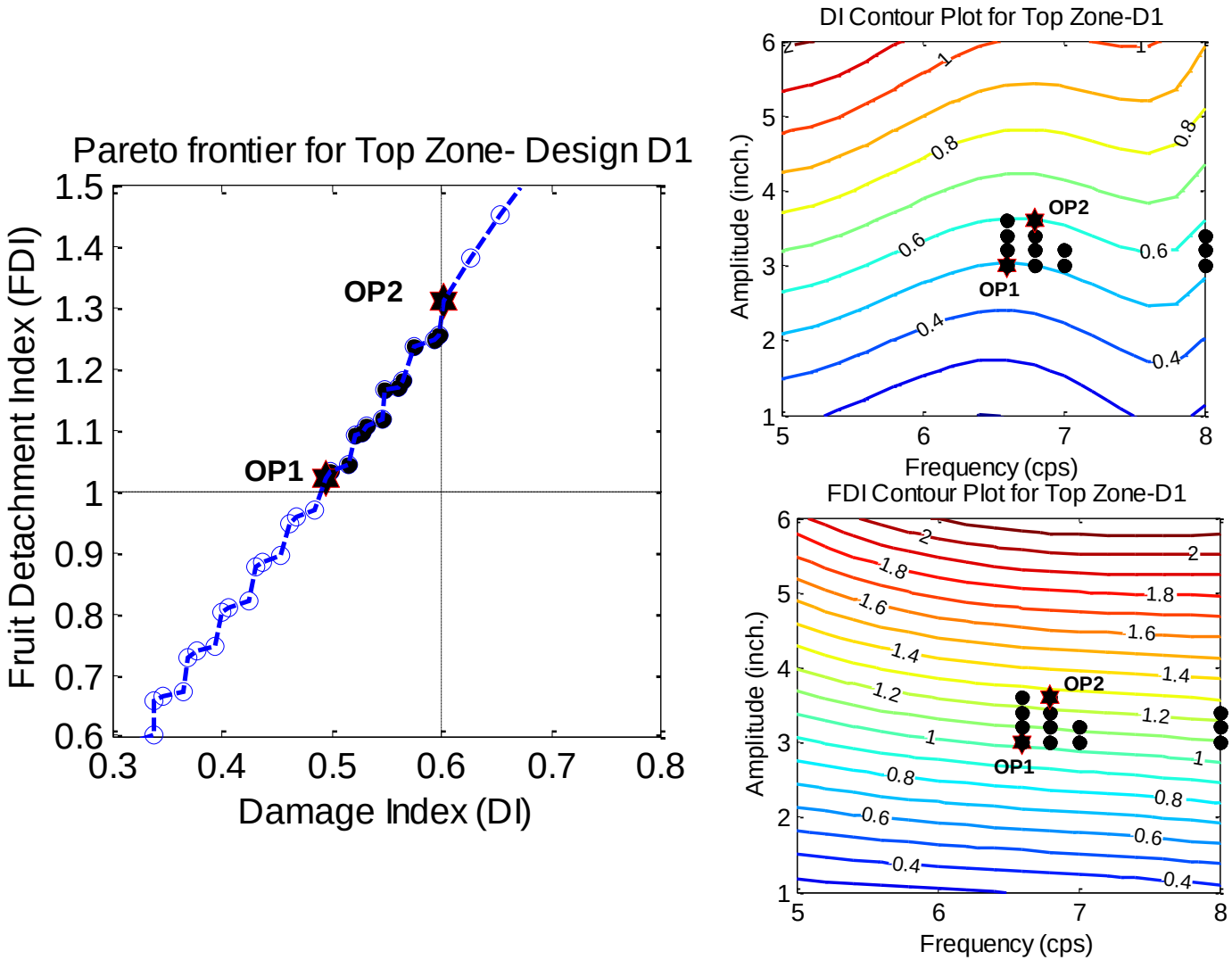


Figure C-7. Pareto front and contour plots of the best tine design D1 to predict optimum configuration of top section of a canopy shaker.

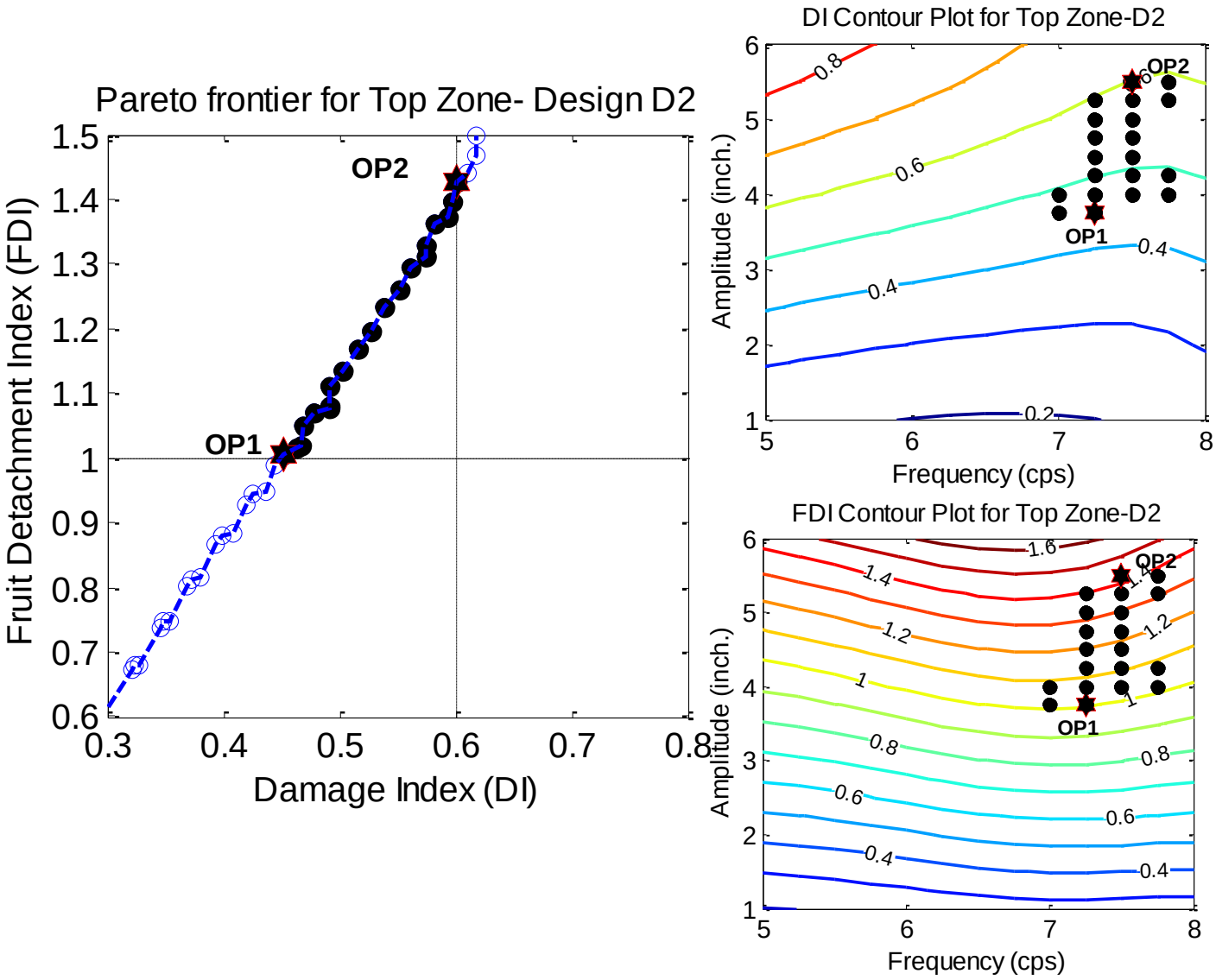


Figure C-8. Pareto front and contour plots of the best tine design D2 to predict optimum configuration of top section of a canopy shaker.

Table C-5. Error norms of RBNN meta models used to predict objective functions for the bottom zone tine designs

| MODEL | | Fruit Removal Index | | Damage Index | |
|---|---|---|---|---|---|
| Error Norms | | PRESSRMS | RMS | PRESSRMS | RMS |
| D1 | Design P5 | 0.040 | 0.032 | 0.036 | 0.013 |
| D2 | Design P4 | 0.063 | 0.037 | 0.064 | 0.037 |
| D3 | Design P3 | 0.057 | 0.049 | 0.054 | 0.031 |

Table C-6. Optimum operating parameters of the tines in the bottom section of canopy shaker

| ZONE | Phase-1 Best Designs | Best Operating Range | Frequency (Hz) | Amplitude (inch) | Reduction in Damage (%) | Fruit Removal *(%) |
|---|---|---|---|---|---|---|
| BOTTOM | D1 | OP1 | 3.6 | 5.4 | 21.3 | 99.35 |
| | | OP2 | 3.2 | 5.4 | 33.7 | 81.5 |
| | D2 | OP1 | 7.6 | 2.6 | 20.6 | 102.3 |
| | | OP2 | 3.2 | 5.8 | 38.9 | 82 |
| | D3 | OP1 | 7.6 | 2.6 | 25.2 | 100.4 |
| | | OP2 | 3.2 | 6 | 39.2 | 81.8 |

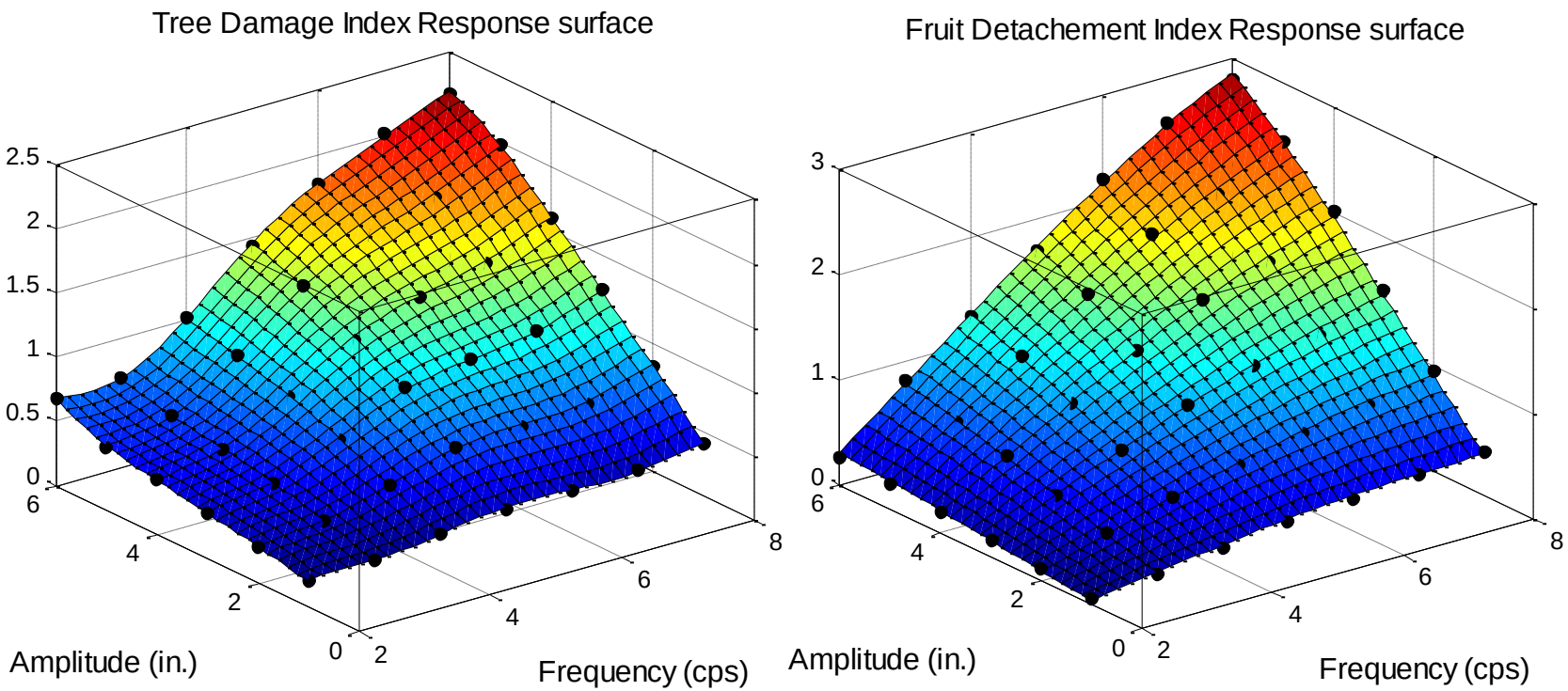


Figure C-9. Response surfaces used to predict the damage index and fruit detachment index of tine design D1 of bottom zone.

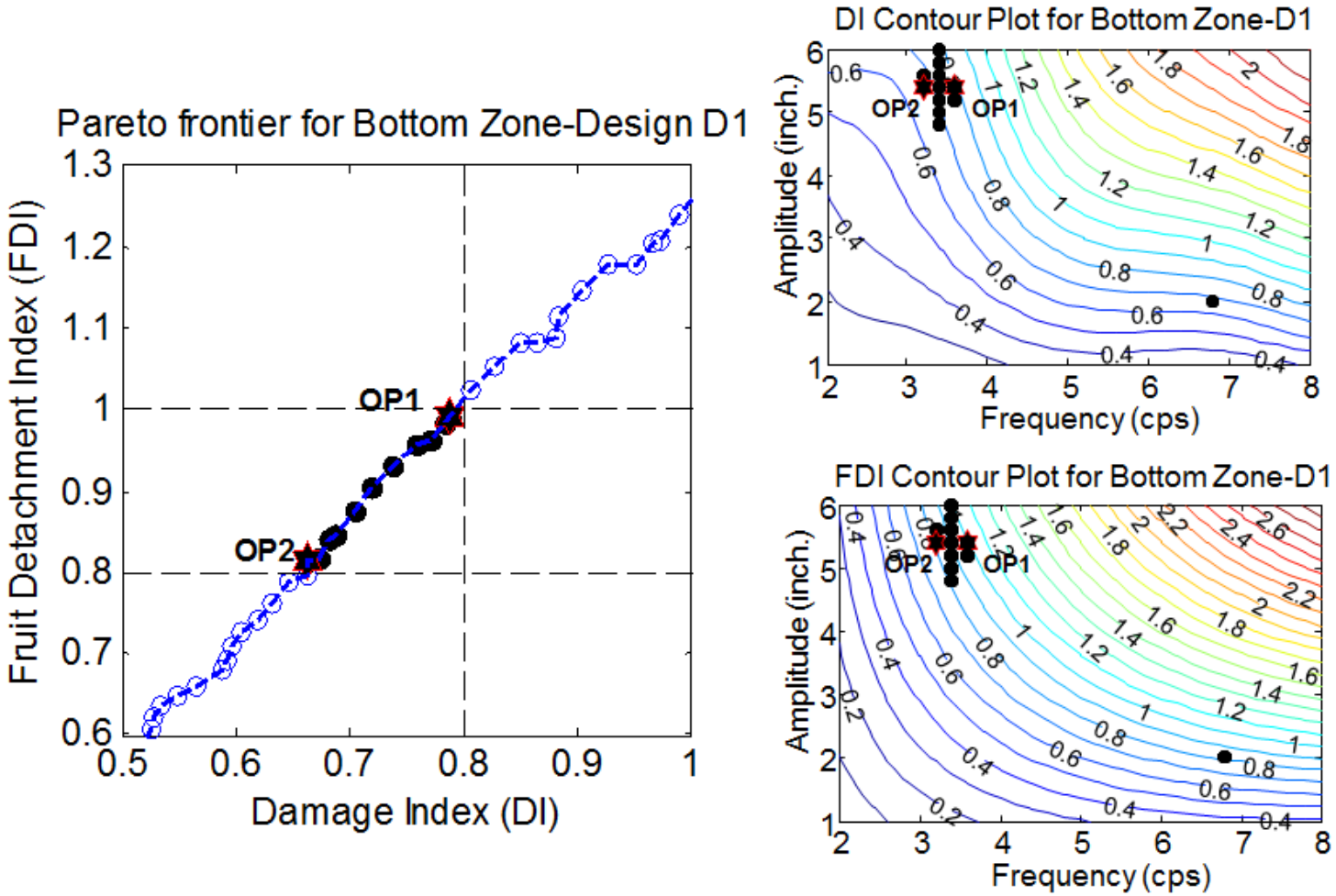


Figure C-10. Pareto front and contour plots of the optimum tine design D1 of the bottom section of a canopy shaker.

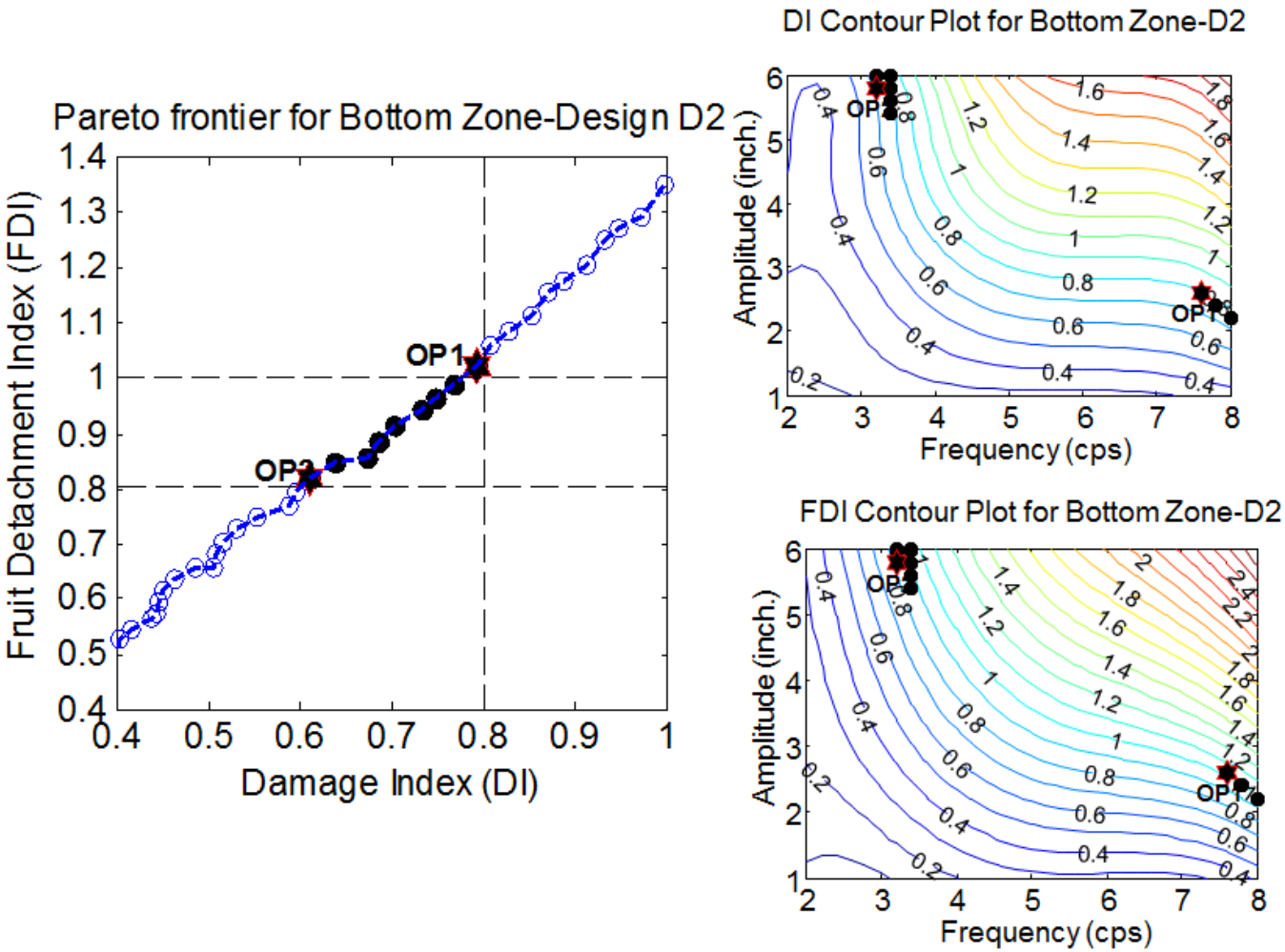


Figure C-11. Pareto front and contour plots of the optimum tine design D2 of the bottom section of a canopy shaker.

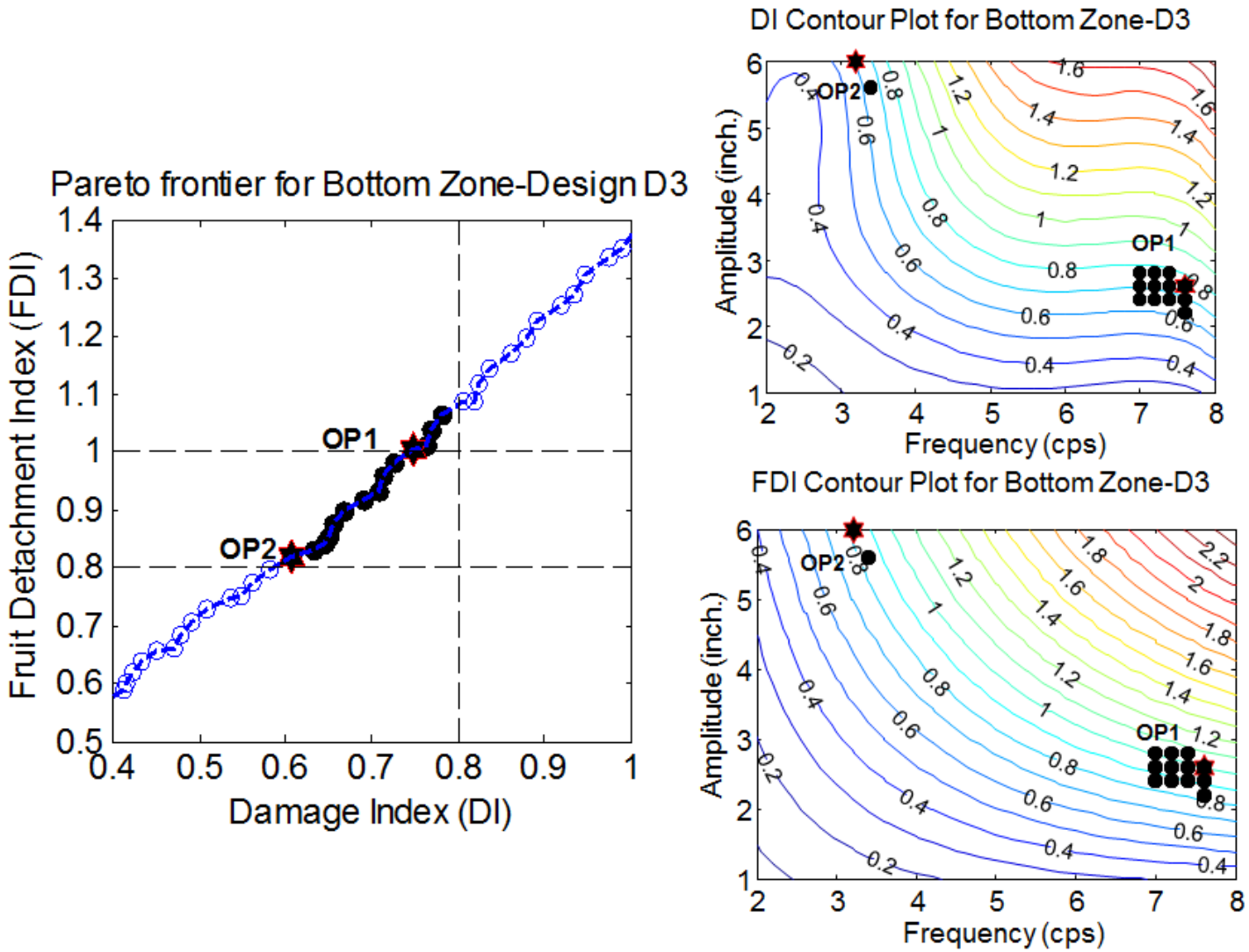


Figure C-12. Pareto front and contour plots of the optimum tine design D3 of the bottom section of a canopy shaker

# LIST OF REFERENCES


Abaqus 2010. *Finite Element Software*. Ver. 6.10. Providence, RI, USA. Dassault Systèmes Simulia Corp.

Adrian, P. A., and R. B. Fridley. 1965. Dynamics and design criteria of inertia-type tree shakers. *Trans. ASAE* 8(1):12–14.

Allen, D. M. 1971. Mean square error of prediction as a criterion for selecting variables. *Technometrics*. 13, 469-475.

Archer, J. S. 1965. Consistent matrix formulation of structural analysis using finite-element techniques. *AIAA J*. 3(10): 1910-1918.

Arora, J. S., O. A. Elwakeil, A. I. Chahande,and C. C. Hsieh. 1995. Global optimization methods for engineering applications: A review. *Struct. Optim.* 9: 137–159.

ASTM. D143-03.: *Standard Test Methods for Small Clear Specimens of Timber.*

Baier, H. 1977. Uber Algorithmen zur Ermittlung und Charak-terisierung Pareto-optimaler L¨osungen bei Entwurfsaufgaben Elastischer Tragwerke. Z. Angew. Math. Mech. 57, 318–320.

Bathe, K. J. 1996. *Finite Element Procedures in Engineering Analysis*. Englewood Cliffs, NJ: Prentice hall.

Berlarge, A. G., and F. M. Willmorth.1974. Fruit removal potential of high frequency vibrations. *Trans. ASAE* 17(2). 233,234.

Brown, G. E., P. F. Burkner, and C. E. Schertz. 1969. Mass harvest problems in California citrus. Proc. Int. Citrus Sym. 2: 667-674.

Carmichael, D. G. 1980. Computation of Pareto optima in structural design. *Int. J. Numer. Methods Eng*. 15: 925–952.

Cavalchini, A. G. 1999. Harvesters and threshers: Forage crops. In CIGR handbook of agricultural engineering Vol.III Plant production engineering, 348–380. International commission of agricultural engineering ed. St. Joseph, Mich.: ASAE.

Chen, P., J. J. Mehlschau, and J. Oritz-Canavate. 1982. Harvesting Valencia oranges with flexible curved fingers. *Trans. ASAE* 25(3): 534–537.

Cheng, F. Y., and D. Li. 1998. Genetic algorithm development for multi objective optimization of structures. *AIAA J* 36: 1105–1112.

Choi, K. K., and N. H. Kim. 2005. *Structural Sensitivity Analysis and Optimization I: Linear Systems*. New York, N.Y.:Springer. Choi, K.K., and N.H. Kim. 2005. *Structural Sensitivity Analysis and Optimization II: Nonlinear Systems and Applications*. New York, N.Y.:Springer.

Choi, K.K., and N.H. Kim. 2005. *Structural Sensitivity Analysis and Optimization II: Nonlinear Systems and Applications*. New York, N.Y.:Springer.

Chopra, A. K. 1995. *Dynamics of Structures:Theory and Applications to Earthquake Engineering*. Prentice Hall. Englewood Cliffs. NJ.

Cook, J.R., and R. H. Rand.1969. Vibratory fruit harvesting: A linear theory of fruit stem dynamics. *J. Agric Eng. Res*. 14(3), 195-209.

Coppock, G.E., and P. J. Jutras. 1960. An investigation of the mobile picker's platform approach to partial mechanization of citrus fruit picking. *Proc. Fla. State Hort. Soc*. 73:258–263.

Das, I., and J. E. Dennis. 1997. A closer look and drawbacks of minimizing weighted sums of objectives for Pareto set generation in multi criteria optimization problems. *Struct Optim* 14:63–69.

Das, I., and J. E. Dennis. 1998. Normal-boundary intersection: a new method for generating the Pareto surface in nonlinear multicriteria optimization problems. *SIAM J Optim.* 8: 631–657.

Deb, K. 2001. *Multiobjective Optimization using Evolutionary Algorithms*. Wiley. New York.

Diener, R. G., J. H. Levin, and R. T. Whittenberger. 1969. Relation of frequency and length of shaker stroke to the mechanical harvesting of apples. ARS 42-148. US Dept. Agric.

Ebner, A. M., and D. P. Billington. 1968. Steady state vibrations of damped Timoshenko beams. *Journal of the Structural Division (ASCE) Vol. 3: 737*.

Freescale Semiconductor Inc. 2008. ±1.5g - 6g three axis low-g micromachined accelerometer (Document number: MMA7260QT). Austin, TX: Freescale Semiconductor Inc. Available at: http://www.freescale.com/files/sensors /doc/data_sheet/MMA7260QT.pdf. Accessed 01 July 2013.

Freitas, A. D. 2012. Pareto fronts according to dominance relation http://www. mathworks.com/matlabcentral/fileexchange/37080-pareto-fronts-according-to-dominance-relation.

Fridley, R. B., and C. Lorenzen. 1965. Computer analysis of tree shaking. *Trans. ASAE* 8(1): 8 -11, 14.

Fridley, R. B. and C. Yung. 1975. Computer analysis of fruit detachment during tree shaking. *Trans. ASAE* 18(3): 409-415.

Fridley, R. B., H. T. Hartmann, J. J. Mehlschau, P. Chen, and J. Whisler. 1971. Olive harvest mechanization in California. Calif. Agric. Exp. Sta. Bull. 855.

Fridley, R. B., and P. A. Adrian. 1966. Mechanical harvesting equipment for deciduous tree fruits. Calif. Agric. Sta. Bull. 825.

Futch, S. H., J. D. Whitney, J. K. Burns, and F. M. Roka. 2005. Harvesting: From manual to mechanical. Institute of Food and Agricultural Sciences. University of Florida. Pub.: HS-1017.

Halderson, J. L. 1966. Fundamental factors in mechanical cherry harvesting. Trans. ASAE 9 (5): 681-684.

Hedden, S. L., D. B. Churchill, and J. D. Whitney. 1984. Orange removal with trunk shakers. *Proc. Fla. State Hort. Soc*. 97: 47–50.

Hedden, S. L., and G. E. Coppock. 1971. Comparative harvest trials of foliage and limb shakers in Valencia oranges. *Proc. Fla. State Hort. Soc*. 84:88–92.

Hilber, H. M., T. J. R. Hughes, and R. L. Taylor. 1977. Improved numerical dissipation for time integration algorithms in structural dynamics. *Earthquake Eng. and Struct. Dynamics* 5: 283–292.

Hoag, D. L., J. R. Hutchinson, and R. B. Fridley. 1969. Effect of proportional, non-proportional and non-linear damping on the dynamic response of tree limbs. *Trans of the ASAE* 13(6): 879-884.

Hoag, D. L., R. B. Fridley, and J. R. Hutchinson. 1971. Experimental measurement of internal and external damping properties of tree limbs. *Trans. ASAE* 14(1): 20-28.

Horvath, E., and G. Sitkei. 2005. Damping properties of plum trees shaken at their trunks. *Trans. ASAE* 48(1): 19–25.

Hughes T. J. R. 1987. *Finite Element Method-Linear Static and Dynamic Finite Element Analysis.* Englewood Cliffs. New Jersey: Prentice Hall.

Hurty, W.C., and M.F. Rubinstein. 1964. *Dynamics of Structures*. Englewood Cliffs. New Jersey: Prentice Hall.

Hussain, A. A. M., G. E. Rehkugler, and W. W. Gunkel. 1975. Tree limb response to a periodic discontinuous sinusoidal displacement. *Trans. ASAE* 18(4): 614–617.

Jutras, P. J., and G. E. Coppock. 1958. Mechanization of citrus fruit picking. *Proc. Fla. State Hort. Soc*. 71:201–204.

Khuri, A. I., and J. A. Cornell, 1996. *Response Surfaces: Designs and analyses*. 2nd edition, New York: Marcel Dekker.

Kim, N. H., and B. V. Shankar. 2009. *Introduction to Finite Element Analysis and Design*. New York: Wiley.

Koski, J. 1979. Truss Optimization with Vector Criterion. Report Number 6, Tampere University of Technology, Tampere, Finland.

Koski, J. 1980. Truss optimization with vector criterion, examples. Report Number 7, Tampere University of Technology, Tampere, Finland.

Kristensen E.S., and N.F. Madsen.1976. On the optimum shape of fillets in plates subjected to multiple in plane loading cases. *Int. J. Numer. Methods Eng*.10:1007–1019.

Kutzbach, H. D., and G. R. Quick. 1999. Harvesters and threshers: Grain. In CIGR handbook of agricultural engineering Vol.III Plant production engineering, 311–347. International commission of agricultural engineering ed. St. Joseph, Mich: ASAE.

Leitmann, G. 1977. Some problems of scalar and vectorvalued optimization in linear viscoelasticity. *J. Optim. Theory. Appl.* 23: 93–99.

Lenker, D.H. 1970. Development of an auger picking head for selectively harvesting fresh market oranges. *Trans. ASAE* 13(4):500–504, 507.

Liang, T., D.K. Lewis, J.K. Wang, and G.E. Monroe. 1971. Random function modeling of macadamia nut removal by multiple frequency vibration. *Trans. ASAE* 14(6): 1175-1179.

Lybas, J., and M. A. Sozen. 1977. Effect of beam strength ratio on dynamic behavior of reinforced concrete coupled walls. Report SRS No. 444, University of Illinois, Urbana–Champaign.

Manfredi, E., and R. Peters. 1999. Harvesters and threshers: Root crops. In CIGR handbook of agricultural engineering Vol.III Plant production engineering, 381–408. International commission of agricultural engineering ed. St. Joseph, Mich.: ASAE.

Markwardt, E.D., R.W. Guest, J.C. Cain, and R.L. Labelle. 1964. Mechanical cherry harvesting. *Trans. ASAE* 7(1): 70-74, 82.

Marler, R.T., and J.S. Arora. 2004. Survey of multi-objective optimization methods for engineering. *Struct. Multidisc. Optim.* 26: 369–395.

Mayer, H. 1987. Wind induced tree sways. Trees 1: 195–206.

McKenzie W. M.,and H. Karpovich. 1968. The frictional behavior of wood. *Wood Science and Technology*. Vol. 2: 139-152.

Messac, A., A. Ismail-Yahaya, C.A. Mattson. 2003. The normalized normal constraint method for generating the Pareto frontier. *Struct. Multidisc. Optim.* 25: 86–98.

Miller, W. M., and C.T. Morrow.1976. Vibrational characterization of the apple-stem system with respect to stem separation. *Trans. ASAE* 19(3): 409-411,416.

Moore, J. R. 2002. Mechanical behavior of coniferous trees subjected to wind loading. Ph.D. dissertation, Oregon, USA: Oregon State University.

Myers, R.H., D.C. Montgomery. 2002. *Response surface methodology process and product optimization using designed experiments*. 2nd edn., New Work: Wiley.

O'Brien, M., B. F. Cargill, and R. B. Fridley. 1983. *Principles and Practices for Harvesting and Handling Fruits and Nuts*. Westport, Connecticut: The Avi Publishing Company, Inc.

Parchomchuk, P., and J.R. Cooke.1972. Vibratory harvesting: an experimental analysis of fruit-stem dynamics. *Trans. ASAE* 15(4): 598-603.

Pareto, V. 1906. Manuale di Economica Politica, Societa Editrice Libraria. Milan; translated into English by A.S. Schwier as Manual of Political Economy, edited by A. S. Schwier and A. N. Page, 1971. New York: A.M. Kelley.

Park, J. and I. W. Sandberg. 1991. Universal approximation using radial basis function networks. *MIT, Neural Computation* 3: 246-257.

Park, Y.J., and A. H.-S. Ang.1985. Mechanistic seismic damage model for reinforced concrete. *Journal of Structural Engineering, ASCE*, Vol. 111, No. 4, pp.722-739.

Pedersen, P., and C.L. Laursen. 1983. Design for minimum stress concentration by finite elements and linear programming. *Journal of structural mechanics*.Vol. 10, No.4 pp. 376-391.

Pestel, E. C. and F. A. Leckie. 1963. *Matrix methods in elastomechanics*. New York, NY: McGrawHill Book Company.

Peterson, D. L. 1998. Mechanical harvester for processed oranges. *Applied Eng. In Agric*. 14(5): 455-458.

Peterson, D. L., T. Liang, and A. L. Myers. 1972. Feasibility study of shake harvesting macadamia nuts. *Int. Conf.Trop.Subtrop.Agric., ASAE spec. Publ.* SP-01-72

Phillips A. L., J.R., Hutchinson, and R. B. Fridley. 1970. Formulation of forced vibration of tree limbs with secondary branches. *Trans. ASAE* 13(1) 138-142.

Powell, G.H., and R. Allahabadi. 1988. Seismic damage prediction by deterministic methods: concepts and procedures. *Earthquake Engineering and Structural Dynamics*.16(5): 719-734.

Roka, F., J. Burns, J. Syvertsen, and R. Ebel. 2008. Benefits of an abscission agent in mechanical harvesting of citrus. Doc. no. FE752. Food and Resource Economics Department.IFAS. University of Florida.

Roufaiel, M.S.L., and C. Meyer.1987. Analytical modeling of hysteretic behavior of R/C frames. *Journal of Structural Engineering*. 113(3): 429-444.

Ruff, J. H., R. P. Rohrbach, and R. G. Holmes. 1980. Analysis of the air suspension stem vibration strawberry harvesting concept. *Trans. ASAE* 23(2): 288-297.

Rumsey, J. W. 1967. Response of the citrus fruiting system to fruit removing actions. Unpublished master's thesis, Tucson, Arizona: University of Arizona

Rumsey, T. R. 1967. Simulation of forced vibration of a tree limb by finite element methods. Unpublished master's thesis, Davis, California: University of California.

Santos, J. L. T., K. K. Choi. 1989. Integrated computation consideration for larger scale structural design Sens analysis and optimization. Discretization methods and structural optimization –procedure and applications, H.A. Eschenauer and G Thierauf), pp. 229-307, springer-Verlag, Berlin.

Savary. S. K. J. U. 2009. Study of the force distribution in the citrus canopy during harvest using continuous canopy shaker. MS thesis. Gainesville, Florida: University of Florida, Department of Agricultural and Biological Engineering.

Savary, S. K. J. U., R. Ehsani, M. Salyani, M. A. Hebel,and G. C. Bora. (2011). Study of force distribution in the citrus tree canopy during harvest using a continuous canopy shaker. *Computers and Electronics in Agriculture* 76(1): 51-58.

Savary, S. K. J. U., R. Ehsani, J. K. Schueller, and B. P. Rajaraman. (2010). Simulation study of citrus tree canopy motion during harvesting using a canopy shaker. *Trans. ASABE:* 53(5): 1373-1381.

Schertz, C.E., and G.K. Brown. 1968. Basic considerations in mechanizing citrus harvest. *Trans. ASAE* 11(3): 343-346.

Schuler, R.T., and H. D. Bruhn. 1973. Structurally damped Timoshenko beam theory applied to vibrating tree limbs. *Trans. ASAE* 15(5): 886–889.

Spann, T. M., and M. D. Danyluk 2010. Mechanical harvesting increases leaf and stem debris in loads of mechanically harvested citrus fruit. *Hortscience*. 45(8): 1297-1300.

Stadler, W. 1988. *Fundamentals of multicriteria optimization*. In: Stadler, W. (ed.) Multicriteria Optimization in Engineering and in the Sciences, pp. 1–25. New York: Plenum Press.

Tompson, W.T. 1993. *Theory of Vibration with application*, 3rd Ed. Englewood. Cliff. New Jersey: Prentice Hall.

Upadhyaya, S. K., and J. R. Cooke. 1980. Limb impact harvesting: Part III. Model studies. *Trans. ASAE* 24(4):868-871, 878.

Upadhyaya, S. K., J. R. Cooke, R. A. Pellerin, and J. A. Throop. 1980a. Limb impact harvesting: Part II. Experimental approach. Trans. ASAE 24(4):864-867.

Upadhyaya, S. K., J. R. Cooke, and R. H. Rand. 1980b. Limb impact harvesting: Part I. Finite element analysis. *Trans. ASAE* 24(4):856-863.

Veletsos, A. S., and N. M. Newmark.1960. Effect of inelastic behavior on the response of simple systems to Earthquake motions. *Proceedings of the 2nd World Conference on Earthquake Engineering*, vol. 2, pp. 895-912

Viana, F. A. C., R. T. Haftka, V. Steffen Jr. 2009. Multiple surrogates: how cross-validation errors can help us to obtain the best predictor. *Struct. Multidisc. Optim*. 39:439–457.

Viana, F. A. C. 2010. *Surrogates toolbox user's guide*: http://sites.google.com/site/ fchegury/surrogatestoolbox.

Wangaard, F. F. 1950.*The mechanical properties of wood*. New York: Wiley.

Whitney, J. D. 1968. Citrus fruit removal with an air harvester concept. *Proc. Fla. State Hort. Soc*. 81:43–47.

Whitney, J. D. 1995. A review of citrus harvesting in Florida. *Trans. of the Citrus Engineering Conference, Florida Section, ASME* 41:33–59.

Whitney, J. D. 1999. Field test results with mechanical harvesting equipment in Florida oranges. *Applied Eng. in Agric*. 15(3):205–210.

Whitney, J. D., and J.M. Patterson. 1972. Development of a citrus removal device using oscillating forced air. *Trans. ASAE* 15(5):849–855, 860.

Whitney J. D., and T. A. Wheaton. 1984. Tree spacing affects citrus fruit distribution and yield*. Proc. Fla. State Hort. Soc*. 97:44-47.

Wilson, T. R. C. 1932. Strength-moisture relations for wood. U.S. Department of Agriculture Technical Bulletin, Number 282.

Yung, C. and R.B. Fridley. 1975. Simulation of vibrations of whole tree system using finite elements. *Trans. ASAE* 18(3): 475-481.

# BIOGRAPHICAL SKETCH

Susheel Kumar Gupta was born in 1985, to Daya Shankar Gupta and Geeta Gupta in Uttar Pradesh, India. He received his Bachelor in Engineering from Madhav Institute of Technology and Science (M.I.T.S), Gwalior, India in 2007. He worked as a design engineer at Larsen and Toubro Limited from 2007-2011. He joined University of Florida in fall 2011 to pursue Master of Science degree in mechanical and aerospace engineering. He received his MS degree in August 2013.